SD71-191-1

ESTABLISHMENT OF DESIGN CRITERIA FOR ACCEPTABLE FAILURE MODES AND FAIL SAFE CONSIDERATIONS FOR THE SPACE SHUTTLE STRUCTURAL SYSTEM

First Quarterly Progress Report CR-121023
15 June - 15 September 1971

Contract NAS8-27269

Prepared by
R. W. Westrup
Structural Systems and Mechanisms

Prepared for
George C. Marshall Space Flight Center
Marshall Space Flight Center, Alabama 35812

OCT 1971
RECEIVED
NASA STI FACILITY
INPUT BRANCH

Reproduced by
NATIONAL TECHNICAL INFORMATION SERVICE
U S Department of Commerce
Springfield VA 22151

Space Division
North American Rockwell

FACILITY FORM 602

N72-10939 (ACCESSION NUMBER)	(THRU)
97 (PAGES)	63 (CODE)
CR-121023 (NASA CR OR TMX OR AD NUMBER)	31 (CATEGORY)

SD71-191-1

ESTABLISHMENT OF DESIGN CRITERIA FOR ACCEPTABLE FAILURE MODES AND FAIL SAFE CONSIDERATIONS FOR THE SPACE SHUTTLE STRUCTURAL SYSTEM

First Quarterly Progress Report
15 June - 15 September 1971

Contract NAS8-27269

Prepared by
R. W. Westrup
Structural Systems and Mechanisms

Prepared for
George C. Marshall Space Flight Center
Marshall Space Flight Center, Alabama 35812

Space Division
North American Rockwell
Downey, Calif.

Page intentionally left blank

PRECEDING PAGE BLANK NOT FILMED

FOREWARD

This report is the first quarterly progress report submitted under Contract NAS8-27269. It is submitted to George C. Marshall Space Flight Center as a summary of technical investigations and results conducted under the above contract during the period 15 June 1971 through 15 September 1971.

PRECEDING PAGE BLANK NOT FILMED

CONTENTS

Section		Page
1.0	INTRODUCTION	1-1
	1.1 BACKGROUND	1-1
	1.2 STUDY APPROACH	1-3
	1.3 STUDY OBJECTIVES	1-4
2.0	BASELINE VEHICLE MISSION & CONFIGURATION	2-1
	2.1 PROGRAM OBJECTIVE	2-1
	2.2 MISSION PROFILES	2-1
	2.2.1 Operational Mission	2-1
	2.2.2 Ferry Mission	2-8
	2.3 BOOSTER CONFIGURATION	2-11
	2.3.1 General Arrangement	2-11
	2.3.2 Body Structure	2-17
	2.3.3 Aerodynamic Surfaces	2-27
	2.3.4 Body Thermal Protection System	2-30
	2.3.5 Weight Summary	2-33
3.0	STRUCTURAL DESIGN LOADS AND CRITERIA FOR BASELINE VEHICLE	3-1
	3.1 STRUCTURAL DESIGN CRITERIA	3-1
	3.1.1 Design Philosophy	3-1
	3.1.2 Design Requirements	3-2
	3.1.3 Design Conditions	3-3
	3.1.4 Loads and Pressures	3-5
	3.1.5 Design Factors	3-6
	3.1.6 Service Life	3-7
	3.1.7 Design Thickness	3-9
	3.2 DESIGN LOADS	3-10
	3.2.1 Aerodynamic Surfaces	3-10
	3.2.2 Body Loads	3-10
	3.2.3 Propellant Tank Pressures	3-21
	3.3 SERVICE LOAD SPECTRA	3-21
	3.3.1 Wing Load Spectra	3-21
	3.3.2 Vertical Stabilizer Load Spectra	3-21
	3.3.3 Body Load Spectra	3-21
	3.4 STRUCTURAL TEMPERATURES	3-29

Section		Page
4.0	SELECTED STRUCTURAL ELEMENTS	4-1
	4.1 SELECTION SUMMARY	4-1
	4.2 SELECTION RATIONALE	4-1
5.0	FATIGUE AND FRACTURE PROPERTIES	5-1
	5.1 FATIGUE PROPERTIES	5-1
	5.1.1 2219 Aluminum Alloy	5-1
	5.1.2 6 Al-4V Titanium Alloy	5-1

ILLUSTRATIONS

Figure		Page
2-1	Typical Operational Mission Flight Profile	2-3
2-2	Ascent Trajectory Parameters	2-6
2-3	B-9U Booster Entry Trajectory Profile	2-6
2-4	Transcontinental Ferry Route	2-9
2-5	Typical Ferry Mission Profile	2-10
2-6	B-9U Booster Basic Configuration Drawing 76Z0140	2-13
2-7	Booster Structural Arrangement	2-15
2-8	Forward Skirt Structure	2-19
2-9	Liquid Oxygen Tank	2-21
2-10	Intertank Adapter Structure	2-22
2-11	Liquid Hydrogen Tank	2-24
2-12	Thrust Structure	2-25
2-13	Crew Compartment	2-26
2-14	Wing Arrangement and Support Points	2-28
2-15	Canard Structure	2-29
2-16	Vertical Stabilizer	2-31
2-17	Body TPS Shell Structure	2-32
3-1	Wing Bending Moment Distribution	3-13
3-2	Canard Bending Moment Distribution	3-14
3-3	Vertical Stabilizer Bending Moment Distribution	3-15
3-4	Body Loadings - Top ℄	3-16
3-5	Body Loadings - Bottom ℄	3-17

Figure		Page
3-6	Booster Main Engine Thrust vs. Time	3-20
3-7	B-9U Main LOX Tank Pressure Schedule	3-22
3-8	B-9U Main LH_2 Tank Pressure Schedule	3-23
3-9	LOX Tank Limit Pressure Profiles	3-24
3-10	LH_2 Tank Limit Pressure Profiles	3-25
3-11	B-9U Wing Load Spectra	3-26
3-12	B-9U Vertical Tail Load Spectra	3-27
3-13	B-9U Fuselage Sta. 2600 Load Spectra	3-28
3-14	Orbiter Aft Attach Load Spectra	3-30
3-15	B-9U Thrust Spectra	3-31
3-16	Wing Structure Transient Temperatures	3-32
3-17	Vertical Stabilizer Structure Transient Temperatures	3-33
5-1	S-N Curves for 2219 Aluminum (K_t = 4.4)	5-3
5-2	S-N Curves for Ti-6 AL-4V (K_t = 3.0)	5-4
5-3	S-N Curves for Ti-6 Al-4V (K_t = 4.5)	5-5
5-4	Modified Goodman Diagram for Ti-6 Al-4V (Annealed)	5-6

TABLES

Table		Page
2-1	Significant Events During the B-9U Entry Trajectory	2-7
2-2	B-9U Booster Weight Summary	2-34
2-3	B-9U Booster Wing Group Weight Breakdown	2-35
2-4	B-9U Booster Vertical Tail Group Weight Breakdown	2-37
2-5	B-9U Booster Body Group Weight Breakdown	2-38
3-1	Design Factors of Safety	3-8
3-2	Service Life Factors	3-8
3-3	Safe-Life Design Environments	3-11
3-4	Summary of Design Conditions	3-11
3-5	Design Loads for Aerodynamic Surfaces	3-12
3-6	Body Limit Design Loads	3-18
3-7	Booster/Orbiter Connection Loads	3-19
3-8	Estimated Range of Structural Temperatures	3-34
4-1	Matrix of Candidate Structural Elements - Shuttle Booster B-9U	4-3

Page intentionally left blank

PRECEDING PAGE BLANK NOT FILMED

REFERENCES

1. Anon, Space Shuttle Phase B Final Report; Vol. II, Technical Summary; Book 3, Booster Vehicle Definition NR/SD Report SD 71-114-2, 25 June 1971.

2. Fletcher, D. A., and J. E. Jensen, A Study for Developing Safe-Life/Fail-Safe Criteria for the Space Shuttle, First Monthly Progress Report, General Dynamics Convair, 19 April 1971.

3. Garracy, C. A., Space Shuttle Booster Structural Design Criteria, General Dynamics Convair Report No. 76-549-30-007, March 26, 1971.

4. Kruse, G., Space Shuttle Booster B-9U Loads, General Dynamics Convair Report No. 76-549-30-008, June 1, 1971.

5. Jensen, J. E., A Study for Developing Safe-Life/Fail-Safe Criteria for the Space Shuttle, Second Monthly Progress Report, General Dynamics Convair, 22 May 1971.

6. Diller, D. E., A Study for Developing Safe-Life/Fail-Safe Criteria for the Space Shuttle, Third Monthly Progress Report, General Dynamics Convair, 22 June 1971.

7. Diller, D. E., A Study for Developing Safe-Life/Fail-Safe Design Criteria for the Space Shuttle, Fourth Monthly Progress Report, General Dynamics Convair, 22 July 1971.

8. Preston, J. L., Compilation of S-N Fatigue Curves and Modified Goodman Diagrams Applicable to B-1 Structural Materials, North American Rockwell, Los Angeles Division Report TFD-71-845, June 2, 1971.

9. Kaufman, J. E., G. E. Nordmark and B. W. Lifka, Fracture Toughness, Fatigue and Corrosion Characteristics of 2020-T651, 2024-T851, 2219-T851, and 7001-T75, Aluminum Alloys, AFML-TR-66-291 Sept., 1966.

10. Hyler, W. S., and O. L. Deel, Summary of Fatigue Information on Ti-6Al-4V Alloy, DMIC Technical Note, Oct. 5, 1967.

11. Illg, Walter and Claude B. Castle, Farigue of Four Stainless Steel Alloys and Three Titanium Alloys Before and After Exposure to 550F, Up to 8000 Hours. NASA TN D-2899, July, 1965.

12. Dutko, T. R., Effect of Tapered Fasteners on the Fatigue Life of Titanium 6 Al-4V (Annealed) Joints North American Rockwell, Los Angeles Division Report NA-67-822, Oct. 22, 1968.

1.0 INTRODUCTION

1.1 BACKGROUND

The space shuttle missions will subject structures to repeated sequences and combinations of loading and environmental conditions that are unprecedented in the history of aircraft and space vehicles. Although the total flight time associated with the design goal of 100 missions for the space shuttle operational life may be relatively small compared to that of contemporary commercial aircraft, the incidence of repeated high-stress load cycles may remain as a very significant consideration for structural design. This is due to several factors, including the presence of aerodynamic surfaces on booster and orbiter vehicles and the consequent response of the vehicle to wind shear and gust during ascent and entry, the asymmetric configuration and high thrust levels during boost, and the high maneuver load factors anticipated during entry. In addition, repeated cycles of large temperature excursions and, in some cases, associated thermal stresses will occur because of aerodynamic heating and the loading and depletion of cryogenic propellants.

Three general design approaches have evolved over the last two decades to prevent aerospace structures from failing catastrophically because of repeated load cycles: (1) fail-safe design, (2) safe-life design based on conventional fatigue considerations, and (3) safe-life design based on fracture mechanics considerations. The following brief discussion of these approaches includes a tentative evaluation of potential applicability to space shuttle structure.

The fail-safe design concept is based on the premise that a crack may develop and grow in the structure because of fatigue nucleation, material defects, or accidental damage; the growth of the crack will be eventually arrested, however, and a stable condition maintained by suitable design provisions. The residual strength of the structure in this weakened condition must be equal to or greater than a prescribed value, which is frequently taken as limit design load. It is presumed that the damage will be detected and repaired before catastrophic failure occurs during operation. This design philosophy has been extensively applied to the fuselage and main-wing structure of current jet transport aircraft. This basic approach may also have useful application to many of the structural elements of the space shuttle, excluding such areas as propellant tanks. However, before it can be determined that this is the most appropriate criteria for a given structural element, consideration must be given to the specific characteristics of the shuttle with respect to accessibility for thorough inspection, engineering and economic feasibility of damage detection and repair, potential impact on the two-week turnaround time, etc.

Safe-life design using conventional fatigue methods recognizes local stress concentrations due to detail design characteristics such as joints, fittings, section discontinuities, etc. However, it does not consider the potential of undetected crack-like defects existing in the structure before the start of operational service. The useful life of structural elements determined by fatigue test is comprised primarily of the number of cycles required to nucleate a crack, rather than cycles required for crack propagation to a critical value. This approach has also been widely applied to design of military and commercial aircraft over the last 15 years. Good results have been obtained in many cases, particularly for some of the current commercial jet transport aircraft which exhibit minimal structural maintenance problems in airline operation. However, the serious structural problems or failures encountered by some recent high-performance military aircraft after only limited operational service dramatically illustrate that conventional fatigue methods may not adequately guard against premature fracture. This is particularly true for structural designs involving higher operating stresses, lower toughness materials, and material forms or fabrication processes that involve a higher probability of inherent crack-like defects or reduced capability to detect such defects. It is apparent, therefore, that it would be dangerous to apply this approach to space shuttle structure without corollary application of safe-life criteria based on fracture mechanics considerations. However, it is desirable to survey cyclic stresses on typical structural elements of the space shuttle to determine the general magnitude of potential fatigue problems and appropriate criteria to assure a fatigue-resistant design.

Safe-life design based on fracture mechanics considerations is predicated on the assumption that crack-like defects may exist in the structure prior to operational service and the design must be developed so that such defects will not grow to critical dimensions during the operational life. This is accomplished by selecting materials and operating stresses such that (1) flaws of critical initial size are large enough to assure detection by non-destructive inspection or (2) it can be verified by proof test that no flaws of critical initial size exist in the structure. Some investigators in the field believe that no inspection program can be considered 100-percent reliable, and that proof-test verification is mandatory. The fracture mechanics approach to safe-life design has been applied rather extensively to space vehicle pressure tanks in recent years. Proof-test verification was accomplished on nearly all of the Apollo lunar module pressure vessels and on the propellant tanks of booster stages in the Saturn V vehicle. Unfortunately, serious difficulties appear to exist when rigorous proof-test verification criteria are applied directly to space shuttle structure. Proof testing of unpressurized structure, such as wings, fuselage shell, etc., may be impractical because of several factors, including schedule delay, cost, limited accuracy of load simulation, and scars to flight structure caused by attachment of test loading equipment. Valid proof testing of pressurized structure, such as main propellant tanks and crew compartment, will also be difficult and may be impractical. Integral tank design will produce complex load inputs much different than internal pressurization. Body bending and shear loadings on the shuttle vehicle will be much greater than for the Saturn V vehicle. Thus, it may be difficult to conduct a valid proof test by internal pressurization only. An additional problem is related to proof testing of the primary cryogenic propellant tanks.

A critical flaw over most of the surface of these tanks will involve a through-thickness crack rather than a surface crack for the materials and operating stresses currently being considered in space shuttle preliminary design. A leak-before-break characteristic is desirable for proof test, but may not be acceptable for operational service with cryogenic propellants. The proof-test levels required to verify that no initial flaws exist which could grow through the thickness of the tank walls (rather than to critical dimensions as a through crack) may impose unacceptable weight penalties on the shuttle design.

The preceding considerations illustrate that the design criteria for space shuttle structure must be carefully studied to achieve the basic program goals of minimum structural weight, minimum program costs, and demonstrated high reliability. It is further concluded that no single structural design approach will be adequate to achieve these primary goals. The most appropriate criteria will probably contain elements of the fail-safe design approach, fatigue resistant design, and fracture mechanics considerations which include both proof-test verification and nondestructive inspection as essential elements. In addition, it may be necessary to establish quality control criteria for material procurement and fabrication operations and quality assurance procedures for fabrication, checkout and test, and operational usage to assure effective fracture control of space shuttle structure over the entire life history, from raw material to the end of operational service. It is apparent, therefore, that the results of this study program will be an important element of the basic requirements and development approach for the space shuttle during final design, fabrication, and operational phases.

1.2 STUDY APPROACH

The Space Division will conduct this study using, as a point of departure, the space shuttle design definition and data that are available from the space shuttle Phase B study programs. It is believed that this study must be based on typical space shuttle requirements, missions, and structural configurations, rather than generalized concepts, for the following major reasons:

1. To assure that parametric studies cover applicable ranges of variables.

2. To provide realistic focus on problems or limitations associated with design, material characteristics, fabrication processes, nondestructive evaluation, verification tests, and flight and maintenance operations.

3. To make efficient use of analyses and data being developed on the space shuttle Phase B programs that support certain tasks of this study.

4. To permit realistic assessment of the impact of candidate design criteria on structural weight, vehicle performance, maintenance requirements, and program costs.

The booster vehicle and mission characteristics developed by Convair Division of General Dynamics during the space shuttle Phase B study program have been selected as the baseline for this study. This selection has been made in conjunction with the NASA/MSFC COR. The booster configuration is designated as B-9U; the characteristics of the vehicle and its associated mission are described in Reference 1. Typical mission characteristics are used to define reference spectra of structural loadings and environmental conditions that serve as the basis of safe-life, fail-safe, and fatigue assessments. Several major structural elements are selected that serve as the reference structural configurations. Selection is based on design, material, fabrication, and inspectability considerations so that a representative sample of all major structural systems is provided. Failure-mode characteristics of these selected structural elements under the reference loading/environment spectra are investigated by means of fracture mechanics and fatigue analysis methods and data. Parametric studies are performed to determine the effects of variation of load/environment spectra, design configuration, material combinations, and verification methods on structural weight, vehicle performance, maintenance requirements, etc., for the candidate criteria of each appropriate failure-mode approach. Results of the parametric studies are evaluated to determine the most promising criteria candidates, and recommendations are made for criteria selection.

1.3 STUDY OBJECTIVES

The study program has the following major objectives:

1. To develop rational design criteria to implement fail-safe and safe-life considerations of critical primary structure of the space shuttle.

2. To demonstrate that the recommended design approaches and associated criteria are appropriate, practical, and capable of providing the desired structural reliability and safety. This requires consideration of the following factors:

   a. Mission requirements

   b. Performance requirements

   c. Service-life requirements

   d. Maintenance requirements

   e. Material selection

   f. Weight control

   g. Reliability

3. To develop parametric data for evaluation of the effect of changes in mission, configuration, material selection, and design approach or criteria on:

   a. Performance

   b. Service life

   c. Maintenance requirements

   d. Weight

   e. Reliability

4. To bound the magnitude of potential fatigue problems on space shuttle primary structure and to determine the general level of attention and design verification criteria required to assure a fatigue-resistant structure.

2.0 BASELINE VEHICLE MISSION AND CONFIGURATION

2.1 PROGRAM OBJECTIVE

The objective of the Space Shuttle Program is to provide a low-cost space transportation system capable of placing and/or retrieving payloads in earth orbit. To achieve this objective, a fully reusable system capable of rapid turnaround and airline-type operation has been defined.

Three missions have been identified as representing the requirements for the definition of the Space Shuttle System. These missions are (A) "The design mission, 100 n. mi. due east circular orbit. The design mission insertion orbit shall be 50 x 100 n. mi. and for purposes of performance comparison calculations the vehicle shall be considered to be launched from a latitude of 28.5 degrees north; (B) the reference missions of major interest are: (1) 100 n. mi. south polar circular orbit; (2) 270 n. mi. at 55 inclination."

To achieve the objectives of the program, a two-stage vehicle capable of boost and earth entry with cruise-back to a designated landing site has been defined. This cycle is accomplished with reasonable acceleration levels, shirt-sleeve cabin environment, and quick, ground-turnaround time between flights. The significant elements of these missions are ground operations, mating of the orbiter and booster vehicles, and liftoff followed by staging of the two vehicles, with the first-stage booster returning to the launch area and the second-stage orbiter continuing on to the prescribed insertion orbit. Following a series of orbital maneuvers, the orbiter delivers and/or retrieves its payload and, at the appropriate orbital position, reenters the atmosphere, acquires the landing site, and completes the approach and landing. Following safing at the landing area, the vehicle enters a turnaround cycle consisting of thorough postflight inspection, a maintenance cycle, installation of a new payload, and mating with the booster vehicle. This mated system is checked out and returned to the launch area to begin a new mission cycle.

2.2 MISSION PROFILES

2.2.1 Operational Mission

Mission operations are summarized in Figure 2-1. Major phases of the operational mission are discussed below.

Ascent

The ascent phase is defined as beginning with engine ignition and ending with the initiation of separation. In the ignition/liftoff sequence, the thrust rises to 50 percent of full thrust and holds at that level until

main-stage in all engines can be verified and holddown release is verified. Upon verification, the thrust is increased at a controlled rate to 100 percent. The vehicle liftoff occurs when the thrust-to-weight ratio (T/W) is greater than 1.

During the ignition sequence the thrust vector control (TVG) is positioned to point at the vehicle center of gravity, and it maintains this position until the booster clears the holddown mechanism. Then the TVC controls the vehicle to required pitch, yaw, and roll attitudes until the vehicle clears the service towers. Commands to ensure tower clearance are either calculated by the onboard guidance, navigation, and control (GN&C) system or are programmed to a fixed time.

After the vehicle has cleared the service towers, the TVC is commanded by the GN&C system to provide roll, orienting the vehicle to the correct azimuth, and pitch, to provide the proper trajectory, such that the vehicle assumes a wing-level, pilot-side-up attitude and correct azimuth. TVC continues to control the vehicle to a preprogrammed pitch rate and fixed roll/yaw attitudes. During the period of 60 to 90 seconds, a yaw plane acceleration feedback system is switched in to reduce sideslip angle to minimize the induced roll.

At 125 seconds a closed loop guidance steering command is mixed with commanded pitch rate and the yaw attitude command to minimize trajectory dispersions and to steer the vehicle to the desired staging point. As propellant is depleted, along with increased thrust at altitude, the vehicle acceleration reaches 3g. At this point, approximately 160 seconds after launch, the main engines are throttled to maintain 3g for crew comfort and vehicle design loads. Ascent phase is terminated by initiation of separation based on indication of propellant depletion. Ascent trajectory parameters are given in Figure 2-2. The booster weight decreases from 4,188,000 lb at launch to about 806,000 lb at separation, while achieving a velocity of 10,800 fps at an altitude of 245,000 ft.

Separation

Near booster burnout, a signal from the booster LO_2 depletion sensor initiates the separation sequences. At depletion sensor signal, the booster engines are stepped to 50-percent thrust. Concurrently the orbiter engines are started and brought to 50-percent thrust. When both sets of engines are at 50-percent thrust and propellant depletion is imminent, the restraint mechanism between orbiter and booster is released, booster thrust decays to zero, and the orbiter rotates upwards and aft, relative to the booster, on separation system linkages until the orbiter is freed and accelerating under its own thrust. The control of all sequencing functions necessary for separation and maintaining control of both orbiter and booster is accomplished by software in the main computers of each vehicle.

After separation, the orbiter continues on its orbital mission and the booster positions itself for entry, using ACPS engines.

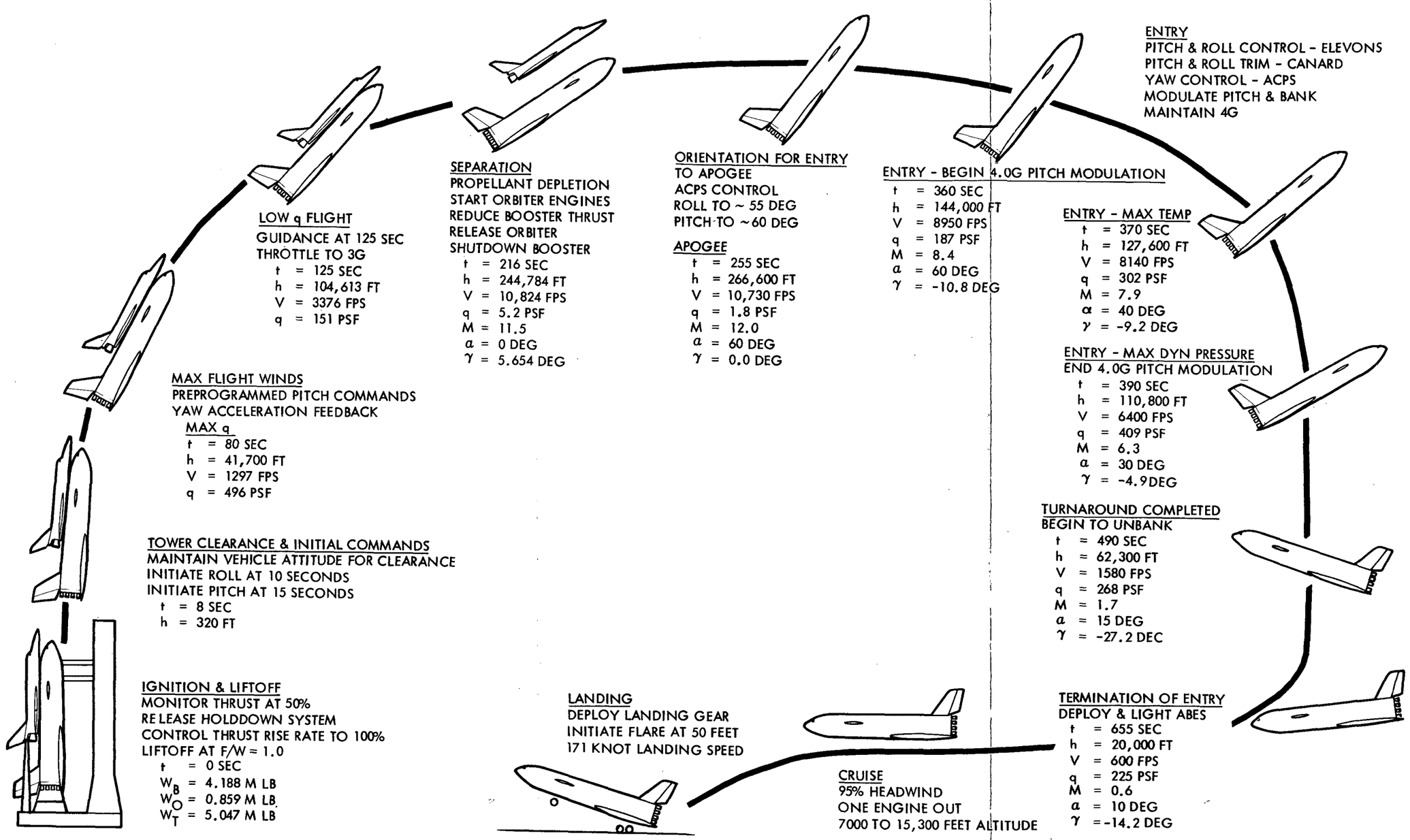

Figure 2-1. Typical Operational Mission Flight Profile

Entry

The booster entry phase starts at separation and terminates when the booster descends to 20,000 feet and deploys air-breathing engines for cruise back to the launch site. The entry mode for the B-9U booster is a supersonic transition. The angle of attack is reduced as Mach number is decreased; the angle of attack schedule is presented in Figure 2-3. Pitch and bank angle scheduling is used to minimize the flyback distance to the landing site with a 4.0g maximum load factor constraint. The entry phase is assumed to be concluded when the booster descends to an altitude of 20,000 feet.

The baseline entry trajectory is for a 100-n.mi. south polar circular orbit mission launched from the Western Test Range. Significant events during the booster entry are listed in Table 2-1. Staging occurs 216 seconds after launch. During the next 40 seconds the booster banks to a 55-degree angle and then pitches to a 60-degree angle of attack. That attitude is maintained until the load factor builds up to a maximum limit of 4.0g, which occurs 360 seconds after launch, at Mach 8.4. For the next 30 seconds the angle of attack is modulated downward. A peak dynamic pressure of 409 psf occurs at the end of the pitch modulation at Mach 6.3 and at an attitude of 30 degrees. Between Mach 6.3 and 2.5 the booster is kept at an angle of attack of 30 degrees and banked at 75 degrees. After 490 seconds, at Mach 1.7, the vehicle has turned around 180 degrees and is headed back to the launch site. The bank angle is reduced to 0 degree. From Mach 2.5 to 1.1 the angle of attack is reduced to 5 degrees, which is held through the transonic region. The subsonic attitude is 10 degrees. By 655 seconds after launch the booster has come down to an altitude of 20,000 feet, where the remaining flyback distance to the landing site is 399 n.mi. At the completion of the entry phase the gross weight of the booster has decreased slightly to 787,000 lb.

Cruise

The flyback profile is initiated at 20,000 feet, where the cruise engines are assumed to be fully deployed and operating normally; flyback range is determined from this point. An idle power descent is made to the optimum cruise altitude; this is the altitude for maximum specific range. The vehicle is then operated at the best cruise altitude for the duration of the cruise flight. For the mission with all engines operating in still air, the idle power descent is made to 14,500 feet, and a cruise climb at the optimum cruise altitude is performed between 14,500 feet and 18,500 feet. For the engine out case, the vehicle is operated at the optimum cruise altitudes between 5000 ft and 13,500 ft. An idle power descent is made from the end of cruise altitude to sea level for the completion of the flyback segment.

The flyback range requirement from the 20,000-foot altitude point is 399 n.mi.

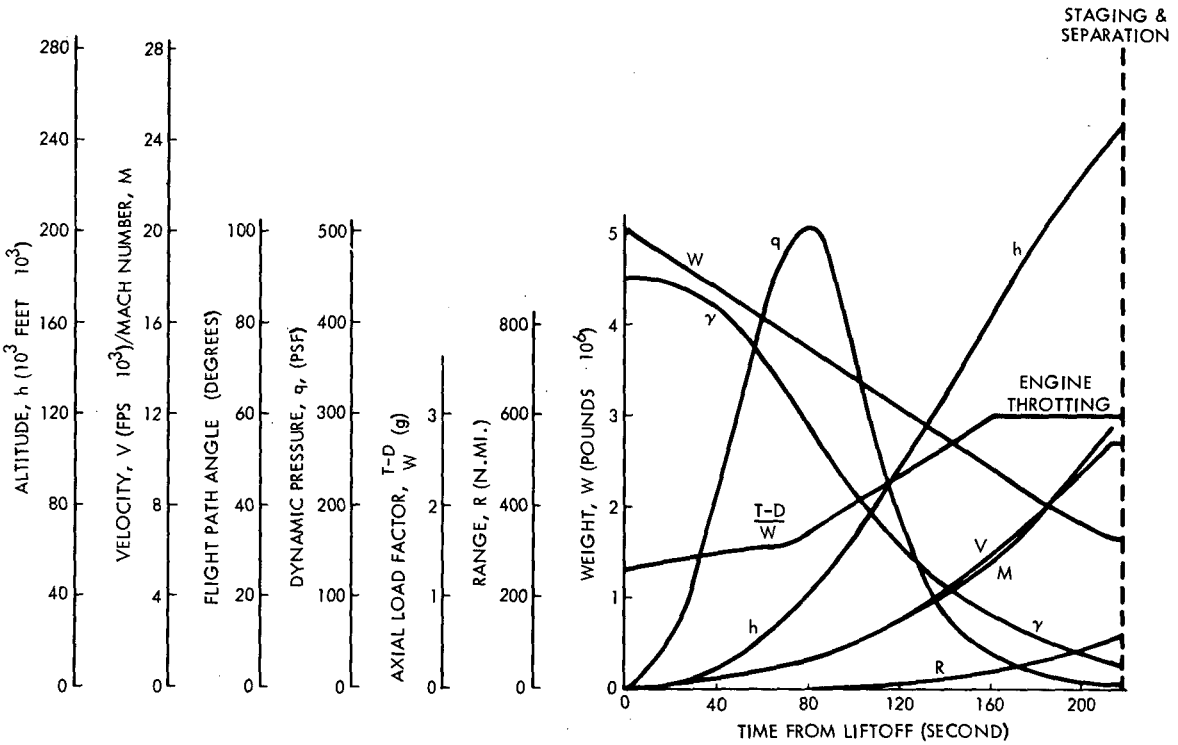

Figure 2-2. Ascent Trajectory Parameters

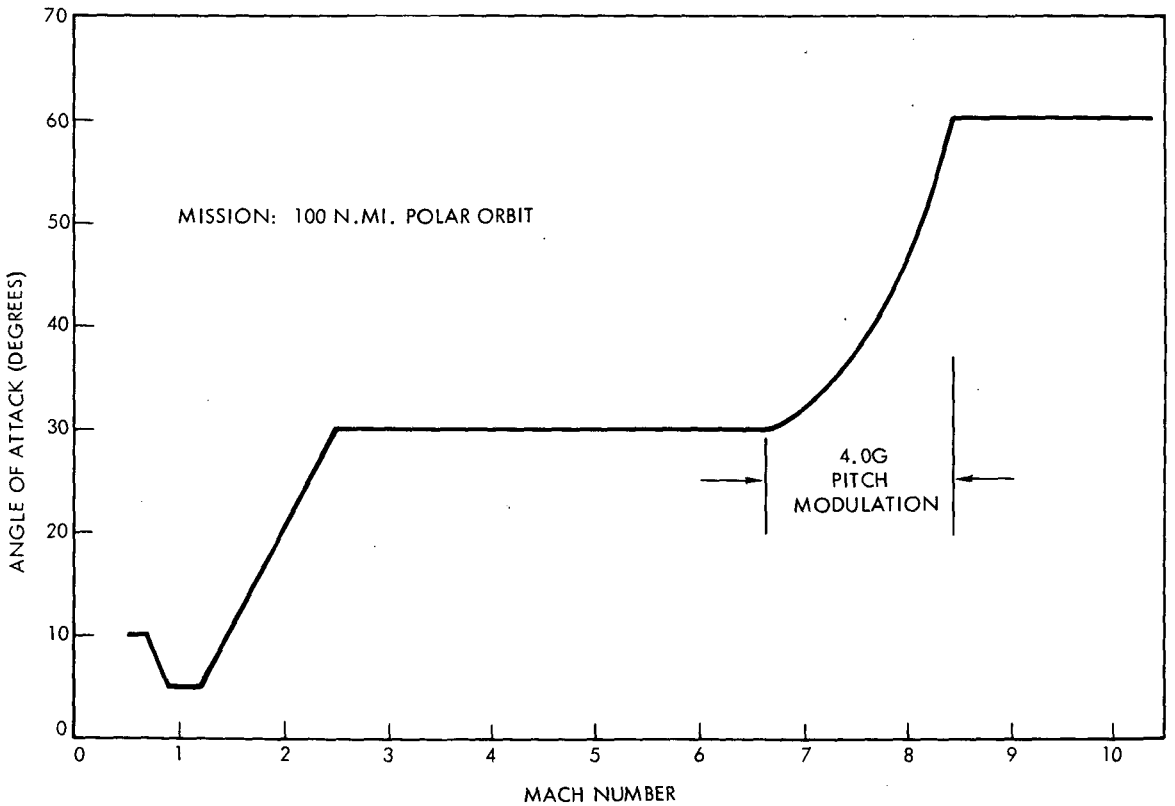

Figure 2-3. B-9U Booster Entry Trajectory Profile

Table 2-1. Significant Events During the B-9U Entry Trajectory

Event	Time (sec)	Altitude (feet)	Relative Velocity (fps)	Mach	Relative Gamma (deg)	Q (psf)	Load Factor	Alpha (deg)	Bank Angle (deg)	Range (n.mi.)	Gross Weight (10^3 lb)
Staging	216	244,784	10,824	11.5	5.6	5.2	0.0	0	0	116	806
Apogee	255	266,600	10,730	12.0	0.0	1.8	0.0	60	55	186	
Begin 4.0g Pitch Modulation	360	144,000	8,950	8.4	-10.8	187	4.0	60	55	363	
Peak Supersonic q/End Pitch Mod.	390	110,800	6,400	6.3	-4.9	409	4.0	30	55	400	
Begin Pitchdown	455	84,000	2,420	2.5	-12.0	208	2.6	30	75	428	
Begin to Unbank	490	62,300	1,580	1.7	-27.2	268	1.9	15	75	423	
Peak Transonic q (1.2g)	590	24,700	915	0.9	-18.3	450	1.2	5	0	407	
Conclude Entry Phase	655	20,000	600	0.6	-14.2	225	0.9	10	0	399	787

Space Division
North American Rockwell

Landing

The requirement for landing performance of the booster is that it land on a 10,000-foot runway on standard day conditions. This has been interpreted to include a 50-foot obstacle.

The basic landing technique for the B-9U booster is to approach from a 50-foot obstacle at a three degree glide slope and touchdown at 110 percent of the free air minimum velocity for the landing configuration. This results in a touchdown angle of attack of about 11.5 degrees. The booster has a 3 fps sink rate at touchdown, and there is a three second delay from touchdown until the nose gear is down and a one second delay from nose gear down until the brakes are applied. The baseline landing configuration is with 3 degree elevons, trimmed with the canard at 15 degrees. The entire landing is executed with the booster in this configuration.

2.2.2 Ferry Mission

Requirements and Criteria

Self-ferry performance requirements are defined as a selected flight route from KSC to Edwards AFB with several intermediate stope, as illustrated in Figure 2-4. Two segments from this route appear to require the greatest ferry capability, i.e.:

1. 300 n.mi. segment from KSC to Robbins AFB requiring takeoff capability from a 10,000-foot runway under sea level hot day conditions.

2. 235 n.mi. segment from Biggs AFB to Davis-Monthan AFB requiring takeoff capability from 13,600-foot runway at an elevation of 4000 feet under hot day conditions.

In determining self-ferry performance of the B-9U booster, the following mission profile was assumed:

1. Takeoff over a 35-foot obstacle utilizing the balanced field concept.

2. Climb to cruise altitude at maximum rate of climb against a 50-knot headwind.

3. Cruise at constant altitude at maximum specific range against a 50-knot headwind to the point of no return.

4. Continue cruise at constant altitude with one engine inoperative against a 50-knot headwind at maximum specific range from point of no return to beginning of descent.

5. Descend at L/D_{max} at idle power with one engine inoperative against a 50-knot headwind.

6. Fuel reserves equal to 20 minutes at maximum endurance at sea level with all engines operating were included.

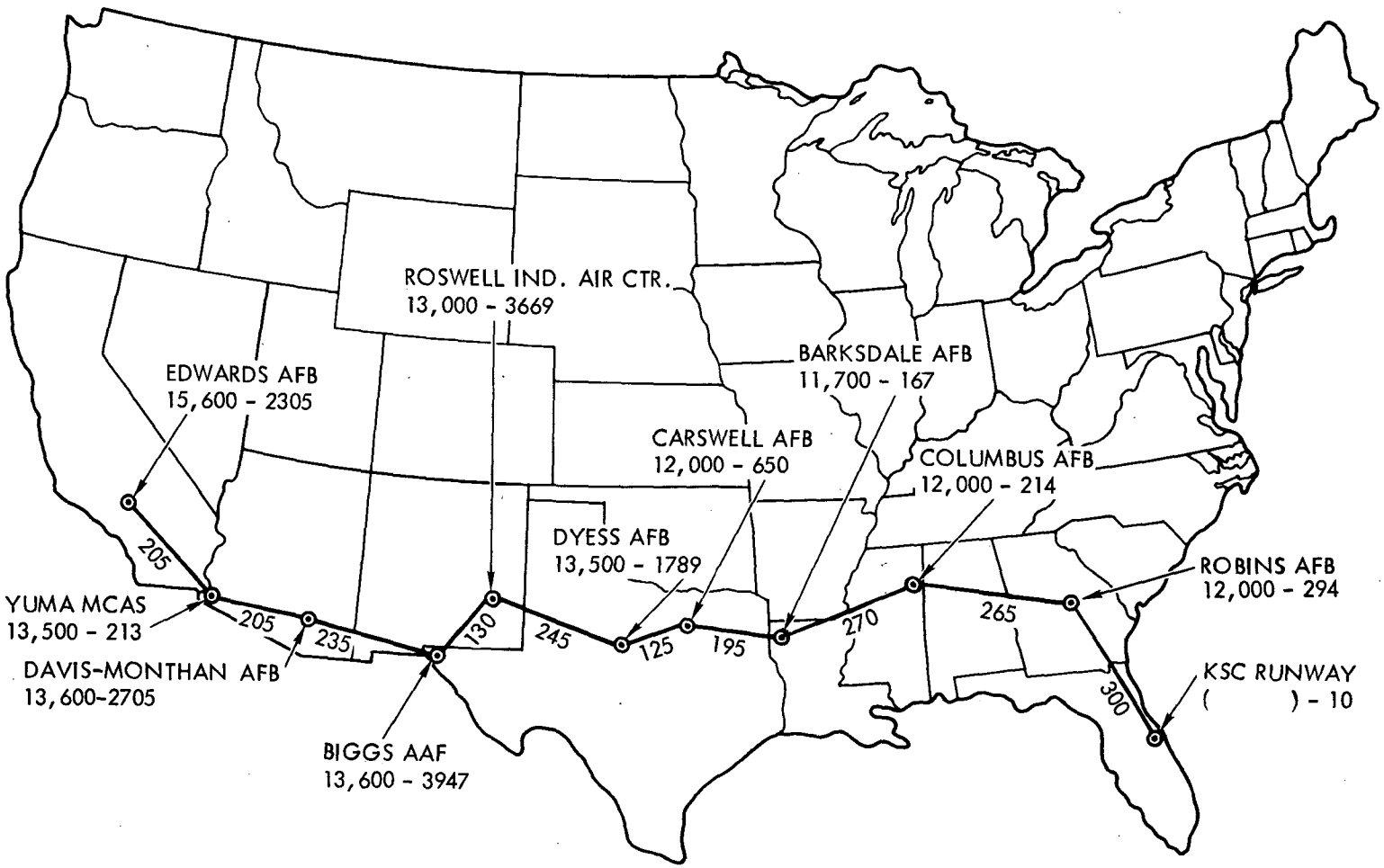

Figure 2-4. Transcontinental Ferry Route

Space Division
North American Rockwell

Figure 2-5. Typical Ferry Mission Profile

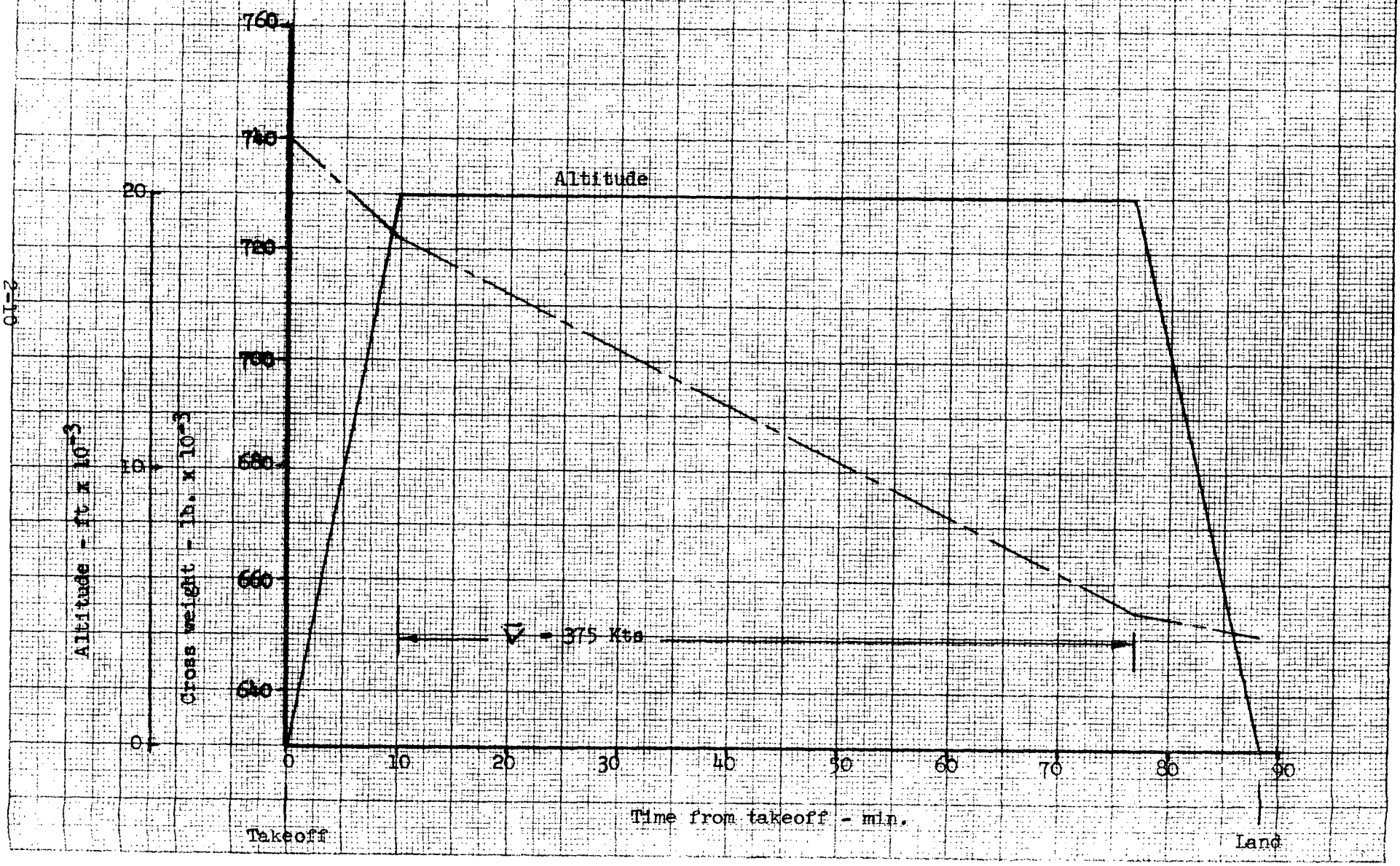

B-9U Ferry Configuration

The B-9U ferry configuration is a modification of the baseline configuration that includes a tail cone which eliminates the blunt base region and improves the aerodynamic efficiency significantly.

Four rocket engines are removed for ferry operations to maintain the required balance. This results in an overall weight reduction of 8000 pounds. For ferry performance calculations, the following range of weights was used:

	Pounds
W_{min}	= 631,828
W_{fuel}	= 143,786
W_{max}	= 775,614

Typical Mission Profile

The characteristics of a typical ferry mission are given in Figure 2-5. These characteristics are based on the following operating modes.

For ferry takeoff the canard is set at $\delta_c = +10$ degrees and control is provided with the elevon. The ground roll attitude is equivalent to an angle of attack of $\alpha = -2.7$ degrees. At sea level under hot day conditions the maximum takeoff gross weight is limited to 724,000 lb for a 10,000-foot runway. At 4000 feet under hot day conditions, the maximum takeoff gross weight is limited to 765,000 lb for a 13,600-foot runway.

Climb performance is based on the air-breathing engines operating at maximum continuous power and the vehicle trimmed at an attitude that results in a maximum rate of climb at a given gross weight and altitude. A cruise altitude of 20,000 feet provides maximum specific ground range. Descent performance is based on operating at $(L/D)_{max}$ with idle power.

2.3 BOOSTER CONFIGURATION

2.3.1 General Arrangement

The booster is shown in three view in Figure 2-6. The layout shows the external shape, major component arrangement, and the overall dimensions of the booster. A perspective cut-away drawing is given in Figure 2-7 which shows the general arrangement and structural configuration.

The B-9U booster is a low, delta wing vehicle with a single vertical tail and a small canard surface mounted forward above the body centerline. The body is basically a cylinder with fairings added to streamline the intersections with the aerodynamic surfaces.

Twelve main liquid-oxygen/liquid-hydrogen (LO_2/LH_2) high-chamber-pressure rocket engines of 550 thousand pounds sea level thrust each are installed in a cruciform pattern in the body base. These engines have an expansion ratio of 35:1 with ±10-degree gimbal provided for thrust vector control. Twelve turbofan engines, used for the subsonic flyback approach and landing, are shown in the extended position below the wing and body.

The landing gear is shown in the down position. The dual-wheel, steerable-nose-gear assembly and the two four-wheel-bogie main landing gear assemblies are of conventional design. The main gear retracts forward in a manner to avoid flow interference with the air-breathing engine inlets.

The crew compartment is conventionally located in the forebody. Visors are used to protect the forward windshields during the boost and entry flights.

Internally the booster is arranged with the LO_2 tank forward and the LH_2 tank aft. The tanks are of aluminum alloy, and they provide the primary load-carrying structure of the booster as well as functioning as pressure vessels. The tank diameter is 33 feet. The tanks are joined by a cylindrical intertank section that supports the canard pivot point and the forward attach links to the orbiter. The aft end of the LH_2 tank picks up the cylindrical thrust skirt, which is also 33 feet in diameter and includes truss-type thrust beams that intersect to form the main engine thrust pad/gimbal support points. The forward end of the LO_2 tank supports a tapered skirt that terminates in a bulkhead that supports the nose landing gear (Station 1339). The main landing gear is supported from trunnion points on external frames attached to the LH_2 tank. All the structural frames are external to the main tanks. The LH_2 tank is internally insulated. The orbiter forward attach points are at the aft LO_2 dome/intertank joint and take the axial loads as well as pitch and side loads, while the aft attach points, which take pitch and sideloads only, are at Station 2666 in the LH_2 tank region (Section C-C). The top of the booster is flat in the stage interface region to fair out the attach frames of the booster and to accommodate the booster linkage after separation.

The outer heat shield provides an aerodynamic surface for the body, which varies from a circular cross section at the nose gear station to a gradually flattening lower surface-transitioning into the wing fillet. The heat shield is also formed to provide the fairing to the fully pivoting canard at Station 2024, as well as the fairing for the orbiter interface. The heat shield is primarily of shallow corrugated frame stiffened panels utilizing Rene' 41 alloy principally, and titanium alloy in the regions of lower aerodynamic heating. The heat shield is supported via links from the primary structure to allow for expansion. The forebody ahead of Station 1479 is supported as an extension of the heat shield itself and moves with it, except for the nose gear that, as previously explained, is supported from an extension skirt on the primary load-carrying LO_2 tank.

The delta wing is mounted below the LH_2 tank. The wing carrythrough spars are reduced in depth in the center section to allow the wing to overlap the tank in the side view and thus minimize base area. The wing

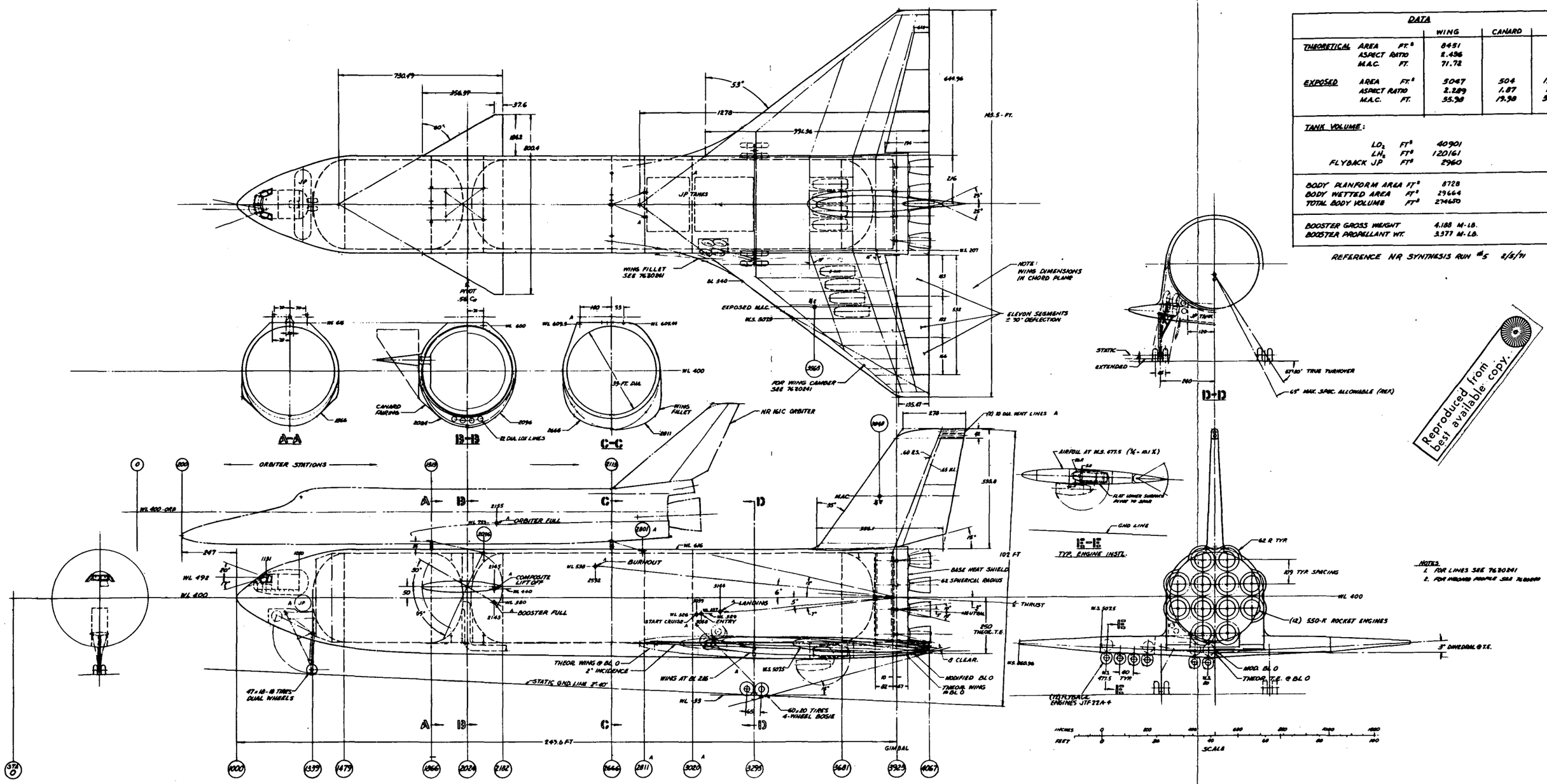

DATA		WING	CANARD	TAIL
THEORETICAL	AREA FT.²	8451		
	ASPECT RATIO	2.496		
	M.A.C. FT.	71.72		
EXPOSED	AREA FT.²	5047	504	1500
	ASPECT RATIO	2.289	1.87	1.28
	M.A.C. FT.	55.38	19.38	36.08

TANK VOLUME:		
LO_2	FT³	40901
LH_2	FT³	120161
FLYBACK JP	FT³	2960

BODY PLANFORM AREA	FT²	8728
BODY WETTED AREA	FT²	29664
TOTAL BODY VOLUME	FT³	274650

BOOSTER GROSS WEIGHT	4.188 M-LB.
BOOSTER PROPELLANT WT.	3.577 M-LB.

REFERENCE NR SYNTHESIS RUN #5 2/5/71

Reproduced from best available copy.

Figure 2-6 . B-9U Booster Basic Configuration Drawing 76Z0140

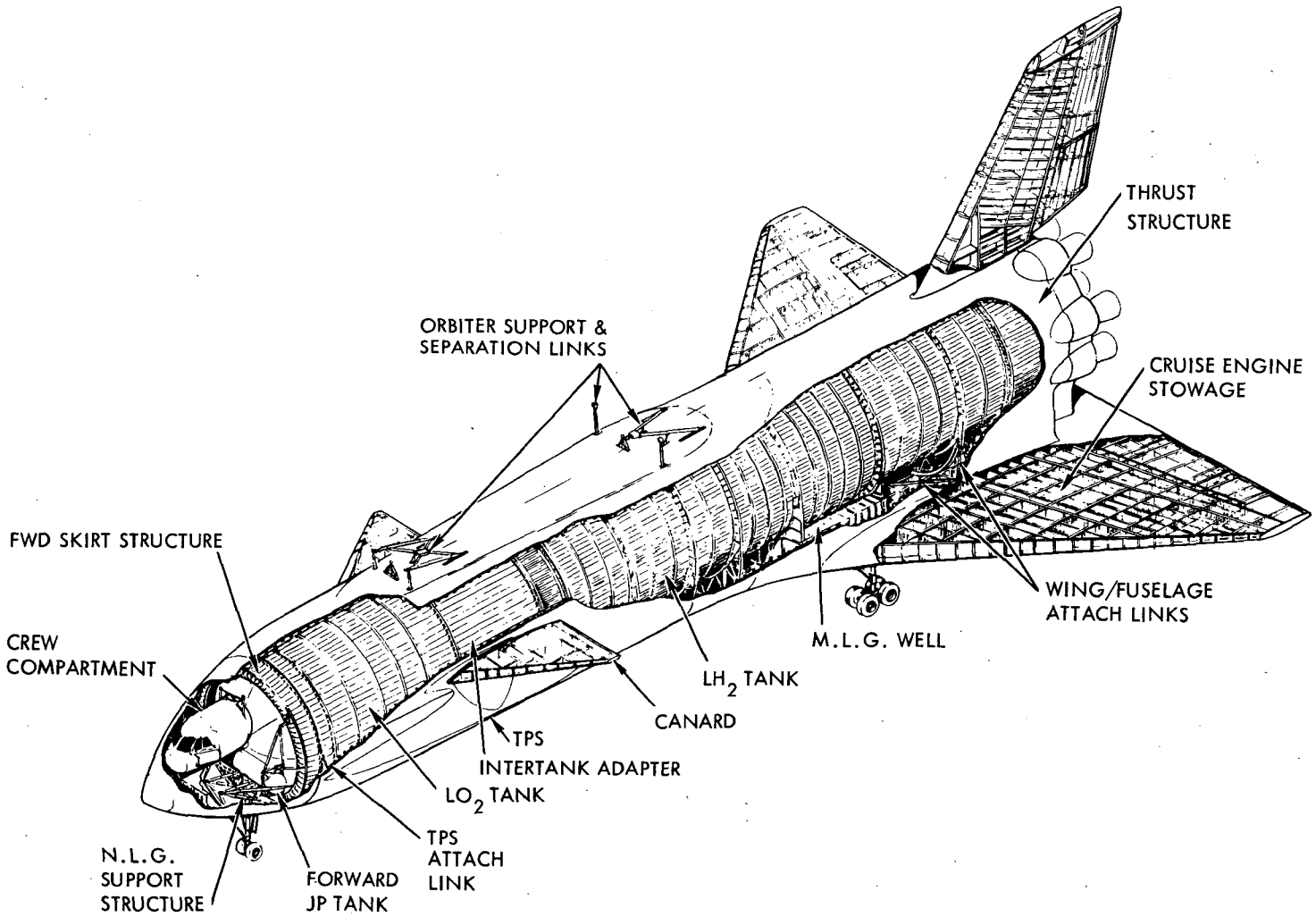

Figure 2-7. Booster Structural Arrangement

Space Division
North American Rockwell

attaches to the hydrogen tank frames and to the thrust structure via a series of links designed to take out relative expansion differentials between the wing and the body.

The delta wing has a theoretical area of 8451 sq ft and an exposed area of 5047 sq ft installed at +2-degree angle of incidence to the body centerline to facilitate cruise and to reduce landing angle within the constraints of the boost loads on the wing. The leading edge sweep is 53 degrees. The installation of the JTF22A-4 air-breathing engines in the wing requires a maximum thickness chord ratio of 10.3 percent at wing Station 507.5 just outboard of the outboard engine. Installation of these engines below the body in the center section requires a 7.1-percent theoretical root thickness at the vehicle centerline. The airfoils are NASA four digit series with modifications to the leading edge radii and with conical camber at the tips to improve L/D. The trailing edge of the wing is perpendicular to the body centerline with elevons segmented into three spanwise parts for varying degrees of control. The wing structure is primarily titanium alloy with two main structural boxes. The forward box accommodates the airbreathing engines. The lower surface of the wing is thermally protected by a system of dynaflex insulation with metallic radiation cover panels.

The vertical tail is located on the body centerline. It has an area of 1500 sq ft with a leading edge sweep of 35 degrees to provide orbiter separation clearance consistent with weight and aerodynamic considerations. The tail thickness varies from 13 percent at the root to 11 percent at the tip. A 35-percent chord rudder is provided with ±25 degrees of travel. The base of the rudder is cut off at 15 degrees to provide clearance for the upper rocket engines. Vent and exhaust lines are terminated at the fin tip trailing edge. The leading edge of the vertical tail has increased material thickness to act as a heat sink during the brief period of plume impingement during orbiter separation.

The canard provides a total exposed area of 504 sq ft. The leading edge sweep is 60 degrees and the thickness is 14 percent. The entire surface is pivoted at 56 percent of the root chord and moves 65 degrees nose down to decouple the effect of the surface during hypersonic entry. The surface wipes a body fairing to maintain a seal at all points along the down travel. This seal is to minimize entry heating. Upward travel of the leading edge of the canard is 30 degrees.

The main landing gear retracts forward into the wing fillet region. The main gear bogies incorporate 60-inch x 20-inch 40 PR tires. The nose gear has dual 47 x 18 tires.

Four main LO_2 lines are routed through the lower body main structure/heat shield interspace, past the main landing gear and aft to the vehicle base.

The outboard rocket engine powerhead packages are protected by local fairings tailored to keep the base area reduced to a minimum. A base heat shield is provided across the entire base station in the plane of the engine throats.

The crew compartment is conventionally located. Swivel seats adjustable for the vertical flight, entry, and cruise flight are provided for the captain and co-pilot, in conventional locations. The crew compartment is pressurized for shirtsleeve environment. Heat shields are provided over the windshields, which are sized for adequate landing visibility at the maximum 15-degree touchdown angle. Access with the booster in the vertical position is via a door to the left of the pilot seat. Access with the booster in the horizontal position is via a door in the compartment floor reached through the nose-gear wheel well. Aft of the crew compartment are the booster avionics systems installed in a controlled environment but separate from the crew compartment. Below the crew and avionics compartments is the nose-gear wheel well. The attitude control propulsion system (ACPS) engines are installed at Station 1300, eight on each side for yaw and four on top for pitchdown. (Pitchup and roll are provided by five engines on each wing.) The ACPS engines use LO_2/LH_2 propellants and deliver 2100 pounds of vacuum thrust each.

The flyback JP fuel is contained, as shown, in two compartments under the body between the main landing gears and in a tank in the nose. The fuel is fed to the four JTF22A-4 airbreathing engines under the body at Station 3560 and to the four similar engines in each wing.

Four auxiliary power units are installed in the wing root and ahead of the airbreathing engine bays and are accessible through doors in the wing upper surface.

The airbreathing engines are installed in podded configurations, pivoted at the aft support point. Each engine assembly has its own deployment rotary actuators. Longitudinal doors in the lower surface open to allow deployment of the airbreathing engines to the subsonic cruise position. The engines rotate through 180 degrees to the locked-extended position. Upon engine deployment the engine bay doors close to present a clean surface for cruise and landing.

2.3.2 Body Structure

The load-carrying body structure consists of five component assemblies which are bolted together to comprise the assembled structure. They are:

1. Forward skirt structure.
2. Liquid oxygen tank.
3. Intertank adapter.
4. Liquid hydrogen tank.
5. Thrust structure and base heat shield.

All of the components, except the thrust structure, are fabricated from aluminum alloy. The thrust structure is built of titanium and utilizes boron-aluminum composite materials for selected structural elements to

reduce weight and to increase stiffness. The base heat shield is coated columbium and Rene' 41. Its supporting structure uses titanium, Rene' 41 and tubular members of beryllium.

The wing (including the airbreathing engines), vertical stabilizer, canard surfaces, nose landing gear, rocket engines and the orbiter are attached to the basic body structure. The body is a "cold" structure while the aerodynamic surfaces are "hot" structure. Attachment method allows for thermal expansion of the hot structures with minimum restraint from the body. This is accomplished by the use of axially loaded links in correct number and orientation to carry all load combinations. All links contain mono-ball end fittings to preclude lateral restraint.

The enveloping body thermal protection system is a "hot" structure and is attached to the body structure by a series of fixed and linked connections. Air loads and inertia loads from the thermal protection system shells are applied to the body structure through these connections. The crew compartment is integrated with the forward segment of the body thermal protection system.

Forward Skirt

The forward skirt structure is shown in Figure 2-8. It consists of two stiffened aluminum alloy shells, one a short cylindrical section, the other a short conical section, and machined aluminum alloy frames. A circumferential pattern of tension bolts at the skirt's aft edge attaches it to the forward end of the liquid oxygen tank. The main trunnion of the nose landing gear is supported by the forward frame and a truss arrangement of tubes supports the upper end of the landing gear drag strut from the two frames. Vertical and side loads from the nose gear are introduced into the shell by the two frames. Longitudinal loads are introduced directly into the shell by back-up members behind the main trunnions. Sheet metal frames stabilize the skin/stringer shell between the machined load-introduction frames.

A cylindrical JP fuel tank is supported from the forward frame of the skirt. Vertical support loads are passed to the skirt shell through the deepened lower segment of the frame; longitudinal loads are carried to suitable stiffeners on the shell skin. Side load brace tubes are provided at each end of the tank.

The most forward attachment of the thermal protection system is also made through the skirt structure. Vertical links on each side and rollers, in tracks, at the top and bottom carry vertical and lateral reactions from the thermal protection system into the shell. There is no longitudinal restraint for the thermal protection system at this station.

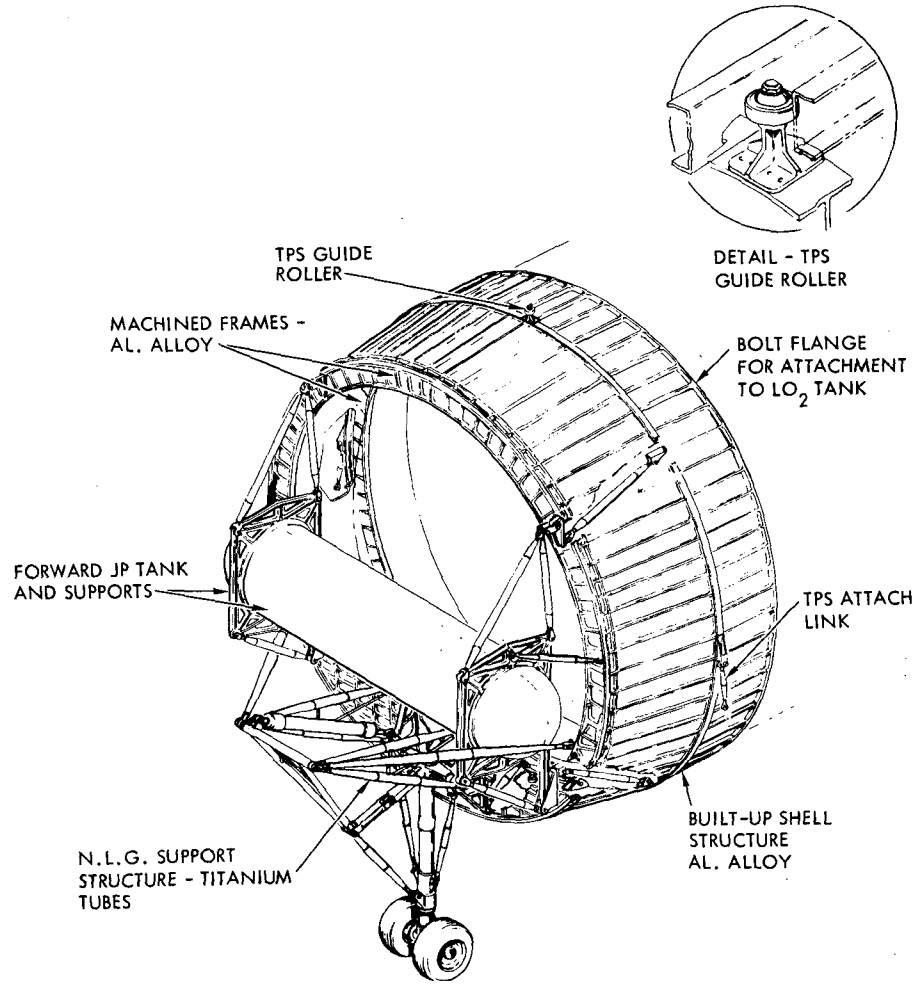

Figure 2-8. Forward Skirt Structure

LOX Tank

The liquid oxygen tank is designed largely by internal pressure resulting from the high density of the oxidizer and the axial accelerations of the vehicle. Bending moments are not as great as those further aft in the liquid hydrogen tank.

The oxygen tank is a welded assembly of 2219T87 aluminum alloy with forward and aft circumferential bolt patterns for joining it to the forward skirt and to the intertank adapter structures. Tank wall segments, with integral stringers, are milled from aluminum alloy plates, age formed to radius and buttwelded together to make the cylindrical tank section.

End bulkheads are ellipsoidal ($\sqrt{2}$ diameter ratio) consisting of gores edge-welded together. The bulkheads are welded to the ends of the cylindrical section. Pressurization inlet and vent ports are provided. An access door is installed in the forward dome. A cylindrical sump, from which four liquid oxygen ducts lead to the main propulsion system, is incorporated in the aft dome.

Stabilizing frames, external to the tank, are spaced at 77-inch intervals. The frames are built up of a series of V forgings riveted between an outboard T flange and the longitudinal stringers of the tank. The V's, in conjunction with the outboard flange and the tank wall, form a truss-webbed stabilizing frame. The frame is shown in detail in Figure 2-9.

Since the temperature of liquid oxygen will not liquefy air on the tank's exterior, no cryogenic insulation is installed.

The forward orbiter attachment station is at the tangency of the ellipsoidal dome with the cylindrical section of the oxygen tank. A machined aluminum alloy internal/external bulkhead is integrated with the tank wall at this station. To achieve maximum bulkhead depth, part of the bulkhead extends beyond the tank skin to support the forward orbiter attachment links. A projecting section of bulkhead, on each side of the booster, provides for two attachments between the booster and the launch tower. The tower supports the booster during high wind conditions and reduces body bending.

Intertank Adapter Structure

The intertank adapter is a shell structure with a circumferential bolt pattern at each end to match those on the aft end of the oxygen tank and on the forward end of the hydrogen tank. It is of aluminum alloy construction consisting of integrally stiffened skins and six frames. It is a mechanically fastened structure since liquid containment is not required. In addition to carrying body bending loads, orbiter longitudinal loads are transmitted to the booster via the intertank adapter. See Figure 2-10.

The forward pair of orbiter launch links, which are also the orbiter attachment drag struts, are hinged to a longitudinal fitting on each side of the intertank structure. The forward and aft ends of the fitting are supported by frames approximately 144 inches apart.

A webbed external bulkhead extends from the intertank shell to the inboard side of the thermal protection system and forms one of the fixed supports for the TPS. In addition, the bulkhead serves as a purge system barrier in the annular space between the shell wall and the TPS.

Two independent canard surfaces are supported by the intertank structure. The canard spindle extends inboard through the adapter skin and is supported by a pair of large diameter bearings, one outboard and

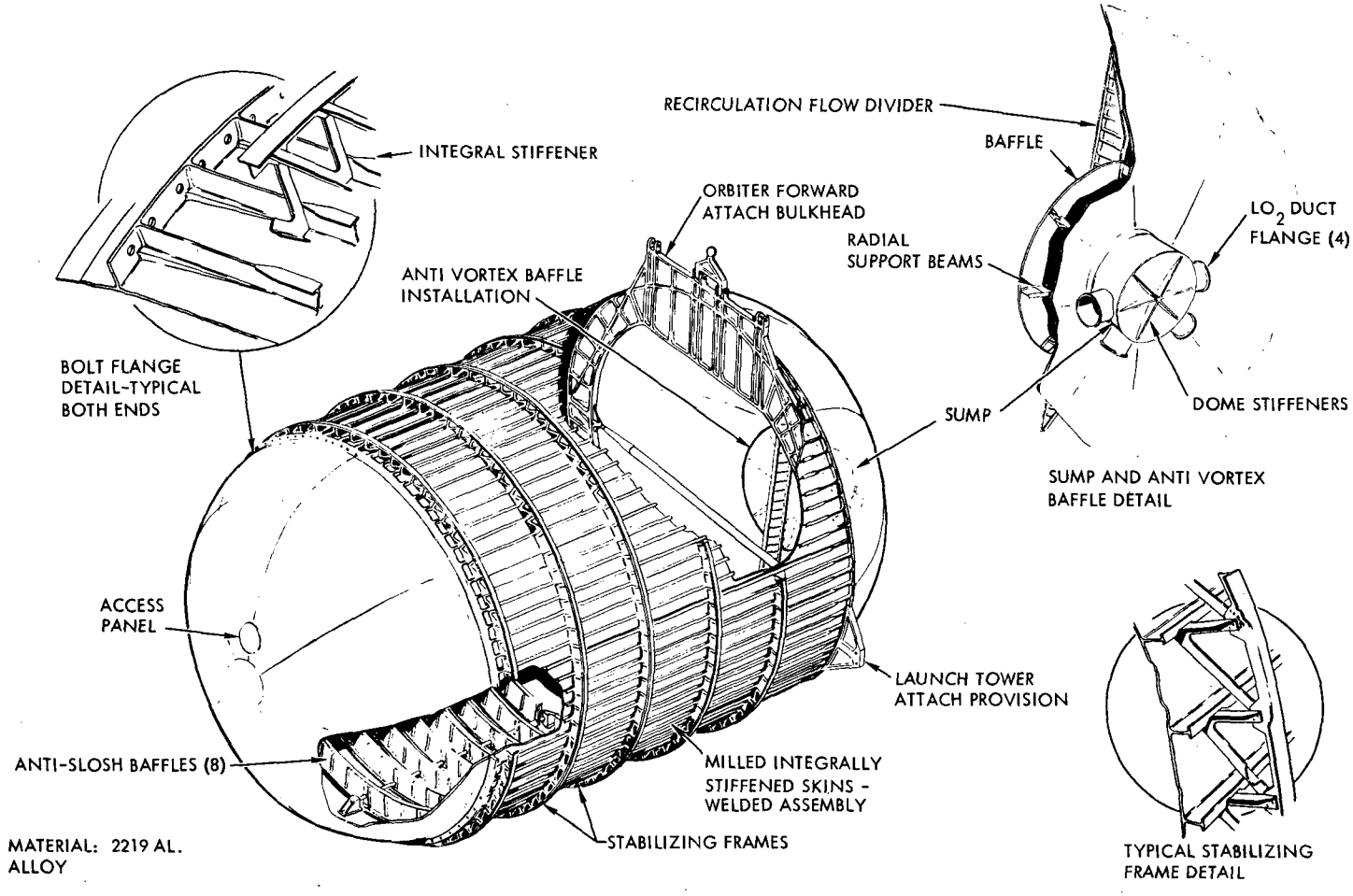

Figure 2-9. Liquid Oxygen Tank

Space Division
North American Rockwell

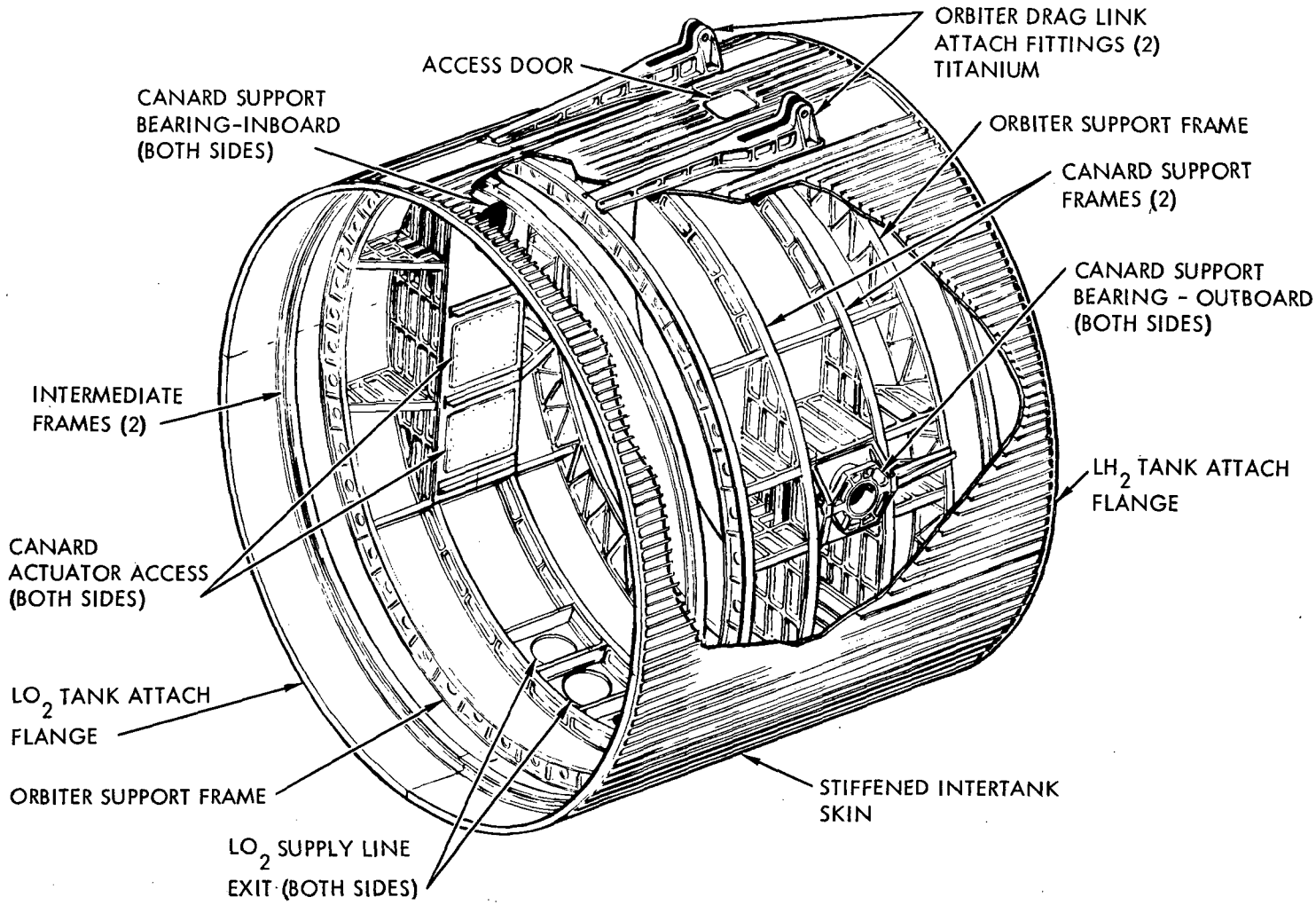

Figure 2-10. Intertank Adapter Structure

Space Division
North American Rockwell

one inboard. The bearing housings are supported between a pair of frames inside the intertank structure. The hydraulic actuator cylinders are also supported by the frames.

The liquid oxygen ducts pass through the skin of the intertank adapter near the bottom of the vehicle and are routed aft between the body structure and the thermal protection system.

LH_2 Tank

The liquid hydrogen tank is shown in Figure 2-11. In construction it is similar to the liquid oxygen tank though the integral T-section stringers are more closely spaced to develop higher compression allowables. Polyphenylene oxide foam bonded to the inside of the tank wall provides cryogenic insulation and prevents condensation of liquid air on the exterior surface.

External tank stabilizing frames are of the built-up type described for the liquid oxygen tank.

An access door is provided in the forward bulkhead of the liquid hydrogen tank.

The orbiter aft support links and the aft separation system links are attached to the tank shell through two external frames machined from 2219 aluminum alloy plate. A circumferential band of thickened tank skin forms the inboard flange for each of these frames; the skin band also incorporates a vertical circumferential rib. A frame web/circumferential rib weld completes the frame installation. All tank frames for the introduction of concentrated loads into the tank shell are of similar construction.

Wing attachment is made by three vertical links and one longitudinal drag link on each side of the body. Three lateral load links also attach the wing to the tank and to the thrust structure. The links contain spherical bearings at each end and carry only axial loads. The wing is able to deflect under load and temperature gradients with minimal restraint from the fuselage.

Thrust Structure and Base Heat Shield

The thrust structure is a stiffened shell and is bolted to the aft end of the liquid hydrogen tank. It contains two transverse trussed-type bulkheads spaced 82 inches apart. These bulkheads distribute loads into the shell structure from the vertical stabilizer, the aft wing attachment struts, and the gimballed rocket engines. Trusses in longitudinal planes between the bulkheads comprise four thrust beams to which the rocket engines are attached. See Figure 2-12.

Intermediate circumferential frames stabilize the shell.

Four fittings, external to the thrust structure shell, support the booster/orbiter in the vertical launch position.

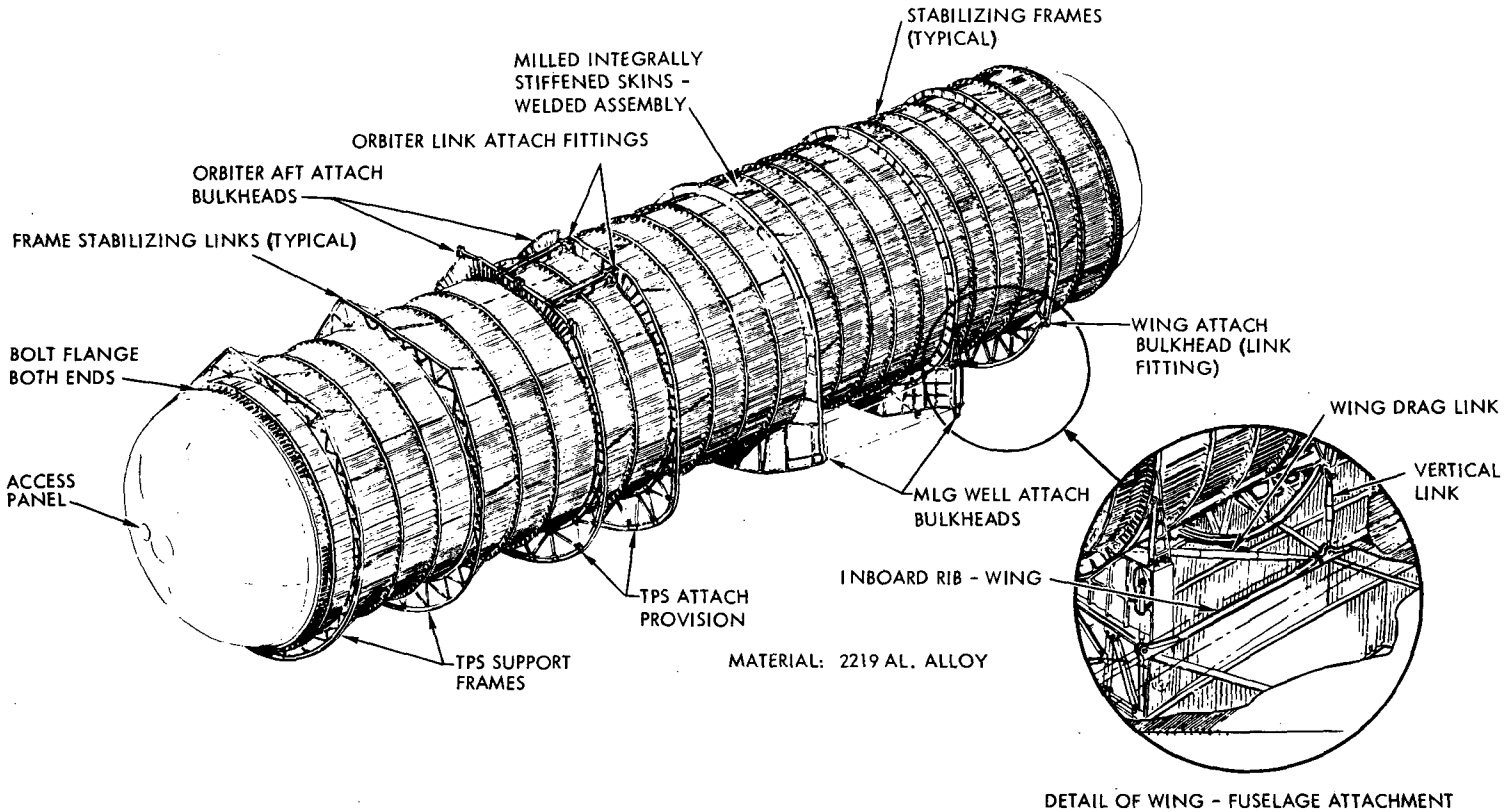

Figure 2-11. Liquid Hydrogen Tank

Space Division
North American Rockwell

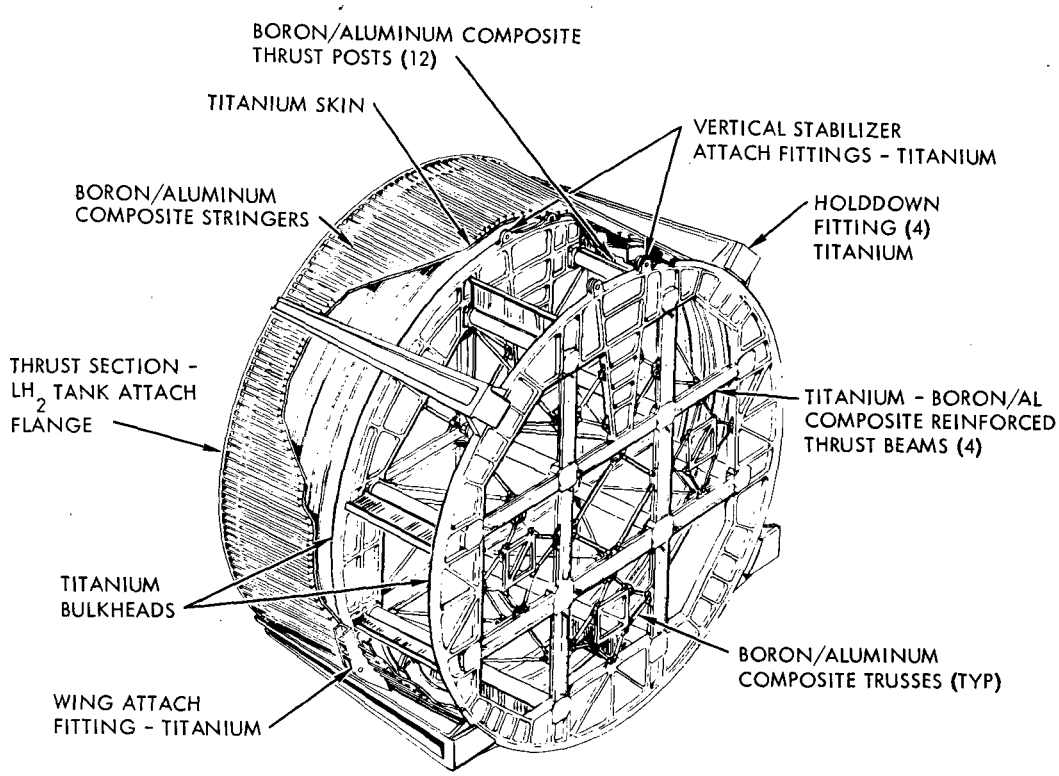

Figure 2-12. Thrust Structure

Spherical segments are installed on each rocket engine to provide a sealing surface for deflected engine positions. A mating ring and seal for each engine is supported from the aft structural bulkhead of the thrust structure. A heat shield consisting of corrugated panels and backed by insulation material is installed between and supported from the seal rings. The circumference of the base heat shield is defined by the rocket engine fairings. The skin extending forward of the base heat shield is part of the body thermal protection system.

Crew Compartment

Figure 2-13 illustrates the general structural arrangement of the crew compartment. It is a semi-monocoque structure incorporating rings and longitudinal stringers. Where possible, the structure is installed on the skin exterior. There are four openings in the structure: the windshield, the aft compartment access hatch, and two hatches opposite the pilots seats. The module consists of two compartments, the pilots station and the electronics compartment. These compartments are separated by an internal bulkhead. The aft end of the module is closed by an ellipsoidal bulkhead. The electronic compartment is cylindrical in section while the crew compartment is faired to maintain as much curvature as is compatible with the hot nose structure contour and internal furnishing envelope.

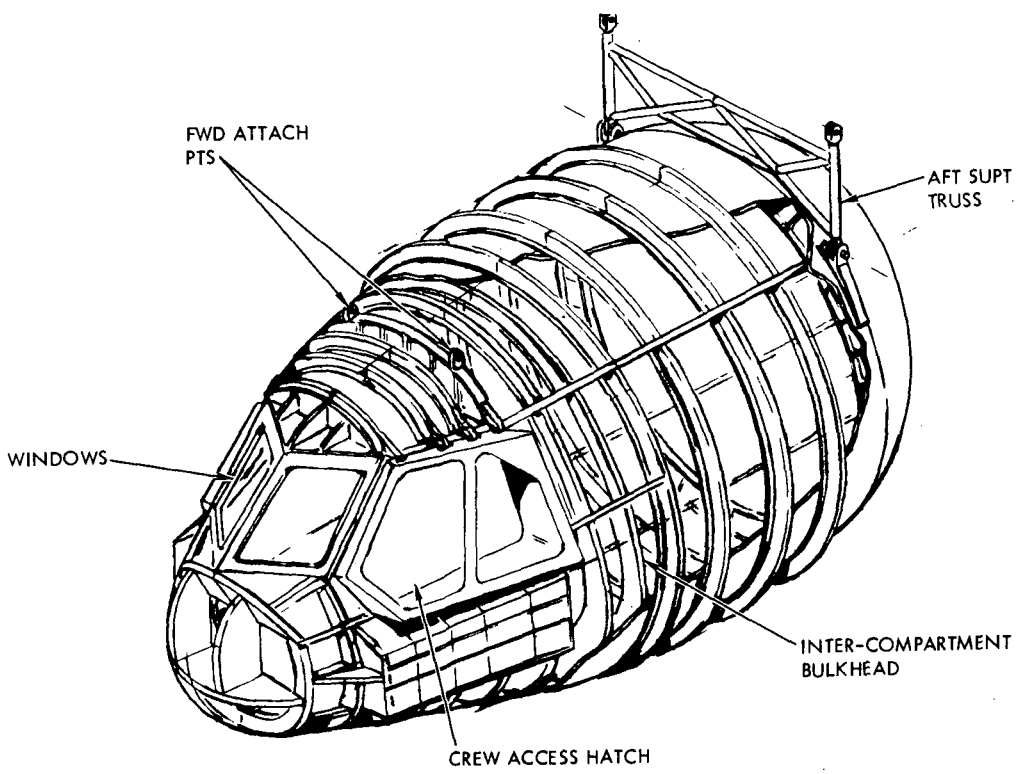

Figure 2-13. Crew Compartment

The compartment is supported by the hot nose shell structure at four points: at two points just aft of the crew compartment hatch and at two points on the frame at end of the electronics compartment. The gap between the nose structure and the crew compartment at the aft support is spanned by a pin ended truss. This truss will minimize thermal loads on both the nose structure and the compartment structure as the outer shell expands.

The structural material of the crew compartment is aluminum alloy except in those areas where the hot nose structure is in close proximity to the compartment structure. In these regions, such as the windshield frame and the pilot's hatches, the structure will be fabricated from 6 Al-4V titanium alloy. With the exception of the glazed areas the entire compartment is shrouded by a fibrous insulation blanket. The inner door windows are fabricated from heat tempered glass. The outer door windows are made from fused silica glass. The windshield is a laminated glass with an electrically conductive film for anti-icing. The floor and the bulkhead separating the electronics compartment from the crew station consist of aluminum alloy honeycomb panels backed up by a grid work of beams.

2.3.3 Aerodynamic Surfaces

Wing

The wing structure is shown in Figure 2-14. The wing structural arrangement is a fail-safe multi-spar, multi-rib configuration utilizing open corrugation cover panels on the upper surface and a thermally protected lower surface. The corrugations are positioned in a chordwise direction to minimize thermal stresses by accommodating skin expansion relative to the spar caps. The covers transmit air loads to the spars and reacts wing torsional loads. The wing has a hot leading edge, two primary structural boxes, an under-body carry-through and trailing edge elevons. Titanium alloy 6 Al-4V is used for the wing box structure. Boost phase venting is accommodated through the gap between the elevon and the fixed trailing edge upper surface. The wing inboard closing bulkhead redistributes spar shear loads to wing-to-body support fittings and the wing loads are reacted to the body through wing-to-body attach links. The corrugated bulkhead shear web allows for differential chordwise thermal expansion and the attach links accommodate wing deflection and relative thermal expansion between wing and body. Twelve flyback airbreathing engines are submerged in the wing structure during boost and recovery and are deployed for subsonic cruise and landing.

The main JP fuel tank is located just forward of the wing carry-through structure between the body TPS and the LH_2 tank. The JP tank is supported from the LH_2 tank and the MLG support structure and is protected by the TPS. The tank is constructed of aluminum alloy honeycomb sandwich panels with aluminum ribs and beams.

Canard

The canard structure is shown in Figure 2-15. The canard is a fully movable surface. The structural box is a multi-spar, multi-rib configuration

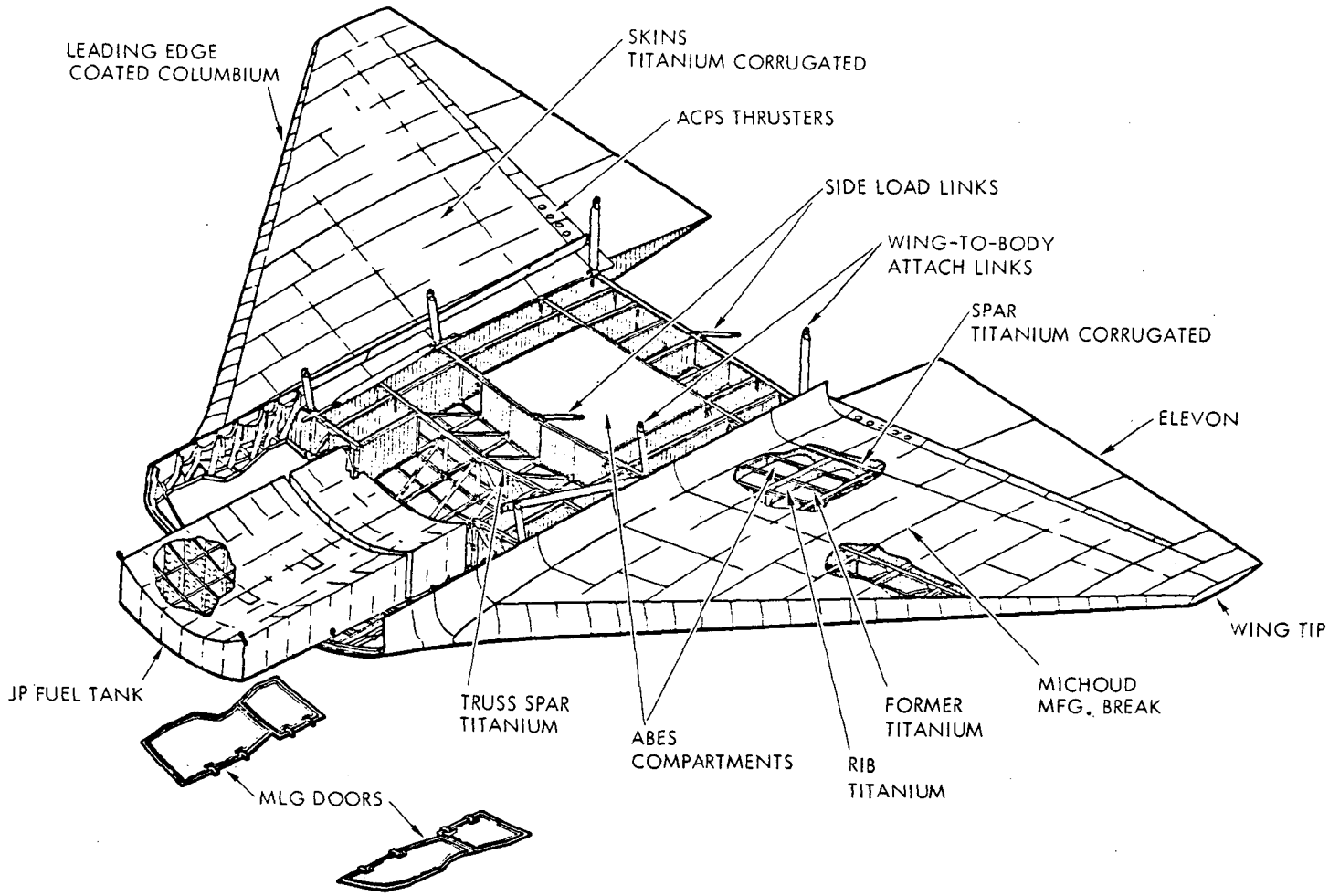

Figure 2-14. Wing Arrangement and Support Points

Space Division
North American Rockwell

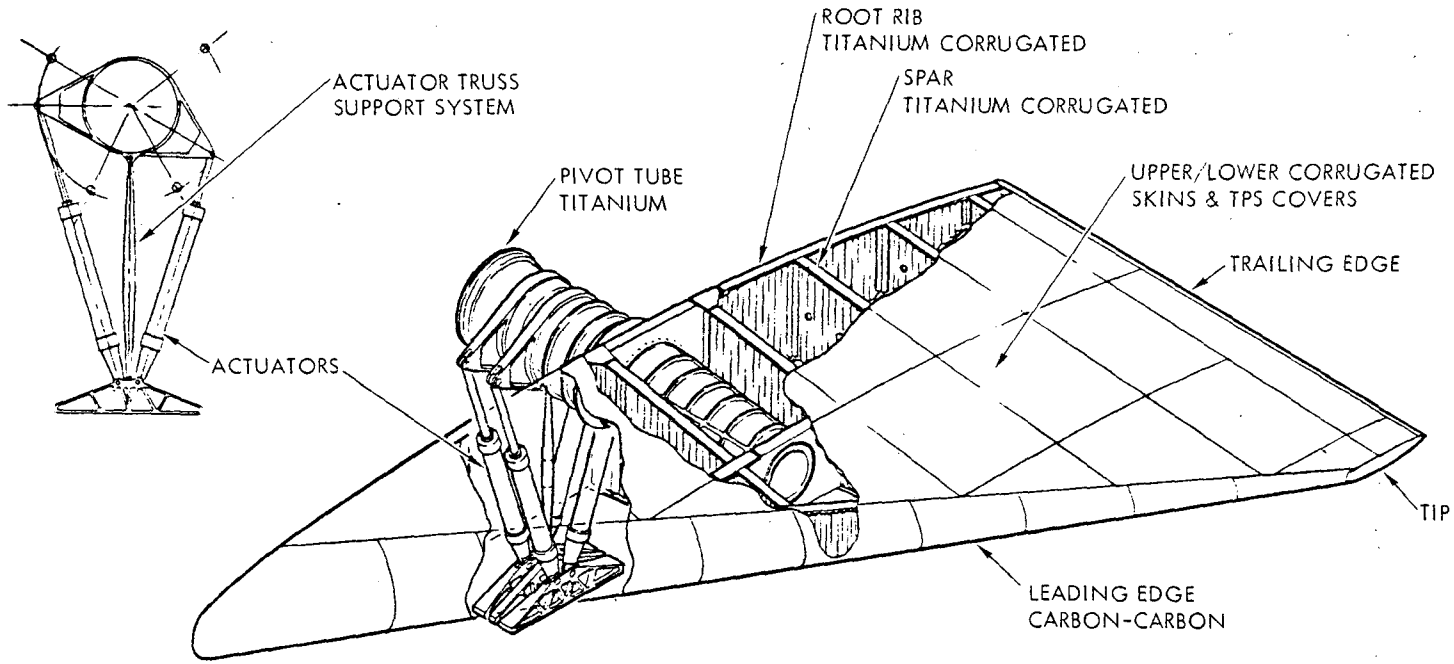

SUBSTRUCTURE SKIN & INTERNAL STRUCTURE - TITANIUM

UPPER & LOWER SURFACE TPS OUTER SKIN - RENE 41

Figure 2-15. Canard Structure

Space Division
North American Rockwell

with corrugated titanium structural skins supported on a welded, corrugated shear web substructure. The structural skins are protected with a TPS. The TPS consists of an insulation material and a semi-smooth outer skin supported from the structural skin by standoffs. The corrugated shear webs of the spars and ribs accommodate differential thermal expansion. A slotted-hinge leading edge is used to allow for spanwise thermal expansion relative to the front spar. The structural box is fixed to a pivot tube at the inboard rib. The outboard pivot tube/rib attachment is a sliding joint to accommodate differential thermal expansion between the pivot tube and the outer surfaces. Bending loads are carried through the pivot tube and reacted through two bearings supported in the intertank structure. Spherical self-aligning bearings are employed to allow for structural deflections. Venting is accommodated through the pivot tube into the intertank structure and then through the body vent ports.

Vertical Stabilizer

The vertical stabilizer structure is shown in Figure 2-16. The vertical stabilizer structural arrangement is a three-spar, multi-rib configuration with integrally stiffened skin/stringer panels. Spar and rib webs are of corrugated or trussed construction to allow for differential thermal expansion. The rudder is of similar construction. The entire structure is 6 Al-4V titanium except for the leading edge which is Rene' 41. The segment of leading edge that is subjected to the orbiter engine exhaust impingement is "heat sink" designed to withstand the increased temperature. Vertical stabilizer bending loads are reacted through spar-to-thrust-structure attach fittings at the center and rear spar. Torsional loads are reacted at the front spar pin joint and the rear spar attach fittings. The APU exhaust and the hydrogen vent lines are vented at the vertical stabilizer tip.

2.3.4 Body Thermal Protection System (TPS)

Figure 2-17 depicts an overall view of the baseline TPS adopted for the body of the booster. The TPS is a metallic radiative system which protects the load carrying primary structure to a peak temperature compatible with the aluminum structural material and the LH_2 tank insulation. No insulation is required to accomplish this. The TPS concept consists essentially of a separate stiffened shell that completely surrounds the basic primary structure. Support of the TPS shell from the primary structure is effected by two means. At each of three body stations, 2096, 2458, and 2811, the shell is rigidly attached around the periphery by mechanical fastening of the shell skin to the outer flanges of deep external primary structure frames. These attachments provide restraint of the TPS shell in all three axes. The restraint locations are selected to minimize thermal displacement of the shell relative to the canard pivot and the orbiter attachment fittings. The other method of support, in addition to the fixed supports, consists of a system of swinging links which attach the TPS shell to the primary structure and permit relative thermal growth longitudinally between these components. Forward of the fixed restraint at Station 2096, the entire forward section of the shell, including the hot nose structure, is free to expand longitudinally relative to the body primary structure. Support is provided by a link arrangement at Station 1423. The TPS shell

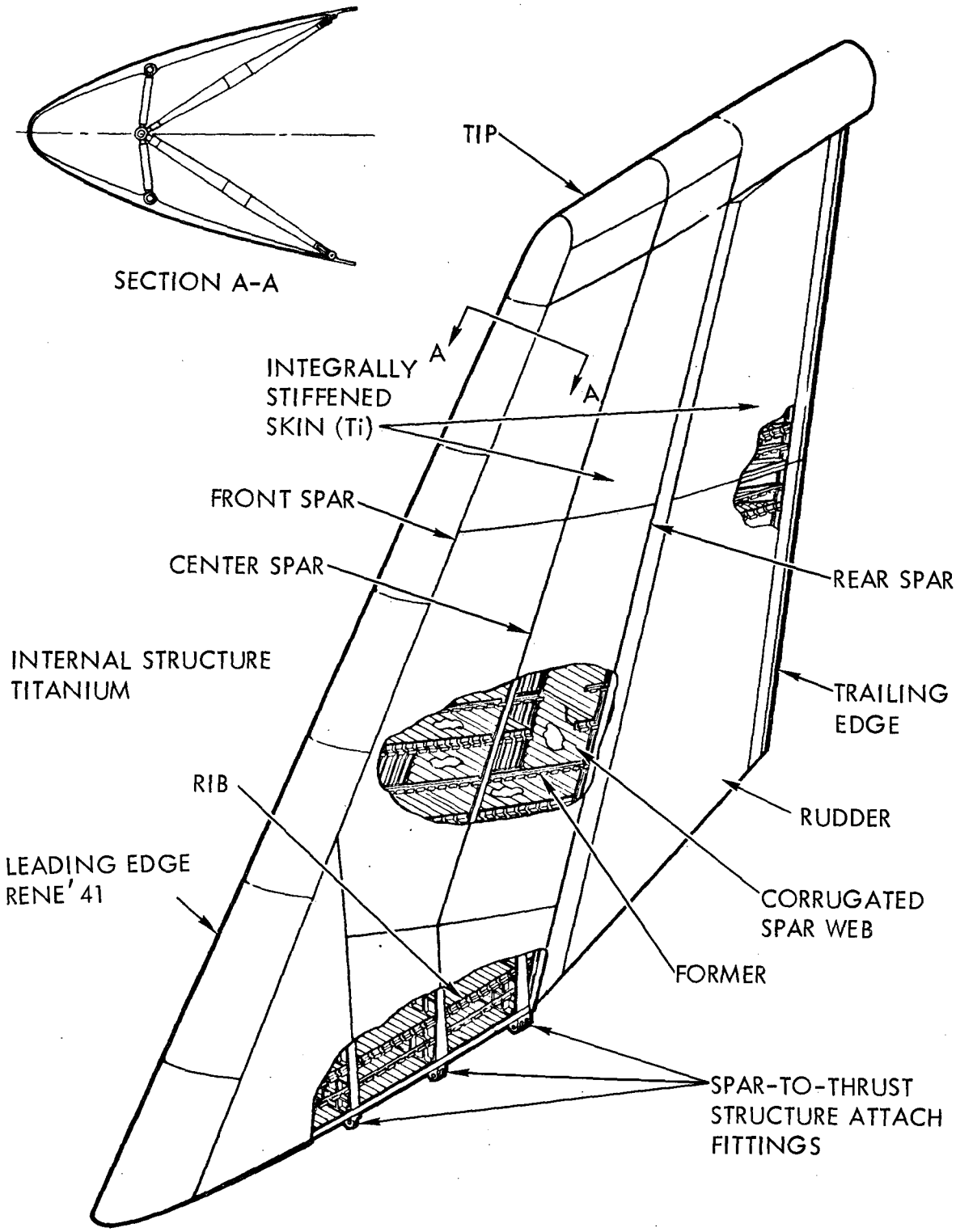

Figure 2-16. Vertical Stabilizer

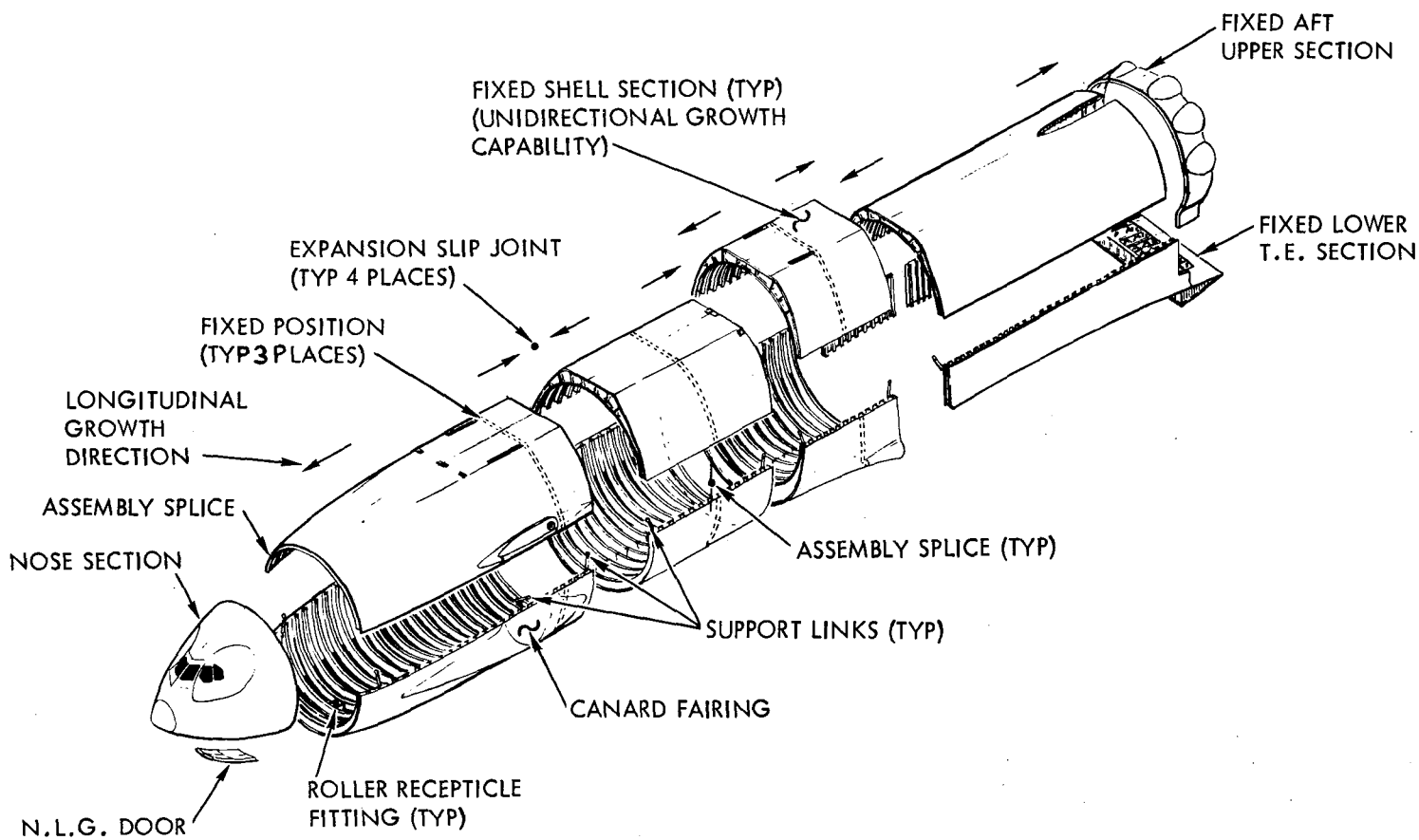

Figure 2-17. Body TPS Shell Structure

Space Division
North American Rockwell

section over the wing is supported by the wing and is free to expand with the wing. Between the fixed stations, peripheral slip joints accommodate displacements due to the thermal expansion of the shell and the cryogenic contraction of the propellant tanks. Swinging links provide support for the free end of each section of the shell at each slip joint.

Each TPS shell section is essentially a frame-supported semimonocoque structure with open corrugation-stiffened skins. The primary loading on this shell structure is the lower surface air pressure induced by the hypersonic pull-out condition during booster recovery. The panel loads induced by this pressure are transmitted by the TPS frames to shear into the side walls of the shell and to be finally transmitted to the body primary structure by the system of fixed and link supports.

The TPS frames are stiffness critical since excessive in-plane deflection would cause interference with the propellant tank structure and subsystem components. A design that incorporates a material of high specific elastic modulus has therefore been adopted. The basic cross-section of the frame is an I section of aluminum, pocket milled to minimize web gages and to provide integral web stiffeners. To each cap of the aluminum section is attached a cap strip of beryllium to produce a frame design of high stiffness to weight ratio. The high specific heat of beryllium is also advantageous in that the beryllium strip adjacent to the hot outer skin provides a heat sink to absorb the "flash heating" effect characteristic of booster recovery and thereby create an acceptable temperature distribution through the frame.

The outer skin of the TPS shell features open corrugations to provide longitudinal stiffening and to accommodate circumferential thermal expansion relative to the cooler frames by flexing of the corrugations. Attachment of the corrugated skin to the frames is by mechanical fasteners in each of the "valleys" of the corrugation.

The TPS shell sections are further broken down into conveniently sized panel assemblies by the provision of bolted splices. This arrangement facilitates panel production, simplifies assembly, and allows periodic "in service" removal of individual panels for inspection and repair of the underlying structure and subsystems. As previously noted, individual skin panels within the panel assemblies are mechanically attached, a feature that will permit easy replacement or repair in service. In addition to these provisions, quick-open access panels will be located where required for the routine maintenance of subsystems.

2.3.5 Weight Summary

A summary weight statement for the B-9U booster is given in Table 2-2. Detail weight breakdowns for the wing group, vertical tail group, and body group are given in Tables 2-3, 2-4, and 2-5, respectively. All weight data are taken from Reference 2.

Table 2-2. B-9U Booster Weight Summary

		Weight (lbs)
Wing Group		70,875
Tail Group		20,634
Vertical Tail	13,121	
Canard	7,513	
Body Group		177,612
LH_2 Tank	67,109	
LO_2 Tank	18,405	
Thrust Structure	30,000	
Other Body Structure	62,098	
Induced Environmental Protection		72,031
Landing, Docking		27,361
Propulsion, Ascent		130,038
Propulsion, Cruise		46,404
Propulsion, Auxiliary		9,864
Prime Power		3,011
Electrical Conversion and Distribution		1,438
Hydraulic Conversion and Distribution		1,862
Surface Controls		7,889
Avionics		5,468
Environmental Control		1,475
Personnel Provision		985
Contingency		49,593
SUBTOTAL (DRY WEIGHT)		626,540
Personnel		476
Residual Fluids		11,534
SUBTOTAL (INERT WEIGHT)		638,550
Inflight Losses		22,080
Propellant - Ascent		3,382,307
Propellant - Cruise		143,786
Propellant - Maneuver and ACS		1,500
TOTAL BOOSTER WEIGHT AT LIFTOFF		4,188,223

Table 2-3. B-9U Booster Wing Group Weight Breakdown

	Weight (lbs)		
Exposed Wing			54,203
Structural Box		29,469	
Spars		14,550	
Webs	4,176		
Caps	6,868		
Splices	3,506		
Ribs		5,156	
Webs	3,512		
Caps	1,644		
Upper Covers		5,360	
Covers	4,378		
Formers	982		
Lower Covers		4,403	
Covers	2,558		
Formers	764		
Engine Bay Formers	1,081		
Leading Edge		3,996	
Trailing Edge		681	
Secondary Structure		11,678	
Thermal Protection Skins, Insulation, and Standoffs		8,122	
Fairings - Wing to Fuselage		1,000	
Engine Bay Doors		2,108	
Door Actuation		448	
Elevons		8,379	

Table 2-3. B-9U Booster Wing Group Weight Breakdown (continued)

	Weight (lbs)			
Wing Carry-Through Structure				16,672
Structural Box			15,450	
Spars		9,073		
Webs	1,669			
Caps	7,404			
Ribs		4,333		
Webs	2,498			
Caps	1,835			
Lower Covers		1,650		
Covers	818			
Formers	292			
Engine Bay Formers	540			
Wing to Fuselage Attach Fittings		394		
Leading Edge			622	
Secondary Structure			600	
Wing to Fuselage Attach Links		600		
TOTAL WING GROUP WEIGHT				70,875

NOTE: The wing carry-through lower surface coverings and doors blanked out by the fuselage act as body heat shield structure; therefore, their weights have been included under Induced Environmental Protection. The items allocated to Induced Environmental Protection include:

Belly Skins, Insulation, and Standoffs	3,765
Engine Bay Doors	1,054
Main Landing Gear Doors	2,108
Total	6,927

Table 2-4. B-9U Booster Vertical Tail Group Weight Breakdown

	Weight (lbs)		
Structural Box			9,301
Spar Caps		779	
Front	49		
Intermediate	351		
Rear	338		
Auxiliary	41		
Spar Webs		1,249	
Front	146		
Intermediate	443		
Rear	464		
Auxiliary	196		
Ribs and Bulkheads		1,485	
Root Rib	271		
Interspar Ribs	379		
Bulkheads	835		
Chordwise Stiffeners		567	
Covers		4,517	
Hinge Fittings (Integral with Spars)		168	
Tail to Fuselage Attach Fittings and Fasteners		536	
Leading Edge			866
Covers		292	
Trusses and Supports		574	
Trailing Edge			316
Covers		235	
Stiffeners		30	
Ribs		51	
Tip			509
Rudder			2,129
TOTAL VERTICAL TAIL GROUP WEIGHT			13,121

Table 2-5. B-9U Booster Body Group Weight Breakdown

	Weight (lbs)		
Main LH_2 Tank			67,109
Forward Dome		1,947	
Aft Dome		1,947	
Barrel Section		57,290	
Skin-Stiffeners	52,658		
Frames	4,632		
Baffles		575	
Orbiter Attach Structure		5,350	
Forward Bulkhead	1,650		
Aft Bulkhead	800		
Load Distribution (weight required for)	2,900		
LH_2 Tank Internal Insulation (PPO Foam)			7,168
Main LO_2 Tank			18,405
Forward Dome		1,405	
Aft Dome		2,902	
Barrel Section		9,583	
Skin-Stiffeners	9,138		
Frames	445		
Baffles		1,200	
Orbiter Attach Structure		3,315	
Forward Bulkhead	2,690		
Load Distribution (weight required for)	625		

Table 2-5. B-9U Booster Body Group Weight Breakdown
(Continued)

	Weight (lbs)	
Nose Section		10,135
Forward Adapter Section		3,652
Intertank Basic Structure		14,141
Orbiter Bulkheads - Intertank Section		5,482
Thrust Structure		30,000
Skin Panels	9,579	
Frames	2,470	
Thrust Beams	6,284	
Thrust Posts	3,060	
Ground Fittings	1,332	
Bulkheads	5,509	
LO_2 Line Backup	200	
Tank Attach Bolts	250	
Joints, Splices, and Fasteners	1,316	
Other Miscellaneous and Secondary Structure		21,520
Crew and Avionics Compartment	1,800	
Engine Heat Protection	5,235	
Orbiter Attach and Separation Mechanism	3,655	
Main Landing Gear and Wing Bulkheads	10,830	
TOTAL BODY GROUP WEIGHT		177,612

3.0 STRUCTURAL DESIGN LOADS AND CRITERIA FOR BASELINE VEHICLE

3.1 STRUCTURAL DESIGN CRITERIA

Structural design criteria that are pertinent to the present study and are reflected in the characteristics of the baseline vehicle are summarized in the following sections. These criteria have been abstracted from Reference 3.

3.1.1 Design Philosophy

The basic structural design philosophy is that the structural components and elements shall be designed for minimum weight consistent with the required service life, degree of damage tolerance, and detail design requirements.

The intent of these requirements is to provide a structural system with the following characteristics:

1. Structures containing no defects or anomalies

    a. Shall withstand ultimate loads and pressures in the expected operating environment without rupture or collapse

    b. Shall withstand limit loads and pressures in the expected operating environments throughout its service life without detrimental deformations

    c. Shall possess a nominal safe-life of 400 missions without fatigue crack initiation.

2. Structures containing defects or anomalies

    a. If designed for safe life, it shall withstand the expected operating loads and pressures in the expected operating environment without rupture or collapse for a nominal safe life of 150 missions

    b. If designed for fail safe, it shall withstand limit loads and pressures after the obvious partial failure of any principal structural element

The use of materials which are considered state of the art and are well characterized shall be the basic general rule.

When ground handling or test conditions are determined to be more critical than flight conditions, their effect should be minimized by investigating alternate ground handling or test methods.

3.1.2 Design Requirements

Program Requirements

The following program requirements shall be used in establishing structural design requirements:

1. Design service life shall be 100 missions and 10 years of operation.

2. The vehicle shall have intact abort capability after liftoff.

3. 550K thrust engines are baseline.

4. JP fuel is baseline for airbreathing engines.

5. The vehicle ascent trajectory load factors should not exceed 3g for passenger-carrying missions.

General Requirements

1. The structure shall be designed to survive the specified number of missions with a minimum of structural refurbishment, and in a manner that does not reduce the probability of the successful completion of any mission. Maximum consideration shall be given to the cumulative deteriorating effect of repeated exposure to the critical environmental conditions, such as temperature, creep, and fatigue.

2. The structure shall be designed by flight conditions wherever possible. The nonflight conditions and environment shall influence the design to the minimum extent possible.

3. The structure shall be designed to have sufficient strength to withstand simultaneously the limit loads, applied temperature and other accompanying environmental phenomena for each design condition without experiencing excessive deformation.

4. The structure shall be designed to withstand simultaneously the ultimate loads, applied temperature and other accompanying environmental phenomena without failure.

5. The vehicle shall be designed such that destructive flutter or other related dynamic instability or divergence phenomena shall not occur on the vehicle, or its components, at any condition along the design trajectories.

6. Structures designed only for positive pressure shall have provisions to prevent inadvertent depressurization.

7. Pressurized structure shall be designed so that any leakage occurring during a mission will permit successful completion of the mission. In no case shall leakage exceed levels stated in safety requirements for toxic and explosive fluids, or levels which might jeopardize system function or rated life.

8. Compartment vent and relief provisions shall be designed with sufficient vent capacity to prevent structural over-pressurization due to failure of pressurizing systems or components.

9. The effects of repeated loads and elevated temperatures shall be considered in the structural design. The design structural adequacy of the vehicle in flight shall not be impaired by fatigue damage resulting from exposure to non-flight and launch environments.

10. The effects of accumulative creep deformation shall be considered. The maximum permissible permanent deformation and creep cracks shall be defined based on the structural application and material behavior.

11. The effects of thermal stresses shall be combined with the appropriate ultimate load stresses when calculating required strength. Thermal stresses shall be based on limit temperatures.

12. If the protection against environments afforded by the overall vehicle design is not sufficient to limit detrimental effects to specified levels, provision shall be made for protection against these environments.

13. The structure shall not be designed to withstand loads, pressures, or environments due to malfunctions that would in themselves result in failure to accomplish the mission.

3.1.3 Design Conditions

The following phases and conditions in the service life of the shuttle vehicle shall be investigated for critical loads, temperatures, and structural response:

Ground Handling

Transportation
Proofing
Towing loads
Jacking loads
Hoisting, mating, erecting, and mooring

Prelaunch/Liftoff

Steady winds, wind shears, and gust
Vortex shedding

Prelaunch/Liftoff (continued)

Dampers, tower structure, and supports
Launcher system, holddown and release
Propellant loading and tank pressurization schedule
Ground thermal environment and thermal transients
Cargo loading conditions
Engine noise and vibration
Engine ignition transients and thrust buildup
Emergency engine shut-down and/or rebound
Purge system vent pressures

Boost/Ascent Flight

Steady winds, wind shears, and gusts
Control system characteristics/engine thrust scheduling
C.g. offsets
Thrust oscillations and engine vibration
Aerodynamic pressure distribution
Boundary layer noise
Buffet and separated flow
Aerodynamic heating

Staging/Separation

Booster engine shut-down
Orbiter engine start
Retro, ullage, and/or RCS engine operation
Separation mechanism activation
Plume impingement

Entry

Heat transfer from external flow field
Shock wave impingement
Aerodynamic loading and differential pressure loads
Steady winds, wind shear, gust
Tank ullage heating and pressurization

Transition and Atmospheric Cruise

Buffet and separated flow during transition
Aerodynamic pressure distribution
Steady winds, wind shears, and gusts
Control system characteristics/maneuvers
Cruise engine noise and vibration
Boundary layer noise
Transient thermal effects
Tank ullage heating and pressurization

Landing

Spin-up and spring back gear loads
Land impact
Symmetric and unsymmetric landing
Taxiing
Braking

Ferry Operations

Engine thrust buildup horizontal takeoff
Engine noise

3.1.4 Loads and Pressures

Loads

Limit loads shall be determined for the vehicle in the mated and unmated configurations for the conditions identified above.

The following effects shall be accounted for:

1. Vehicle external and internal geometry

2. Vehicle mass distribution, stiffness, and damping

3. Aerodynamic characteristics

4. Natural and specification environments

5. Interactions of propulsion, control, and other vehicle systems

6. Trajectory characteristics

The effects of transient loads shall be included in the determination of limit loads for all quasi-static and transient phenomena expected in each design environment. The dynamic loads shall account for the effects of vehicle structural flexibilities and damping, and coupling of structural dynamics with the control system and the external environment. The limit loads shall be calculated by multiplying quasi-static loads by appropriate dynamic load amplification factors. These dynamic factors can be derived by comparison to previous data in lieu of detailed dynamic response studies.

Pressures

Design-limit pressures shall be determined as follows:

1. Regulated pressure (i.e., main propellant tanks, personnel and cargo compartments, ACPS accumulators)

    a. Limit pressure shall be based on the upper limit of the relief valve setting when the pressure is detrimental to the load-carrying capability of the structure.

b. Limit pressure shall be based on the lower limit of the operating pressure when the pressure enhances the load-carrying capability of the structure.

2. Non-regulated pressure (i.e., vented compartments)

a. Upper and lower bounds of pressure shall be established in a rational manner when a range of pressure is possible for a particular structure.

b. Limit pressure shall be based on the upper bound when pressure decreases the load-carrying capability of the structure.

c. Limit pressure shall be based on the lower bound when pressure increases the load-carrying capability of the structure.

3. Combined Loads and Pressures

Pressure vessels (including main propellant tanks) shall be capable of withstanding the following combinations of loads and pressures without rupture or collapse:

a. Ultimate load and ultimate pressure when the pressure is destabilizing

b. Ultimate load and limit pressure when the pressure is stabilizing

c. Ultimate pressure alone

3.1.5 Design Factors

Design factors shall be used to account for structural analysis, environmental, and material uncertainties which are not amenable to rational approaches.

Factors of Safety

Table 3-1 shows the yield and ultimate factors of safety to be used in Phase B studies for various structural components.

Proof Factors

Table 3-1 shows the proof factors to be used in Phase B studies.

In addition to the above factors, when adequate fracture touchness data and sufficient knowledge of operating conditions are available to determine the required proof pressure from fracture mechanics principles, the required proof pressure will be determined from these data and used.

The methods and requirements are provided in the NASA design criteria monograph "Fracture Control of Metallic Pressure Vessels," NASA SP8040.

Service Life Factors and Environments

Table 3-2 shows factors to be used in relation to fatigue, flaw growth, and creep during Phase B studies.

Booster main propellant tanks, pressure vessels, and cabin structures shall be designed to preclude the occurrence of both functional failure (i.e., leakage of fluids and gasses) and structural failure (i.e., rupture). Flaw growth analyses for both types of phenomena shall be performed considering the complexity of structural details, environments, and loadings for each particular design. The factor 1.5 for flaw growth calculations during Phase B studies was selected on the basis of (1) the observation that flaw growth is a better behaved phenomenon than flaw initiation (i.e., fatigue) for which a life factor of 4 is traditionally used; and (2) the desire to maintain a realistic structural design approach with minimum weight impact. This life factor for flaw growth must be re-examined when sufficient flaw growth data for Space Shuttle materials become available.

Due to present uncertainties on (1) the behavior of materials under sustained and cyclic creep conditions, (2) temperature predictions due to lack of substantiating flight data, and (3) potential temperature overshoots due to presently undefined perturbations of nominal trajectories, a rather conservative approach was used in establishing life factors for creep evaluation during Phase B studies. These factors were a factor of four on design service life and, in addition, a factor of two on accumulated creep strain.

The design environments given in Table 3-3 are to be used for safe-life calculations.

Margins of Safety

The margin of safety shall be positive and shall be determined at ultimate allowable levels and at yield levels, when appropriate, at the temperatures expected for all critical conditions.

For minimum-weight design, the margin of safety should be as small as practicable.

3.1.6 Service Life

The combined effects of fatigue, thermal stress, and creep on general structure shall be evaluated.

Load spectra shall be defined to represent analytically the cumulative static, dynamic, and environmental loads and deflections anticipated for all major structural components during the service life of the vehicle.

C2.

Table 3-1. Design Factors of Safety

Component	Yield	Ultimate	Proof	Applied On
Main propellant tanks	1.10	1.40	◁1	Maximum relief valve pressure only
	1.10	1.40	-	Loads (+ limit pressure)
	1.00	--	-	Proof pressures
Personnel compartments, windows, doors, hatches	1.10	1.50	-	Loads (+ limit pressure)
	1.50	2.00	1.50	Maximum operating pressure only
	1.00	--	-	Proof pressure
Airframe structure	1.10	1.40	-	Boost + entry loads
	1.10	1.50	-	Aircraft mode loads
Pressure vessels	--	2.00	1.50	Maximum operating pressure
Pressurized lines fittings	--	2.50	1.50	Maximum operating pressure
Thermal stresses	1.00	1.00		Thermal forces + flight loads
	1.00	1.25		Thermal forces alone

◁1 Proof factor TBD based on Fracture Mechanics Analysis

Table 3-2. Service Life Factors

ITEM	FACTOR	APPLIED ON
Fatigue initiation	4.0	Design service life
Flaw growth to leak	1.5	Design service life
Flaw growth to failure	1.5	Design service life
Creep	4.0	Design service life
	and	
	2.0	Accumulated creep strain

NOTE: Design service life = 100 missions and 10 years of operation.

Flaw growth shall not exceed the growth required to increase the maximum undetectable initial flaw to a size where the stress intensity under limit-stress levels exceeds the threshold stress-intensity values. The effects of short-time load excursions which result in stress intensities above the threshold (e.g., due to maneuver loads, vibratory loads, or gust loads) shall be accounted for in the fatigue-life predictions.

Safe-Life

Safe-life design concepts shall be applied to all structure vital to the integrity of the vehicle or the safety of personnel. The safe-life shall be determined using the factors given in Table 3-2.

The determination of structural safe-life shall take into consideration the effects of the following factors in combination with the expected operating environments:

Material properties and failure mechanisms

Load spectra

Cyclic-loads effects

Sustained-loads effects

Cumulative combined damage

Fail-Safe

Where practicable, fail-safe design concepts shall be applied. For all fail-safe structure, the failure of a single principal structural component shall not degrade the strength or stiffness of the structure below that necessary to carry limit load. All fail-safe structure shall be accessible for periodic inspection.

3.1.7 Design Thickness

The structural design thickness, t_d, for each metallic structural member other than mechanically or chemically milled pressure vessels shall be the minimum thickness obtained by either of the following calculations:

1. t_d = mean thickness based on equal plus and minus tolerances

2. t_d = N times the minimum thickness

where

N = 1.10 for strength design

N = 1.05 for stability design

The mean and minimum design thicknesses, as used above, shall include allowances for cumulative material damage or loss resulting from repeated exposure to the design environment. The design thickness for mechanically or chemically milled pressure vessels shall be the minimum thickness (i.e., mean minus the lower tolerance).

3.2 DESIGN LOADS

Design conditions listed in 3.1.3 were evaluated by GDC to determine critical conditions and resulting external loads on booster primary structure. These limit design loadings are summarized in the following sections; data are abstracted from Reference 4. A summary of characteristics for critical design conditions is given in Table 3-4.

3.2.1 Aerodynamic Surfaces

A summary of design loadings at the root of aerodynamic surfaces is given in Table 3-5. The spanwise distribution of bending moment is given in Figures 3-1, 3-2 and 3-3 for the wing, canard, and vertical stabilizer, respectively.

3.2.2 Body Loads

Body Shell Loads

Internal loads consisting of axial and shear loads and bending and torsion moments were determined along the body length for 25 different load conditions by GDC as part of their Phase B study effort. The results of this analysis are documented in Reference 4. These data have been reviewed and ten loading conditions identified as being of potential interest for the present study. The resulting distributed longitudinal loading (N_x) on the body shell at the top and bottom centerlines is plotted versus body station in Figures 3-4 and 3-5. These loadings are based on limit external loads and limit nominal compartment ullage pressures. The identifying numbers for design conditions are the same as employed in Reference 4.

The body bending moment, axial force, and compartment pressure for these selected design conditions and three body stations of potential interest for the present study are summarized in Table 3-6.

Orbiter Attachment Loads

Design limit loads for the connection between booster and orbiter vehicles are summarized in Table 3-7.

Thrust Loads

The variation of total booster main engine thrust over the boost period is plotted in Figure 3-6.

Table 3-3. Safe-life Design Environments

COMPONENT	DESIGN ENVIRONMENT
LO_2 Tank	LO_2 @ -320°F or GO_2 @ 70°F
LH_2 Tank	Air at 70°F
Intertank Adapter	Air at 70°F
TPS, Wing, Canard Empenage, Thrust Structure, and Orbiter Attachments	3 1/2% salt solution with alternate drying

Table 3-4. Summary of Design Conditions

Condition	Axial Load Factor (g)	Lateral Load Factor (g)	Wind Speed at 60 Feet or αq (βq)	Remarks
Two-week standby	1.0	-	72.1 knots	Unfueled, unpressurized
One-day hold	1.0	-	48 knots	Fueled, pressurized
One-hour to launch	1.0	-	34.4 knots	Fueled, unpressurized
Liftoff				
LO_2 mass	1.31 ±0.15	TBD		
LH_2 mass	1.31 ±0.25	TBD		
Orbiter & other	1.31 ±0.21	TBD		
Maximum dynamic pressure				
αq	1.71	+0.62, -0.20	±2800 deg-psf	
βq	1.71	±0.15	±2400 deg-psf	
Maximum thrust	3.0 ±0.30	TBD	±480 deg-psf	
Booster burnout	3.0 ±0.30	TBD	±100 deg-psf	
Booster recovery		4.0		
Subsonic gust		2.05		
Subsonic maneuver		2.50		
Landing		2.0 ±.35		

Table 3-5. Design Loads for Aerodynamic Surfaces

Surface	Design Condition	Shear		Bending Moment		Torque	
		(lb x 10^3)	MN	(in-lbx10^6)	NM-m	(in-lbx10^6)	MN-m
Wing	Max α-q	646.7	2.90	173.9	1.98	25.7	.293
	Entry	650.6	2.92	163.1	1.86	30.0	.342
	2.5g Man.	518.9	2.33	150.3	1.71	77.1	.880
	Subsonic gust	508.5	2.28	146.3	1.67	74.5	.850
Canard	2.5g Man.	64.0	.287	4.76	.0544	1.55	.0177
	Max α-q	43.9	.197	3.66	.0418	-1.26	-.0144
Vertical Stabilizer	Subsonic side gust	272	1.22	63.0	.719	77.0	.879
	Subsonic rudder kick	204	.915	50.9	.580	45.3	.516
	Max β-q	187	.839	43.2	.492	61.0	.695

NOTE: (1) All loads are limit
(2) Loads are at root of aerodynamic surface
(3) Loads are per panel

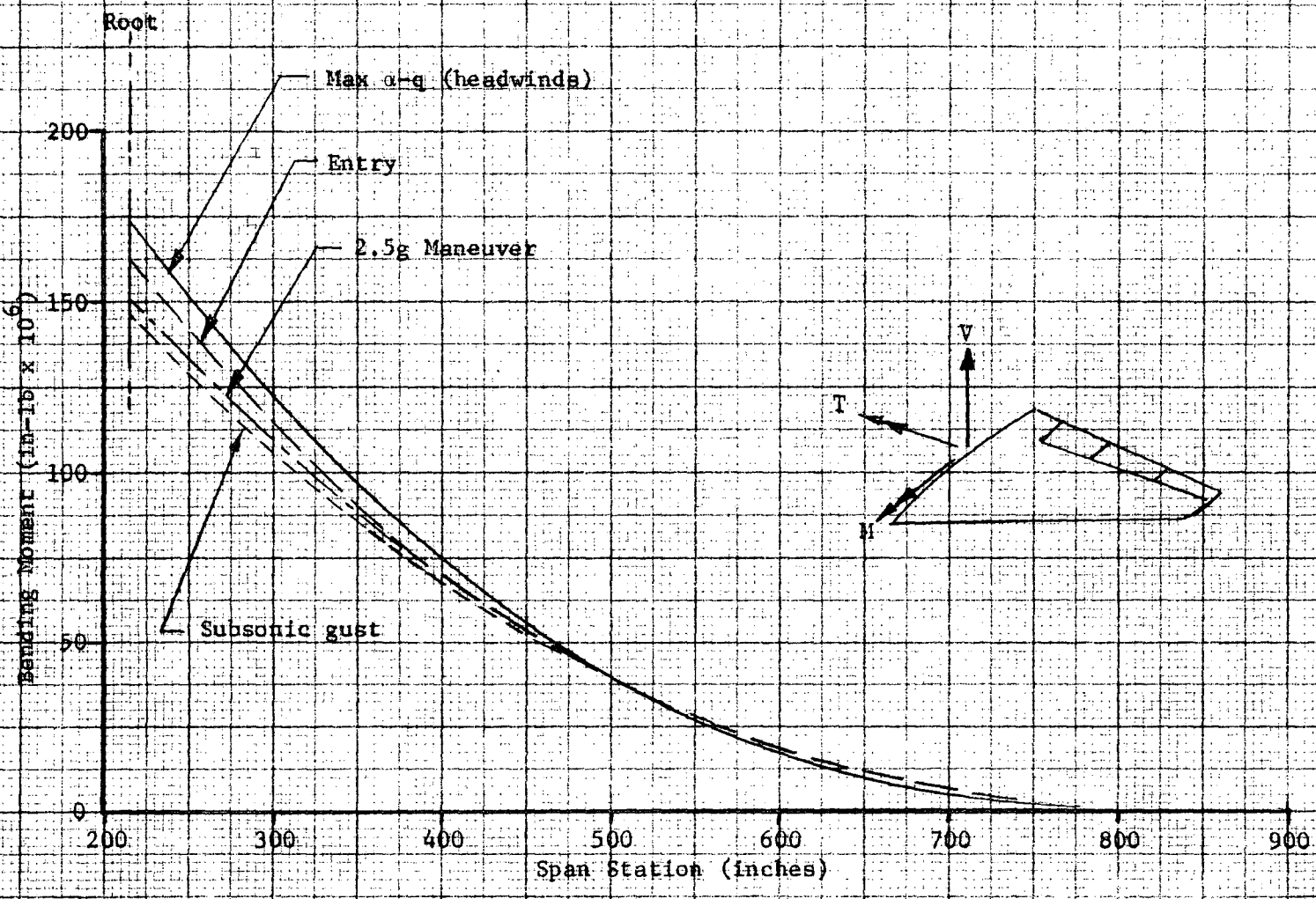

Figure 3-1. Wing Bending Moment Distribution

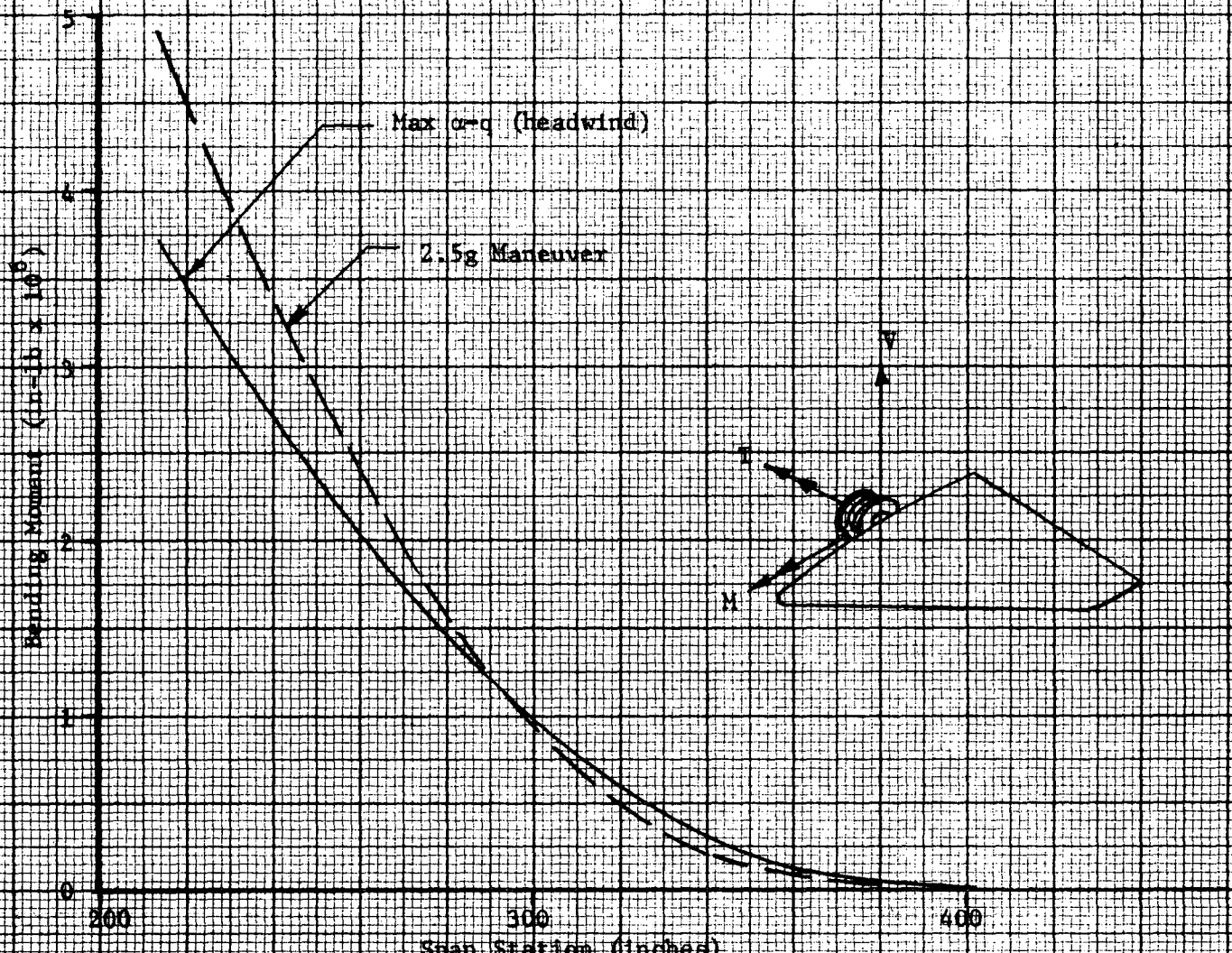

Figure 3-2. Canard Bending Moment Distribution

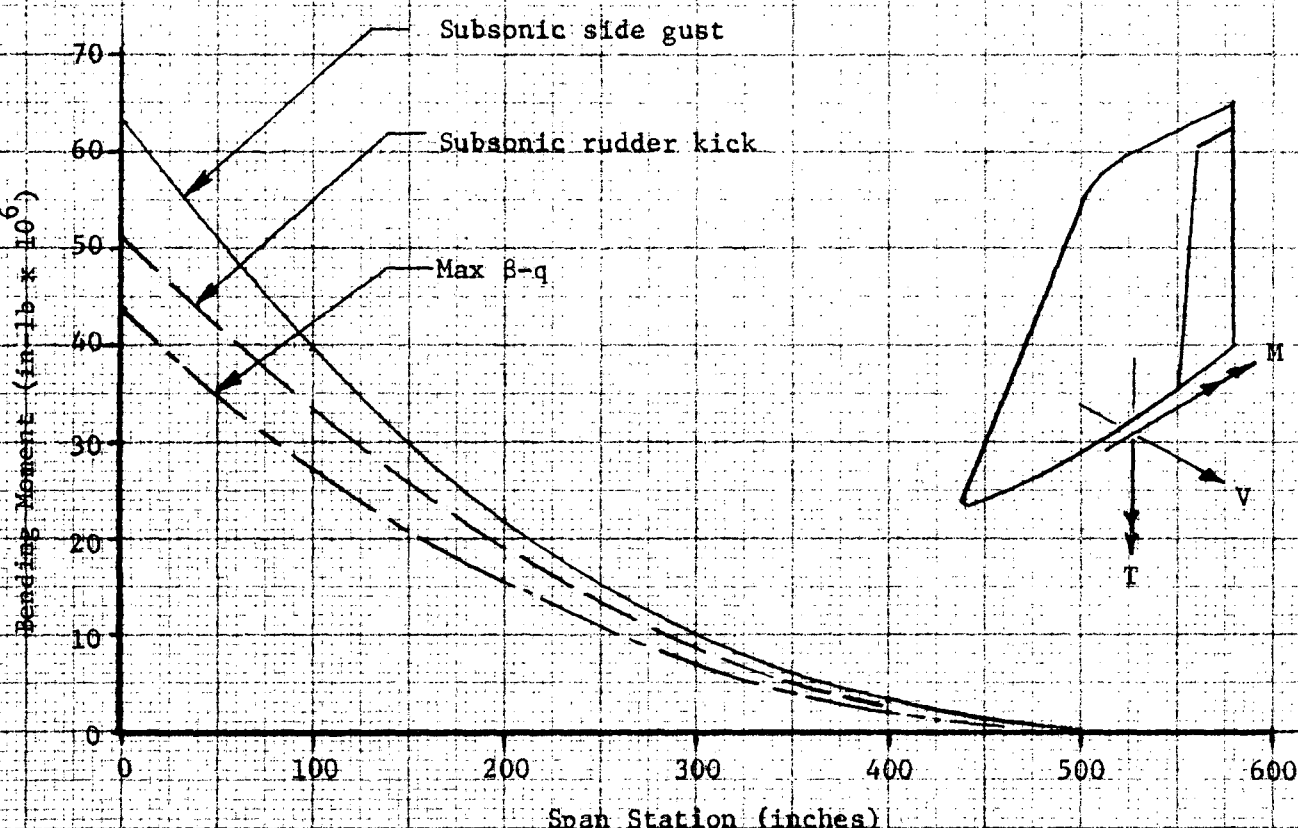

Figure 3-3. Vertical Stabilizer Bending Moment Distribution

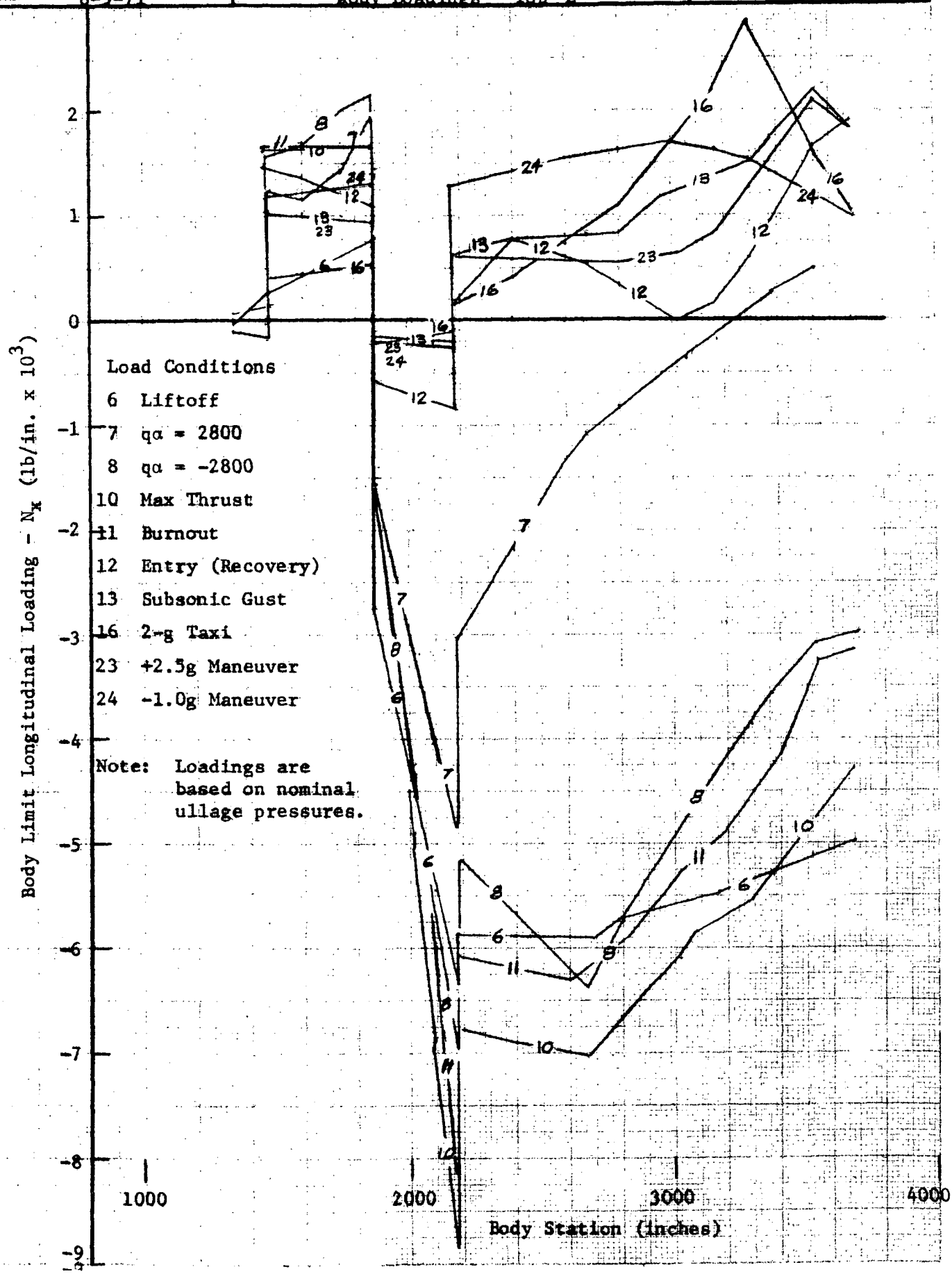
Body Limit Longitudinal Loading - N_x (lb/in. x 10^3)
Body Station (inches)
1000
2000
3000
4000
2
1
0
-1
-2
-3
-4
-5
-6
-7
-8
-9
Load Conditions
6 Liftoff
7 qα = 2800
8 qα = -2800
10 Max Thrust
11 Burnout
12 Entry (Recovery)
13 Subsonic Gust
16 2-g Taxi
23 +2.5g Maneuver
24 -1.0g Maneuver
Note: Loadings are based on nominal ullage pressures.

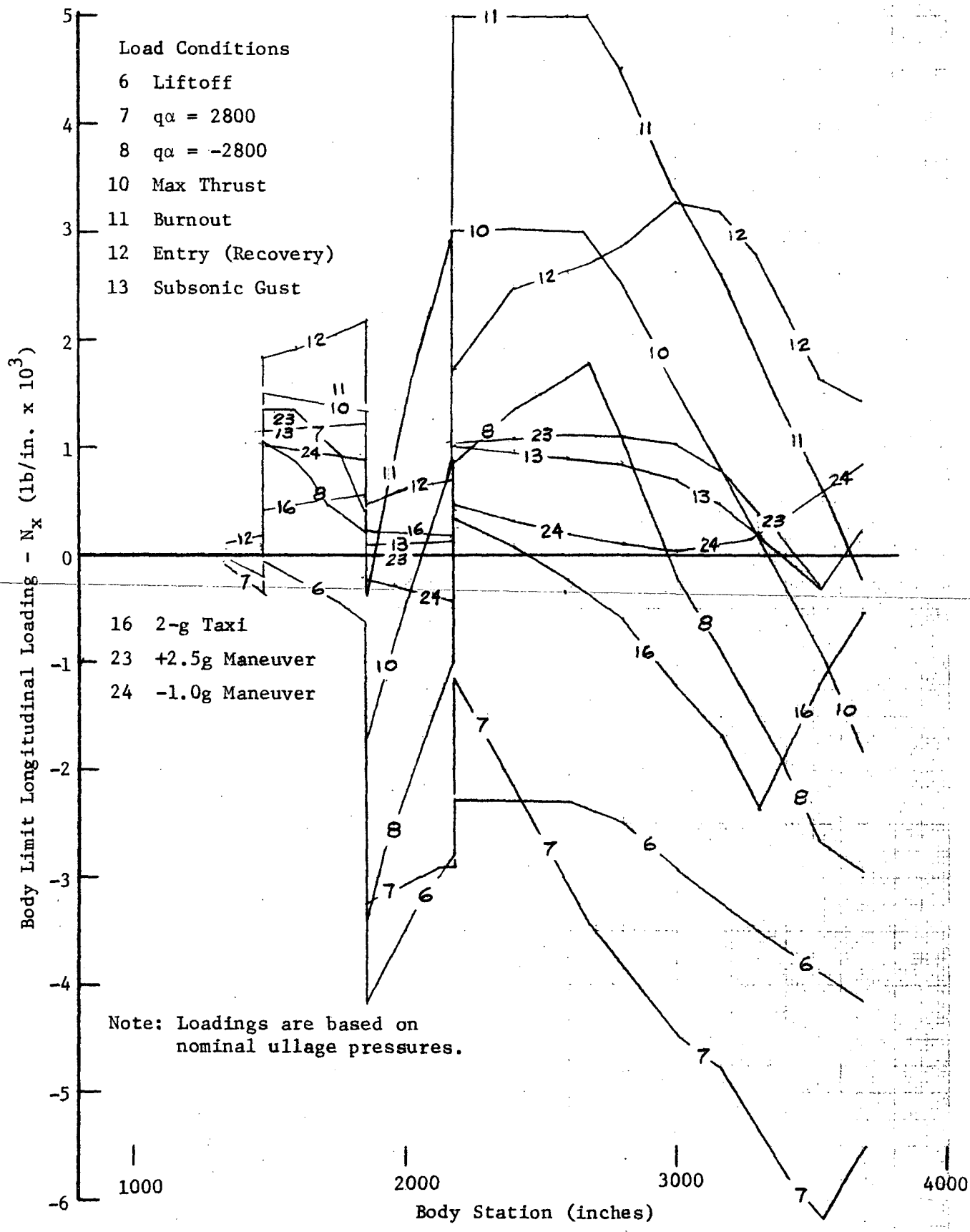
Load Conditions
6 Liftoff
7 qα = 2800
8 qα = -2800
10 Max Thrust
11 Burnout
12 Entry (Recovery)
13 Subsonic Gust
16 2-g Taxi
23 +2.5g Maneuver
24 -1.0g Maneuver
Note: Loadings are based on nominal ullage pressures.
Body Limit Longitudinal Loading - N_x (lb/in. x 10^3)
Body Station (inches)
5
4
3
2
1
0
-1
-2
-3
-4
-5
-6
1000
2000
3000
4000

Table 3-6. Body Limit Design Loads

Cond. No.	Condition	Bending Moment[1] (in-lb x 10^6)			Axial Force[2] (lb x 10^3)			Internal Pressure[3] (psig)		
		Sta. 1864	Sta. 2180	Sta. 2600	Sta. 1864	Sta. 2180	Sta. 2600	Sta. 1864	Sta. 2180	Sta. 2600
6	Liftoff	86.0	-220	-223	104	5660	5730	2.2	0	5.1
7	α-q = 2800	97.2	-118	109	312	4830	5030	14.0	0	18.2
8	α-q = -2800	117	-370	-486	283	4910	5090	14.0	0	18.2
10	Maximum thrust	17.5	-602	-616	226	4880	5050	16.8	0	20.8
11	Burnout	24.6	-679	-695	225	3230	3400	16.8	0	20.8
12	Entry (Recovery)	-64.9	-92.9	-124	56.3	93.5	124	15.0	0	17.2
13	Subsonic gust	-15.9	-16.9	-4.9	26	42.8	58.8	11.0	0	9.0
16	2-g Taxi	-26.4	-9.4	59.5	0	0	0	3.3	0	2.5
23	+2.5g Maneuver	-12.0	-24.2	-33.4	25.6	63.1	78.8	11.0	0	9.0
24	-1.0g Maneuver	24.6	50.1	83.6	12.6	23.6	30.7	11.0	0	9.0

(1) Positive bending moment is tension on upper surface

(2) Positive axial force is compression

(3) Compartment nominal ullage pressure with respect to free-stream ambient

Space Division
North American Rockwell

Table 3-7. Booster/Orbiter Connection Loads

BOOSTER B-9U

BOOST PHASE

SEPARATION SYSTEM

LIMIT LOADS

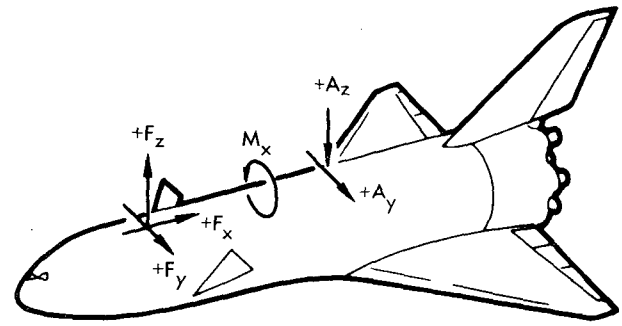

CONDITION		WIND	F_x (KIPS)	F_y (KIPS)	F_z (KIPS)	A_y (KIPS)	A_z (KIPS)	M_x (X 10^6 IN-LB)
TWO-WEEK GROUND WINDS, UNFUELED, WITH TOWER SUPPORT		HEAD	268	0	56.9	0	-33.0	0
		TAIL	268	0	-119.0	0	149.0	0
		SIDE	268	±98.5	28.8	±30.2	34.9	∓17.1
ONE-DAY GROUND WINDS, FUELED, WITH TOWER SUPPORT		HEAD	859	0	95.2	0	62.7	0
		TAIL	859	0	-0.1	0	161.0	0
		SIDE	859	±53.3	80.0	±16.3	99.5	∓9.28
ONE-HOUR GROUND WINDS, FUELED, UNSUPPORTED		HEAD	859	0	89.5	0	76.5	0
		TAIL	859	0	30.0	0	138.0	0
		SIDE	859	±33.3	80.0	±10.2	99.5	∓5.80
DYNAMIC LIFTOFF PLUS ONE-HOUR GROUND WINDS		HEAD	1296	0	119.0	0	134.0	0
		TAIL	1295	0	82.2	0	182.0	0
		SIDE	1296	±20.5	121.0	±2.92	150.0	∓4.14
MAX α-q	α-q = 2800	HEAD	1798	0	224.8	0	234.8	0
	α-q = -2800	TAIL	1804	0	83.0	0	950.3	0
		NO WIND	1808	0	137.4	0	625.6	0
MAX β-q	±2400	SIDE	1802	±81.2	128.8	±166.8	653.7	∓72.3
3g MAX THRUST	$N_x = 3.3$ $N_y = 0$ $N_z = -0.35$		2849	0	135.2	0	424.5	0
	$N_x = 3.3$ $N_y = \pm 0.1$ $N_z = -0.25$		2849	±55.4	179.3	±30.7	394.5	∓7.6
BOOSTER BURNOUT	$N_x = 3.3$ $N_y = 0$ $N_z = -0.46$		2841	0	62.9	0	459.0	0
	$N_x = 3.3$ $N_y = \pm 0.1$ $N_z = -0.36$		2841	±55.4	118.3	±30.7	428.0	∓7.6

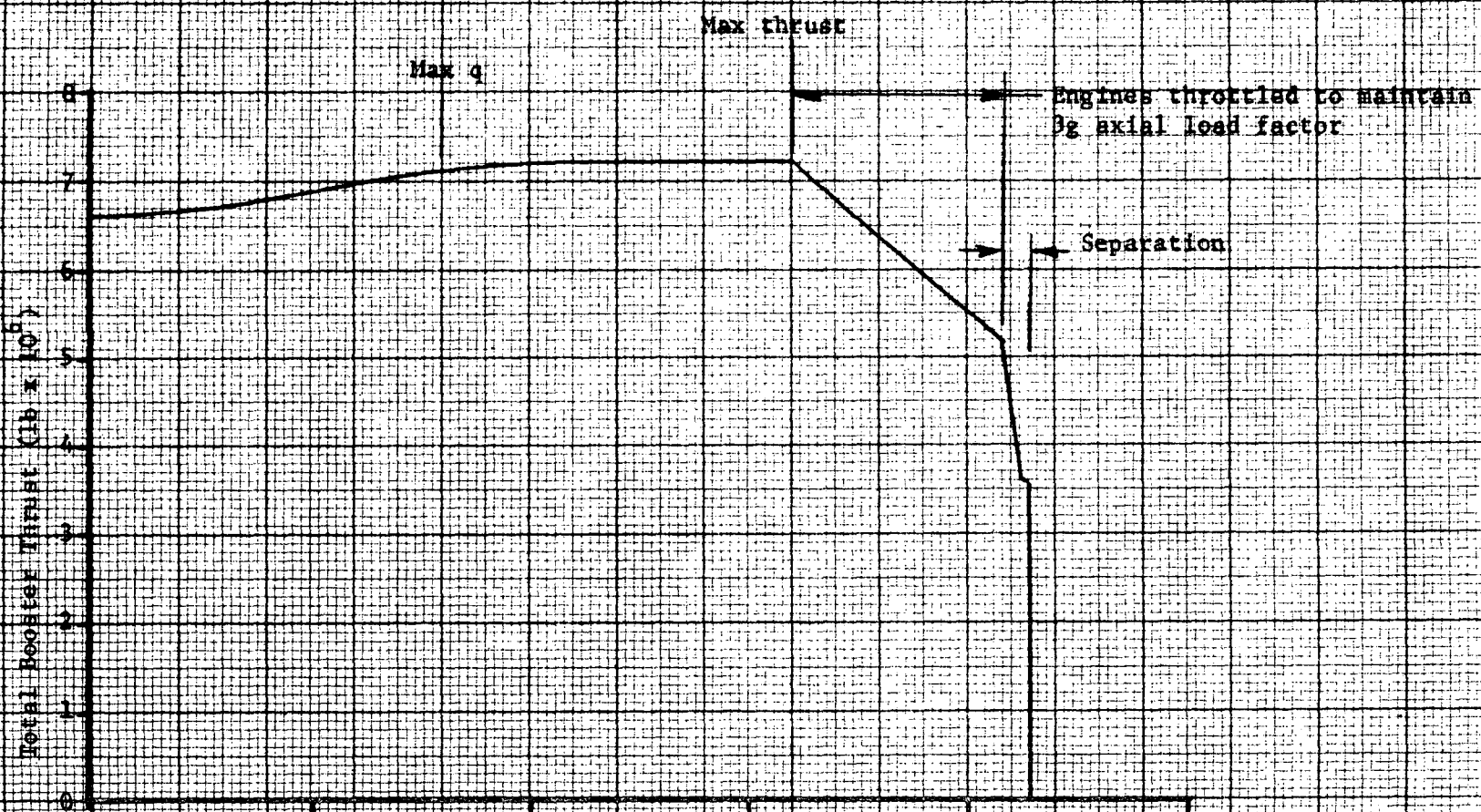

Figure 3-6. Booster Main Engine Thrust vs. Time

3.2.3 Propellant Tank Pressures

The ullage pressure schedule over the complete mission is plotted in Figures 3-7 and 3-8 for the LOX and LH_2 tanks respectively. Also indicated on these curves is the variation of total pressure (ullage plus head) at the bottom of the tanks.

The resulting design pressure profiles over the length of the tanks are plotted in Figures 3-9 and 3-10.

3.3 SERVICE LOAD SPECTRA

Service load spectra for major structural elements of the B-9U booster have been determined by GDC in support of other contracted studies. Data summarized in this section is taken from References 5, 6, and 7. The data is presented in the form of curves giving number of exceedances versus load magnitude for key loading parameters. The number of exceedances are based on a total of 100 operational missions. Ferry missions are not included in these curves, but their effect can be approximated by doubling the number of exceedances indicated for cruise, landing, and taxi flight phases.

3.3.1. Wing Load Spectra

Load spectra for the wing are given in Figure 3-11 in terms of mean and alternating bending moment at the wing root. The bending moments are expressed as a percentage of maximum design bending moment. The ascent phase has been divided into segments, and a series of curves are plotted which give exceedances of alternating bending moment for various values of mean bending moment. Wing bending moment for the entry phase is assumed to increase from zero to a positive maximum; the load magnitude shown for this flight phase refers to the maximum value of this one-sided bending moment distribution.

3.3.2 Vertical Stabilizer Load Spectra

Load spectra for the vertical stabilizer are given in Figure 3-12. The data is presented in the same form as for the wing; the ascent phase is divided into segments and a series of curves are plotted which give exceedance of alternating bending moment at the root of the vertical stabilizer. The alternating bending moment is again expressed as a percentage of maximum design value. The mean bending moment is zero for all flight conditions.

3.3.3 Body Load Spectra

Service load spectra are given in Figure 3-13 for fuselage station 2600; this station is in the region of maximum bending moment on the body. The data is plotted as exceedance of alternating bending moment at Sta. 2600 in conjunction with a prescribed mean bending moment. Two types of loading variation are represented on this figure. The bending moment for maximum thrust and entry conditions increases from zero to a positive or negative peak; this peak value is defined by the load exceedance curves. Transient bending moments due to atmospheric disturbances will alternate about some

KEUFFEL & ESSER CO.
ALBANENE ®
MADE IN U.S.A.

FIGURE 3-7.

B-9U MAIN LOX TANK PRESSURE SCHEDULE

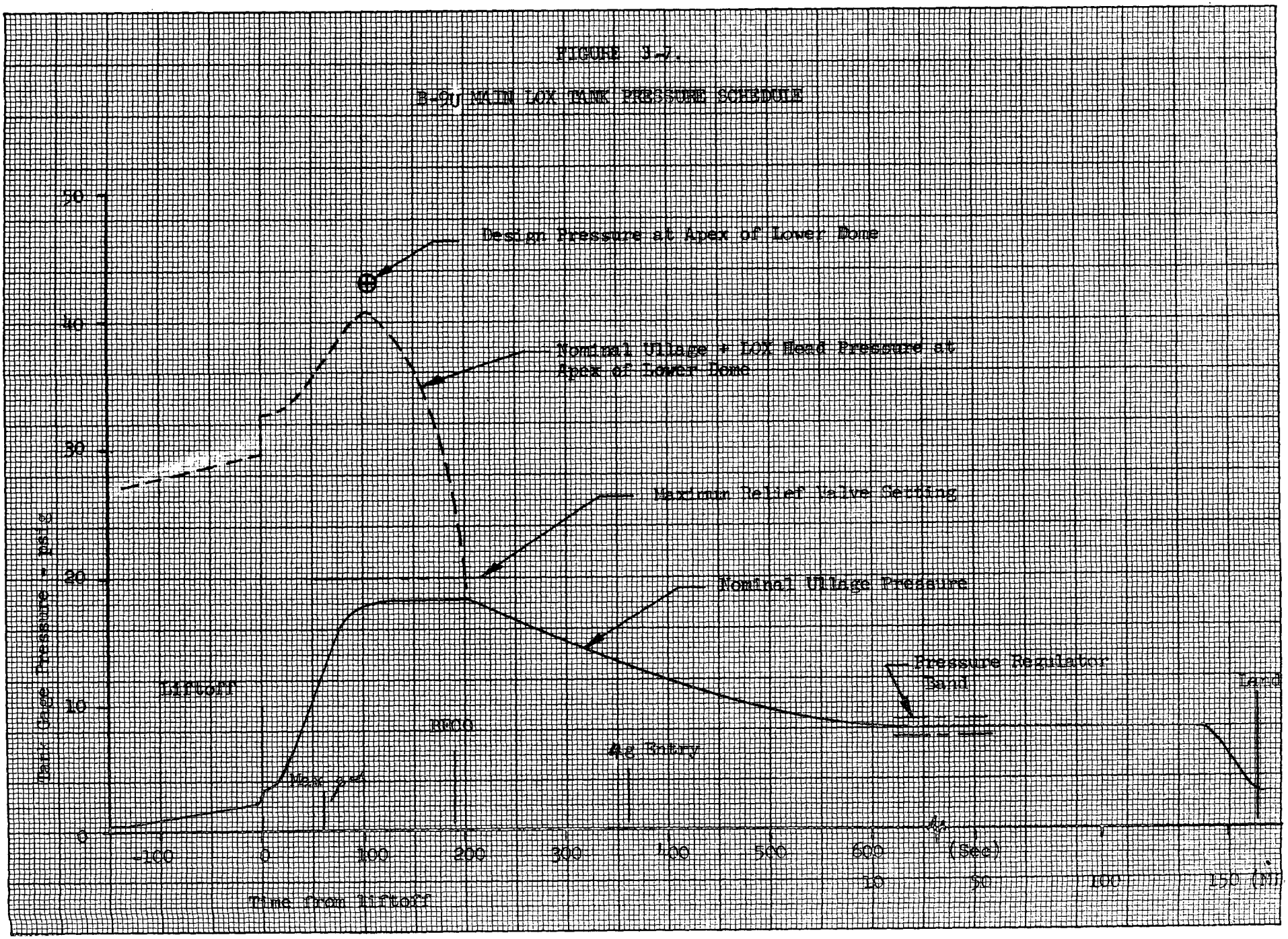

K+E 10 X 10 TO THE C.
KEUFFEL & ESSER CO.
ALBANENE ®
MADE IN U.S.A.

FIGURE 3-8. B-90 MAIN LH_2 TANK PRESSURE SCHEDULE

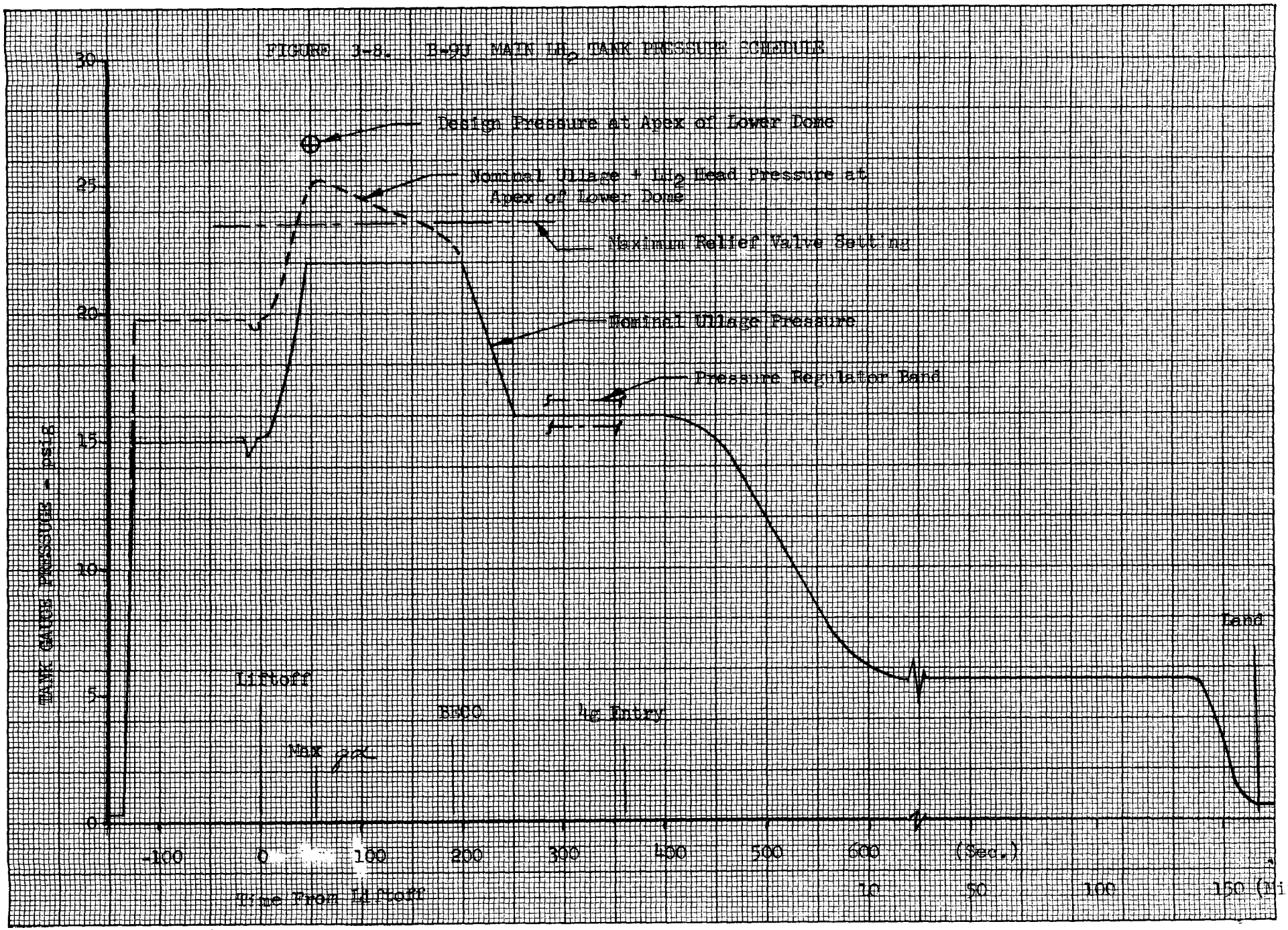

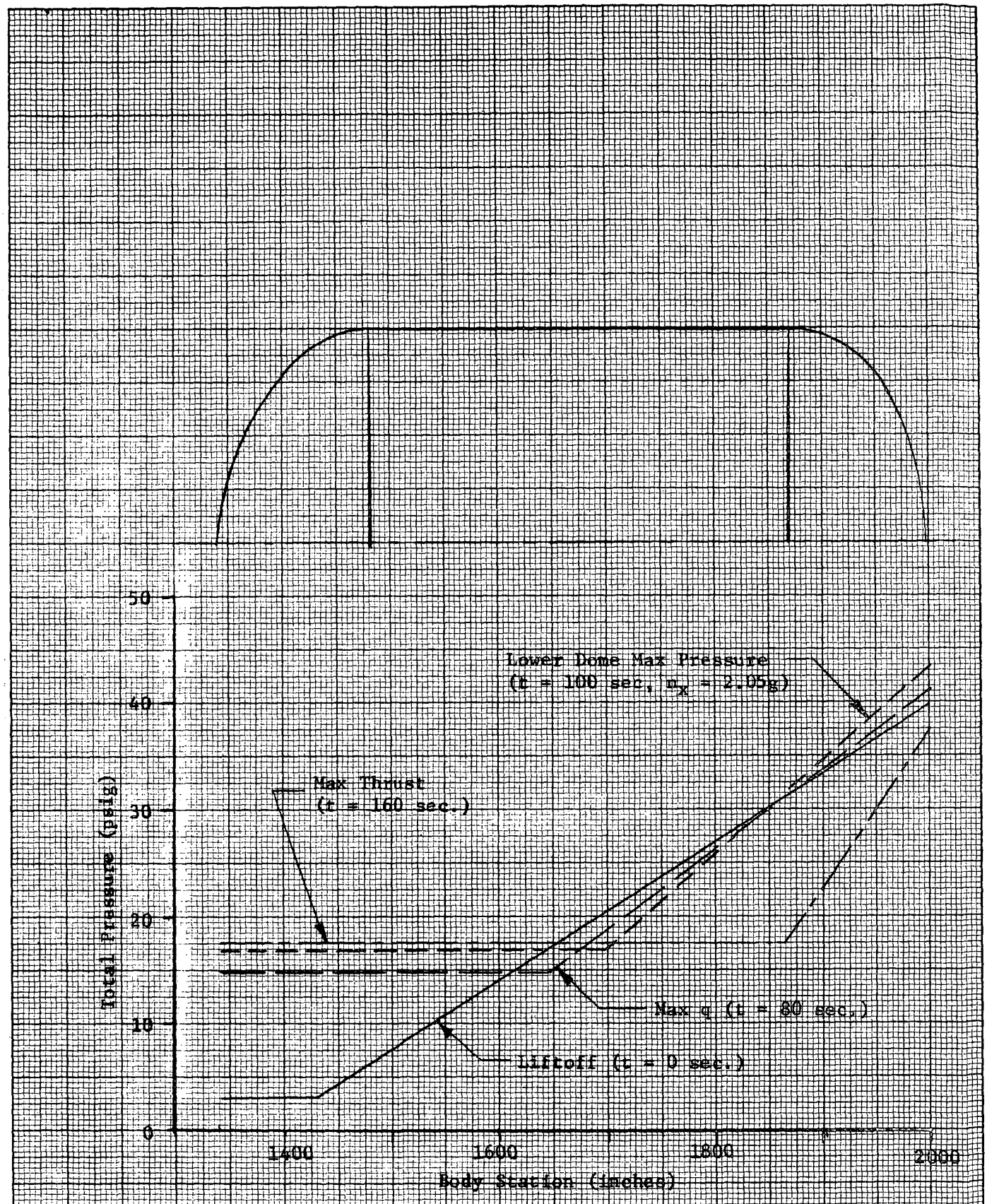

Figure 3-9. LOX Tank Limit Pressure Profiles

KEUFFEL & ESSER CO.

10 X 10 TO THE CENTIMETER 46 1512
KEUFFEL & ESSER CO.

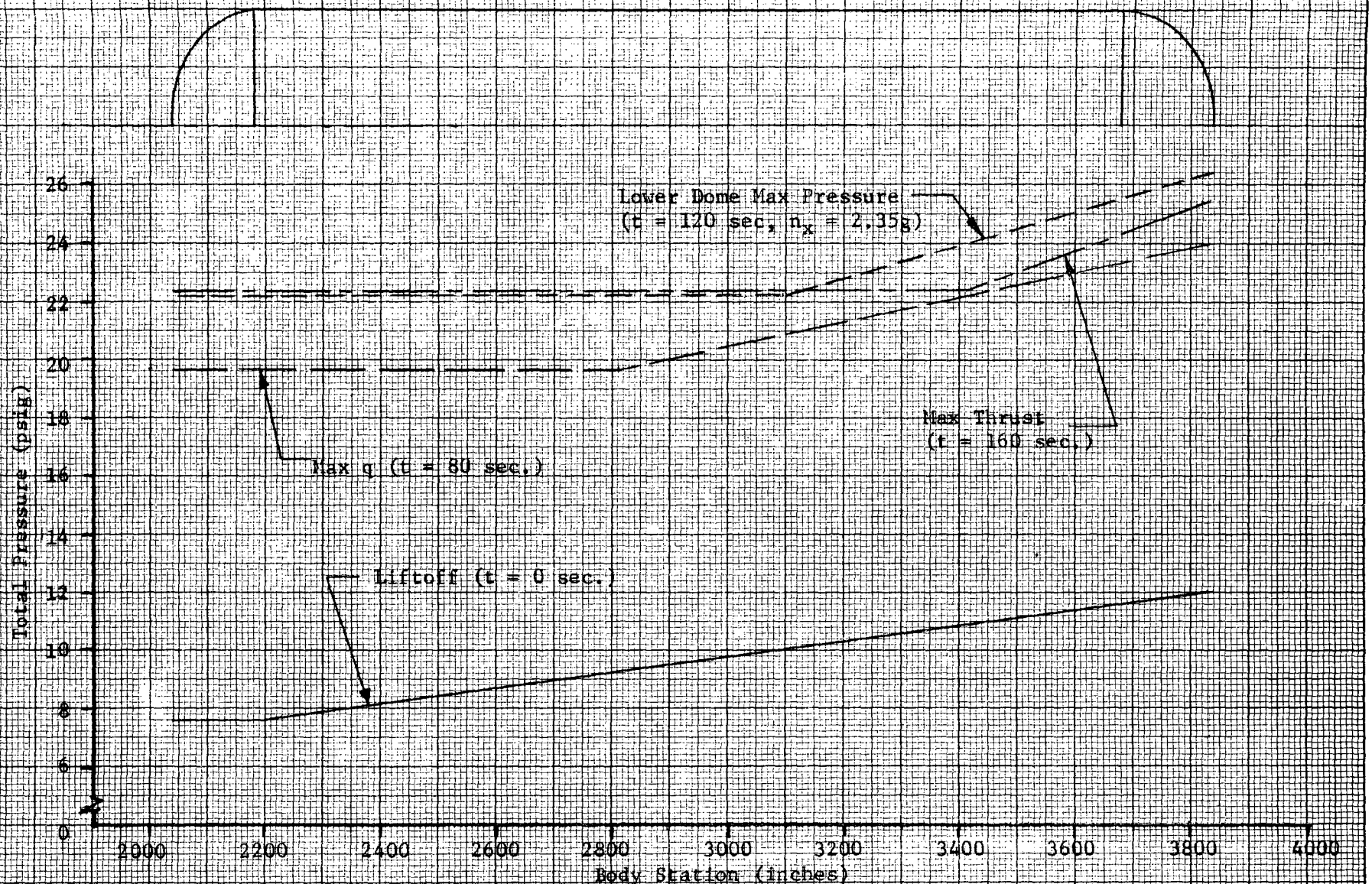

Figure 3-10. LH_2 Tank Limit Pressure Profiles

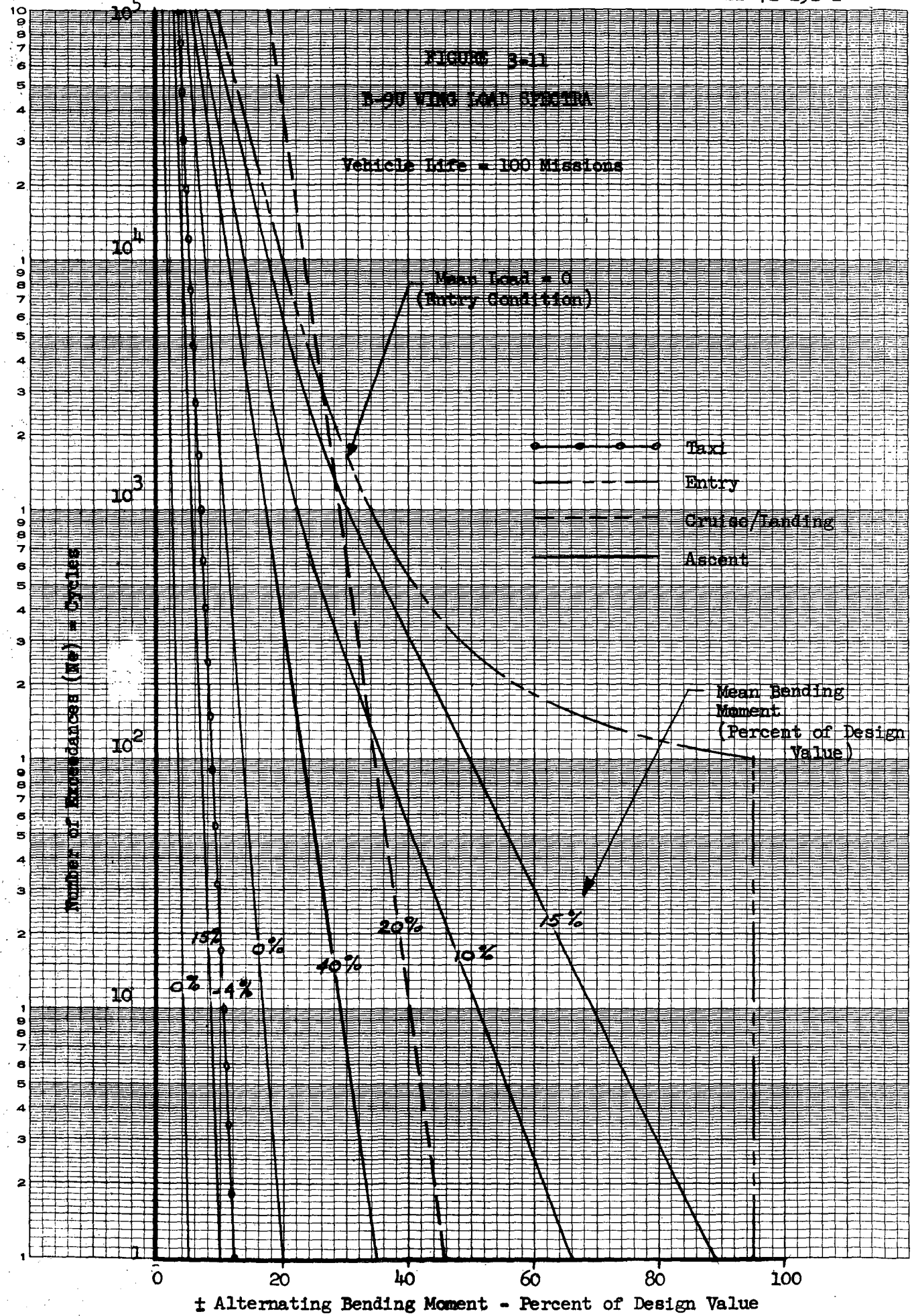

EUGENE DIETZGEN CO.
MADE IN U. S. A.
NO. 340-L510 DIETZGEN GRAPH PAPER
SEMI-LOGARITHMIC
5 CYCLES X 10 DIVISIONS PER INCH

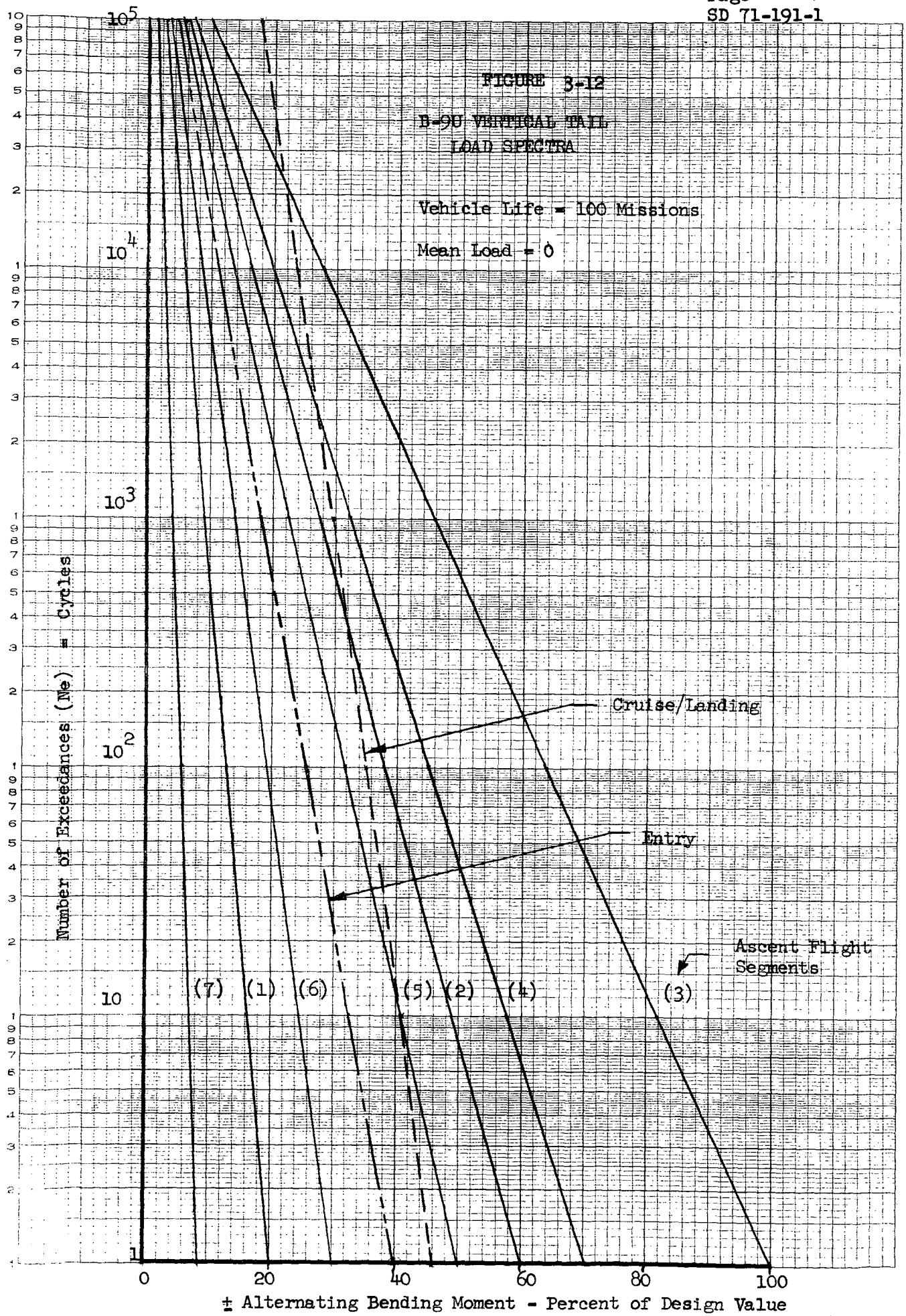

FIGURE 3-12

B-9U VERTICAL TAIL
LOAD SPECTRA

EUGENE DIETZGEN CO.
MADE IN U. S. A.
NO. 340-L510 DIETZGEN GRAPH PAPER
SEMI-LOGARITHMIC
5 CYCLES X 10 DIVISIONS PER INCH

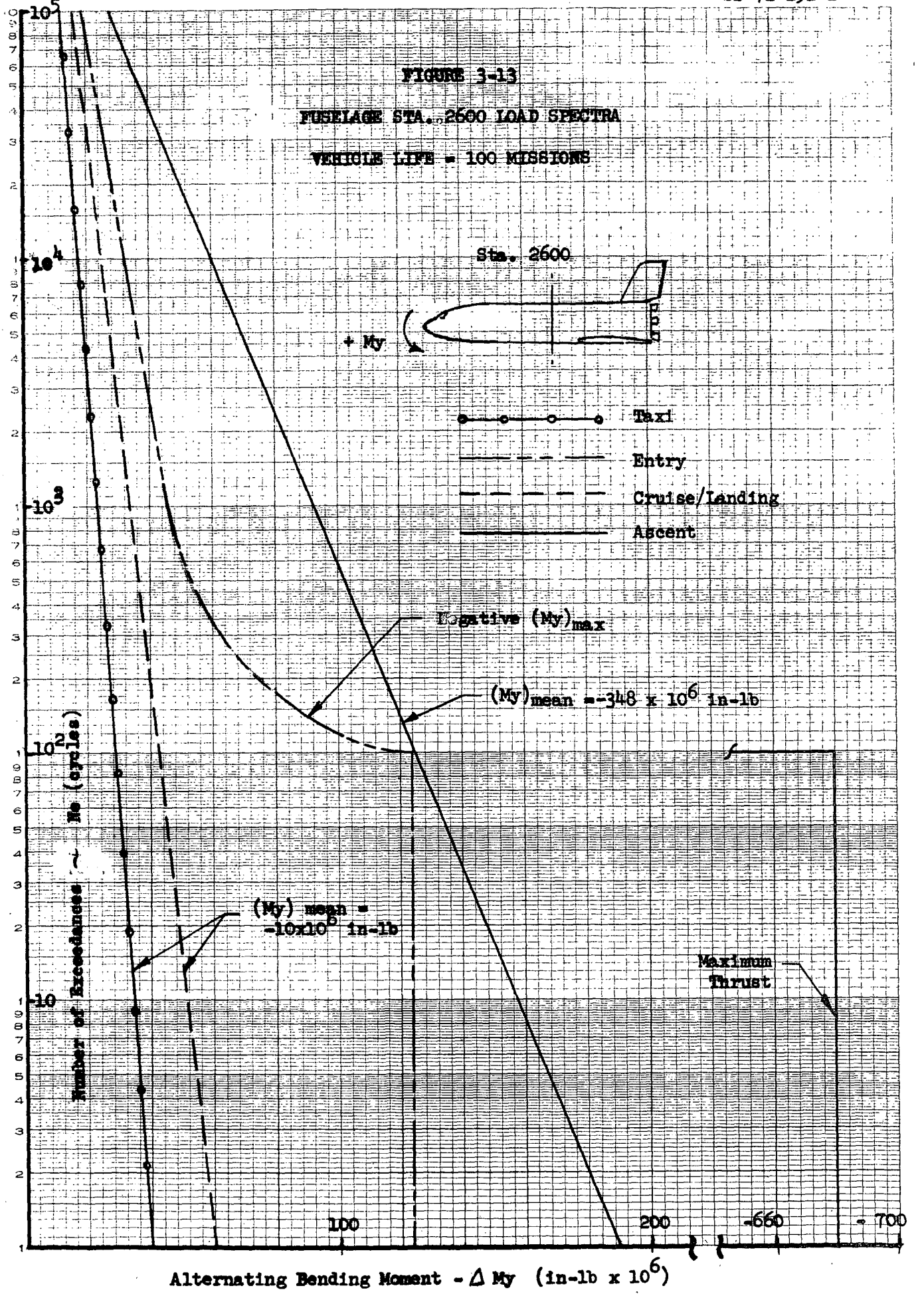

FIGURE 3-13

FUSELAGE STA. 2600 LOAD SPECTRA

VEHICLE LIFE = 100 MISSIONS

mean value which is the result of steady-state aerodynamic and thrust forces. Major aerodynamic transients will occur in the maximum α - q regime during ascent, so a mean bending moment applicable to this condition is used for the ascent flight phase. The effect of axial load and tank ullage pressure must also be considered, of course.

Service load spectra are given in Figure 3-14 for the orbiter aft attachment. The exceedance of alternating loads in the normal and lateral directions are given, expressed as a percentage of maximum design values.

The exceedance of main engine thrust variation for one flight is given in Figure 3-15.

3.4 STRUCTURAL TEMPERATURES

Detailed thermal analysis has not been performed in the Phase B study on all structural elements of present interest. However, typical transient temperature histories on the wing and vertical stabilizer are illustrated in Figures 3-16 and 3-17, respectively. The wing lower surface has a thermal protection system (TPS) over the primary structure. Primary structure of the wing upper surface and the vertical stabilizer main box is exposed to direct aerodynamic heating. The vertical stabilizer is also subjected to heating from plume impingement of the orbiter main engines during the separation phase.

A summary of the estimated range of temperature on each of the selected structural elements for the major mission phases is given in Table 3-8. These estimates are based on the specific data and general trends indicated in Figures 3-16 and 3-17, and consideration of the following factors:

1. The TPS is designed to protect the primary structure by limiting the maximum temperatures to approximately 300F for aluminum sub-structure and 650F for titanium sub-structure.

2. Primary structure covered by TPS will experience thermal lag compared to outer surface temperatures. Peak temperatures will occur at a later time and decay more slowly than for the outer surface.

3. Primary structure involving thick sections, such as wing spar caps and orbiter aft attachment bulkhead, will have significant heat sink capability. Peak temperatures on these members will be much less than for thin skins, and the peak temperature will decay more slowly.

4. Internal insulation is employed in the LH_2 tank; the resulting minimum temperature expected on the structural wall is approximately -200F.

5. The crew compartment will be environmentally controlled for crew habitability.

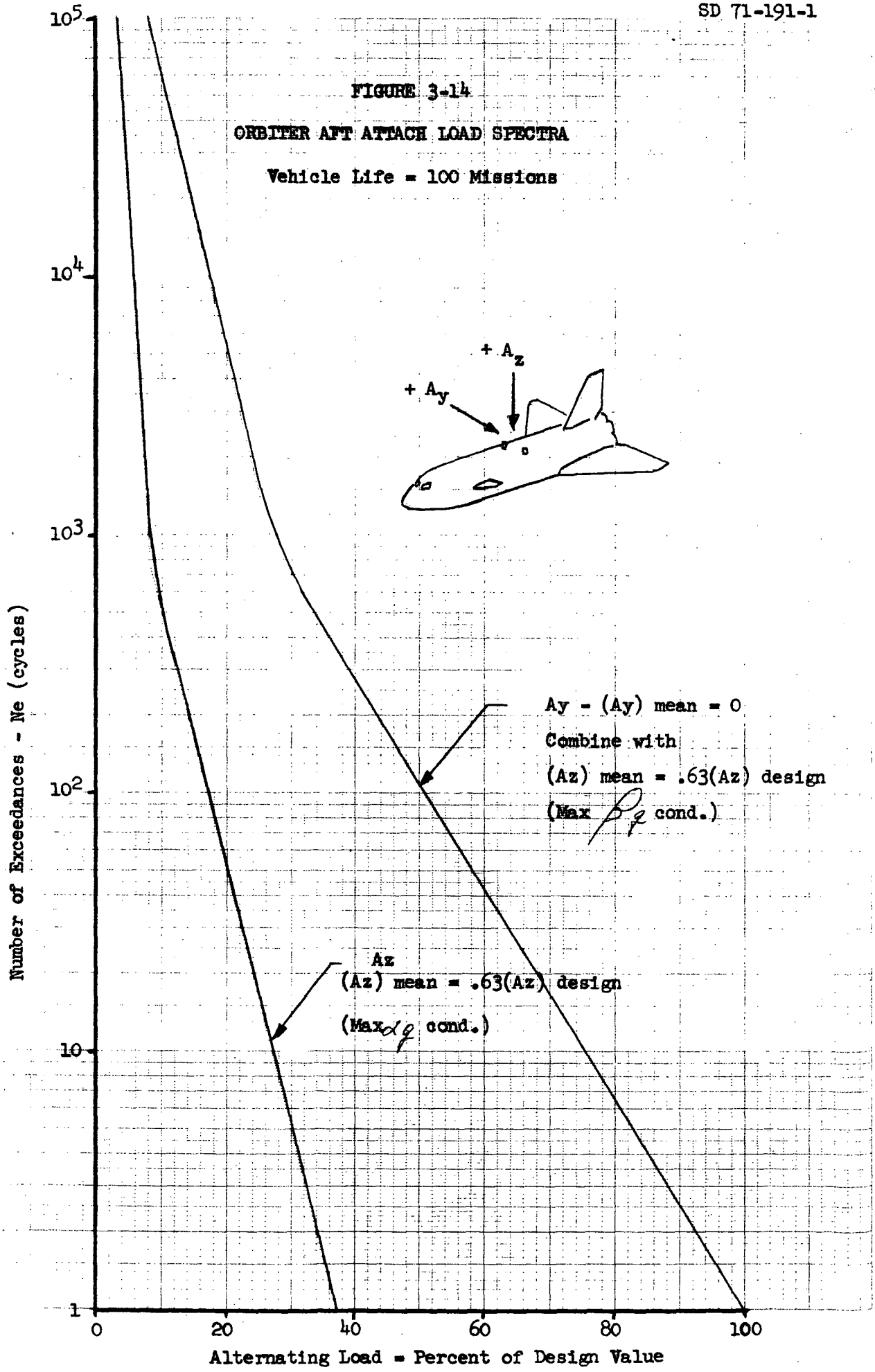
FIGURE 3-14
ORBITER AFT ATTACH LOAD SPECTRA
Vehicle Life = 100 Missions
+ Az
+ Ay
Ay - (Ay) mean = 0
Combine with
(Az) mean = .63(Az) design
(Max ∂/g cond.)
Az
(Az) mean = .63(Az) design
(Max ∂/g cond.)
Number of Exceedances - Ne (cycles)
Alternating Load - Percent of Design Value
10^5
10^4
10^3
10^2
10
1
0
20
40
60
80
100

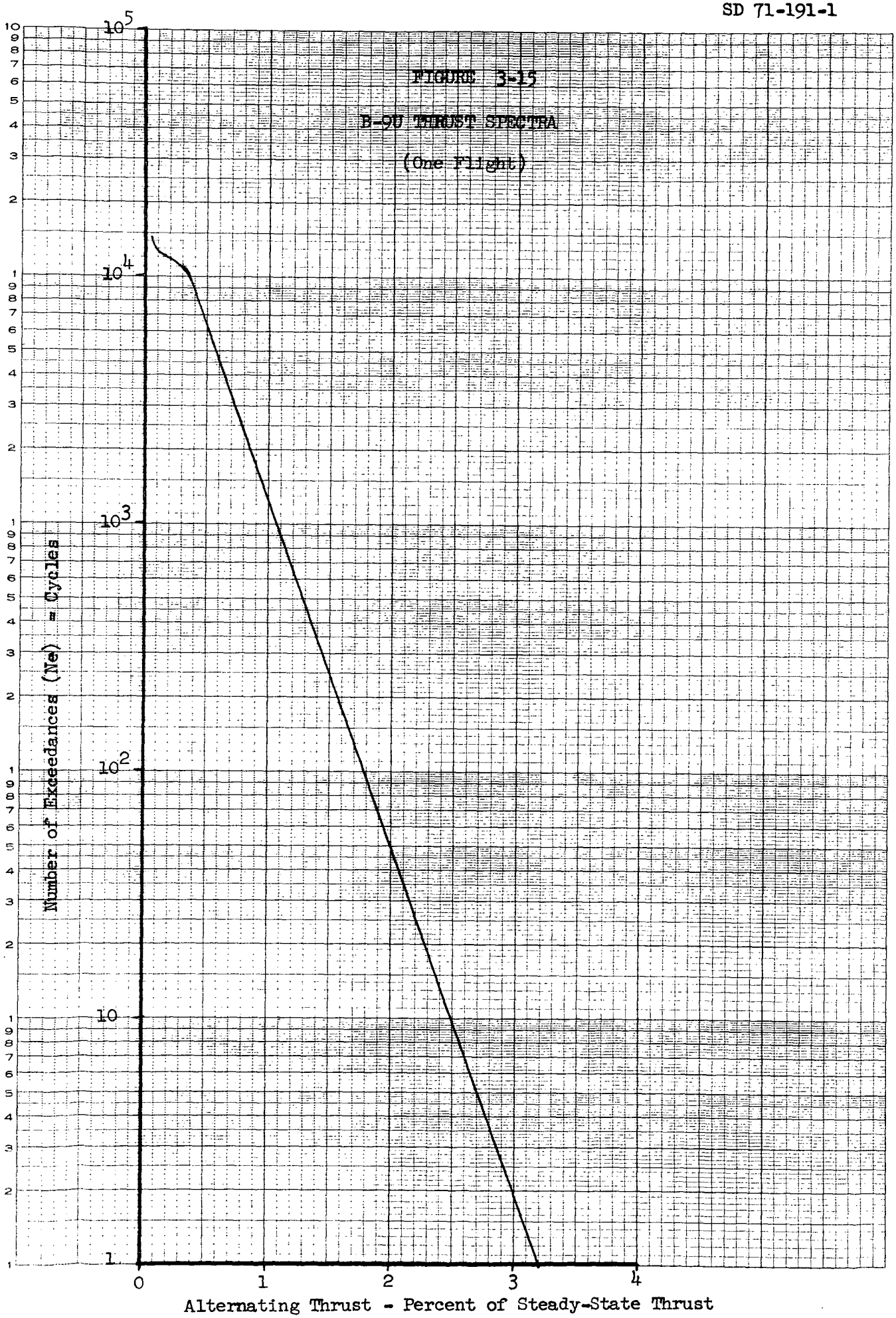

FIGURE 3-15

B-9U THRUST SPECTRA

(One Flight)

EUGENE DIETZGEN CO.
MADE IN U. S. A.
NO. 340-L51D DIETZGEN GRAPH PAPER
SEMI-LOGARITHMIC
5 CYCLES X 10 DIVISIONS PER INCH

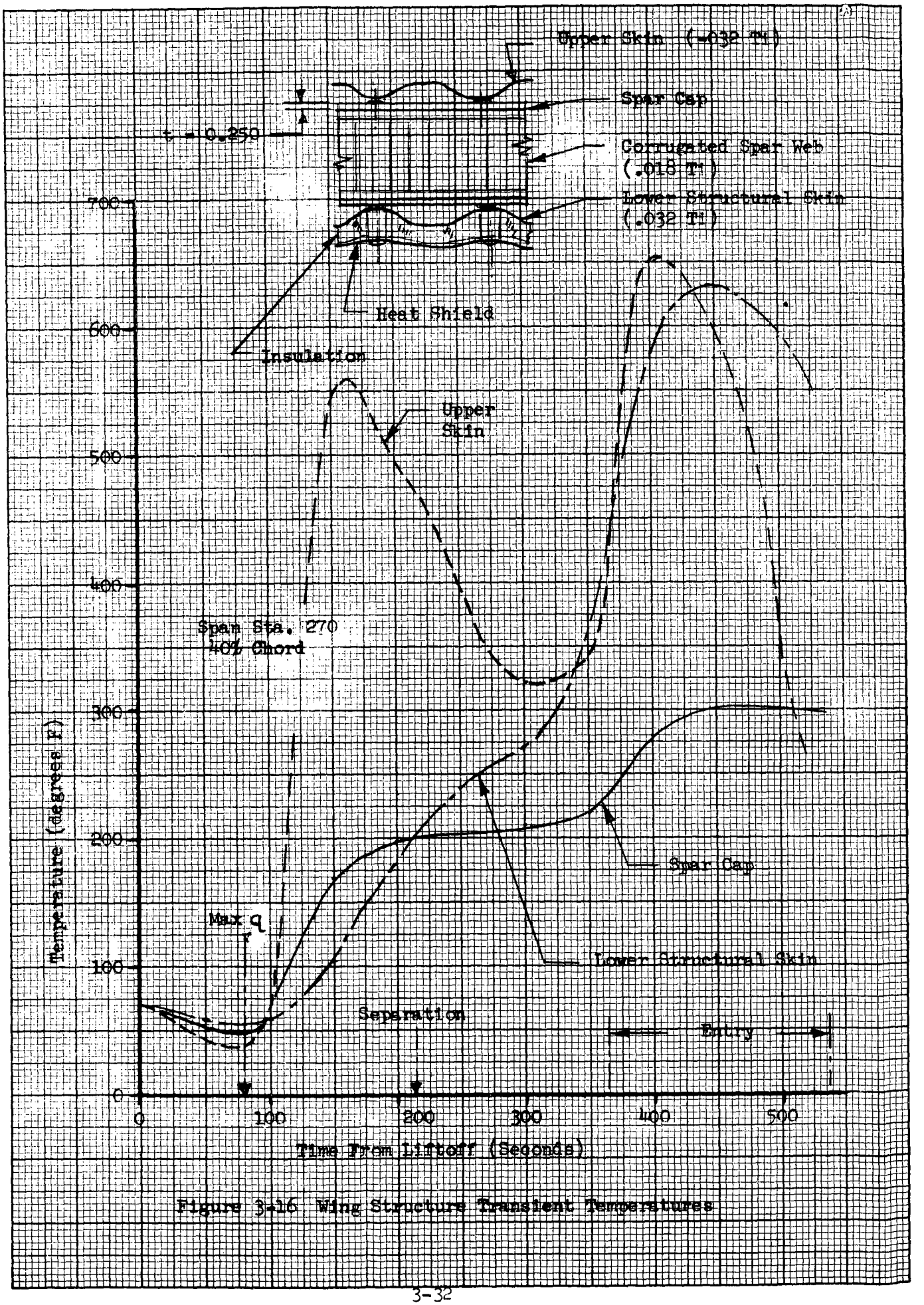

Figure 3-16 Wing Structure Transient Temperatures

K+E 10 X 10 TO THE 1/2 INCH 359I-11
KEUFFEL & ESSER CO. MADE IN U.S.A.
ALBANENE

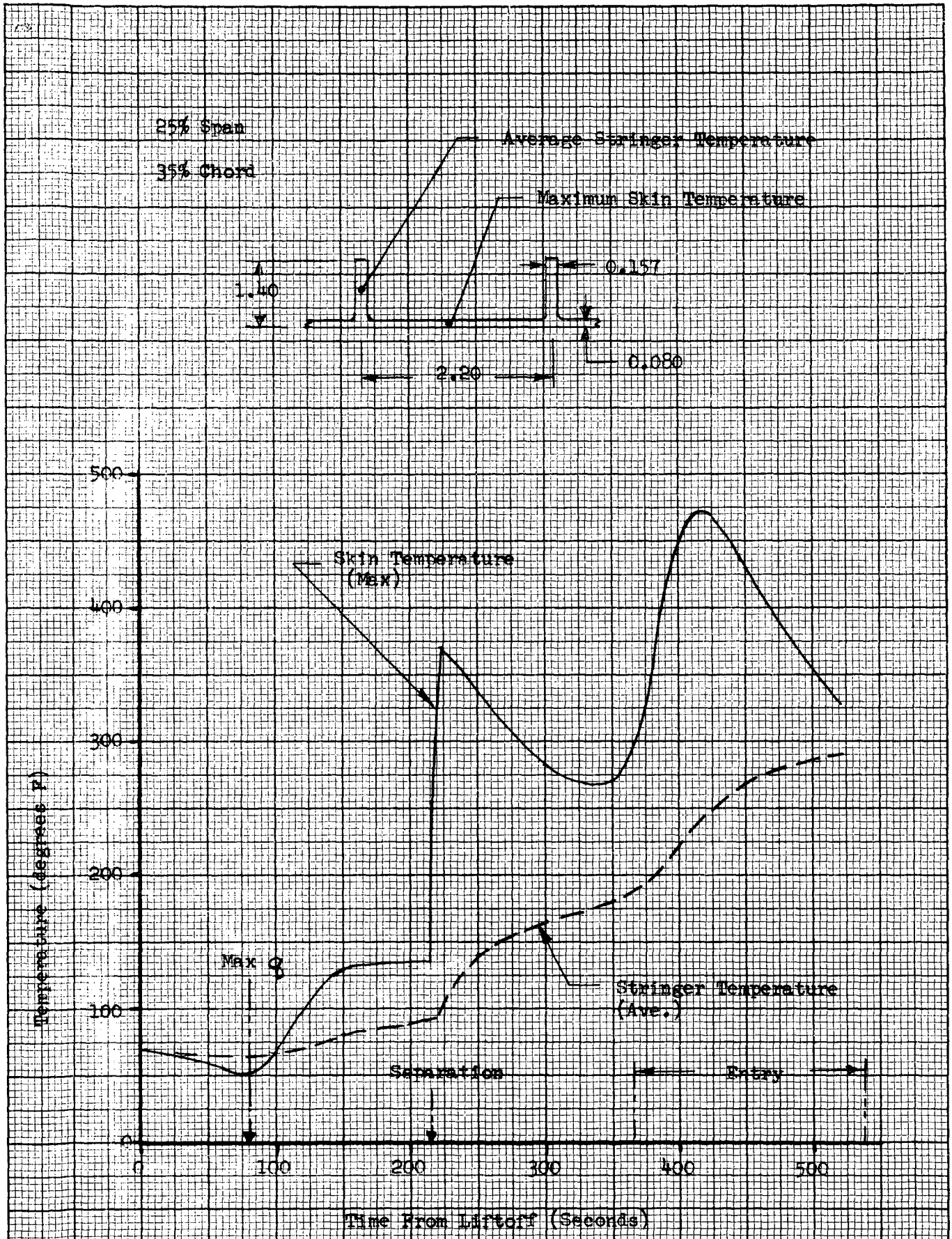

Figure 3-17 Vertical Stabilizer Structure Transient Temperatures

10 X 10 TO THE ½ INCH 3391-11
KEUFFEL & ESSER CO. MADE IN U.S.A.
ALBANENE

Table 3-8 Estimated Range of Structural Temperatures

Structural Element	Flight Phase				
	Ascent	Entry	Cruise	Landing/ Taxi	Ferry
LH_2 Tank Cyl. Shell	-200F to -100F	100F to 300F	100F to 300F	100F to 300F	-65F to 130F
LOX Tank Cyl. Shell	-297F to 0F	100F to 300F	100F to 300F	100F to 300F	
LOX Tank Aft. Bulkhead	-297F	-297F to 100F	100F to 200F	100F to 200F	
Wing Spars	0F to 130F	200F to 300F	200F to 300F	100F to 300F	
Vert. Stab. Main Box Skins (Root)	0F to 130F	300F to 480F	100F 300F	0F to 130F	
Intertank Adapter Cyl. Shell	-250F to 130F	200F to 300F	200F to 300F	200F to 300F	
Orbiter Aft Attach Buklhead	-200F to 0F	0F to 200F	100F to 200F	100F to 200F	-65F to 130F
Crew Compartment Cyl. Shell	60F to 100F				60F to 100F

4.0 SELECTED STRUCTURAL ELEMENTS

4.1 SELECTION SUMMARY

To provide an efficient and effective basis to conduct the study, it is necessary to select discrete structural elements and associated critical sections for detailed strength, fatigue, and fracture mechanics investigations. The elements should be selected to provide a representative sample covering the range of materials, operating environments, design approach, and failure modes expected for the shuttle booster structure. In general, they should also represent structural areas which are a significant portion of the structural weight, so that the influence of different criteria and approaches on vehicle weight and performance will be determined on a realistic basis.

A matrix of candidate structural elements of the B-9U booster is presented in Table 4-1. This table also summarizes the type of structural configuration, selected material, operating stress and temperature environment, weight of similar structure, and proof test and inspection considerations as determined in the Space Shuttle Phase B Study. Review and evaluation of this matrix led to the following selection; reasons for selection are discussed below.

The following structural elements are of primary interest and are selected as the principal basis for detailed investigations:

1. LH_2 tank cylindrical shell-mid region (Sta. 2600)
2. LOX tank cylindrical shell-forward region
3. LOX tank cylindrical shell-aft region
4. LOX tank aft bulkhead
5. Wing spars (lower surface)-root region
6. Vertical stabilizer main box-root region
7. Crew compartment cylindrical shell

The following structural elements are of secondary interest and will be investigated to an extent appropriate to date availability and study scope.

1. Orbiter aft support bulkhead
2. Intertank adapter cylindrical shell.

4.2 SELECTION RATIONALE

The main propellant tanks of the booster are obviously primary elements for investigation because of their susceptability to fracture, the catastrophic consequences of failure, and the large amount of structural weight involved. Because of the low density of liquid hydrogen, the pressure gradient from forward to aft end of the LH_2 tank is relatively small. Therefore, a single section at Sta. 2600 has been selected for analysis. This is in the region of the maximum body bending moment and should therefore

provide a good basis to evaluate the influence of flight loads on fatigue and fracture characteristics of the tank. The evaluation of behavior under hoop stresses due to internal pressure determined at this station should be representative of the entire LH_2 tank. A large pressure gradient exists over the length of the LOX tank, so sections at both the forward and aft ends of the cylindrical shell are selected for analysis. The aft bulkhead of the LOX tank is subjected to a maximum design pressure, so it is selected for evaluation as an example of pressure vessel membrane structure. The general results and trends determined for this member should also be applicable to the other propellant tank bulkheads.

The wing spars are selected as the most appropriate elements of the wing structural assembly for investigation. They represent a significant portion of the structural weight and are loaded by axial tension and compression stresses. In-service accessibility and inspection limitations exist because of attachment of cover skins and thermal protection system; the effects of these limitations should be investigated. Spars on the wing upper and lower surfaces are of similar configuration; however, the lower surface operates at higher tensile stress levels, so it is selected for analysis.

The main box of the vertical stabilizer is also selected for analysis because of the different nature of the aerodynamic loading and because it is of different structural configuration from the wing. Integral-stiffened skin planks resist the spanwise bending loads rather than concentrated spar members.

Although the crew compartment represents only a relatively small portion of the structural weight, it is selected for evaluation in this study because of special problems related to crew safety. The current design approach applied to almost all aircraft pressurized fuselage structure provides a high fail-safe capability such that a skin crack can extend completely between frame members without causing catastrophic rupture. However, this concept may not be practical for space shuttle, considering the loss of cabin atmosphere that will occur before the crew can descend to a safe attitude or don pressure suits. Therefore, it is considered desirable to evaluate the crew compartment cylindrical shell, with special attention to crew safety provisions.

The orbiter aft support bulkhead is of interest as an example of a heavy forged member subjected to repeated load cycles. The same type of structure is also found at the orbiter forward attachment and at wing support frames. However, the basic design and stress analysis data is less well developed for these members than for the other structural elements considered. Also, the total weight involved is a relatively small percentage of the vehicle structural weight, so that fracture mechanics and fatigue design considerations applied to these members should not have a major impact on the total vehicle weight and performance.

The intertank adapter is also of interest as an example of unpressurized fuselage structure. However, because of thrust and inertia loadings during boost, the compression design stresses are much higher than the maximum tension stresses encountered. Therefore, it is unlikely that fracture considerations would cause a significant change in the design approach or the structural weight of this assembly.

FOLDOUT FRAME 1

FOLDOUT FRAME 2

FOLDOUT FRAME 3

Space Division
North American Rockwell

TABLE 4-1 MATRIX OF CANDIDATE STRUCTURAL ELEMENTS - SHUTTLE BOOSTER B-9U

STRUCTURAL ELEMENT	TYPE OF STRUCTURE	MATERIAL	TOTAL WEIGHT OF SIMILAR STRUCTURE	% (1) VEHICLE STRUCTURAL WEIGHT	LIMIT STRESS (TENSION)	POTENTIAL FAILURE MODES	CRITICALITY LEVEL	CANDIDATE DESIGN APPROACH	TYPE OF LOADING	TEMPERATURE CYCLES	POTENTIAL FOR INITIAL FLAWS	PROOF TEST FEASIBLE	ACCESSIBILITY		APPLICABLE NDE METHODS			
													FABRICATION & PROOF TEST	OPERATIONAL SERVICE	DETAIL	ASSEMBLY	POST-PROOF	OPERATIONAL
① LH_2 TANK CYL. SHELL - MID REGION (STA. 2600) ►	INTEGRAL STIFFENED - WELDED PANELS	2219-T87 ALUMINUM ALLOY PLATE	23,800 kg (52,600 LB.)	28.0	310 MN/m² (45 KSI)	LEAKAGE	DEFERRED CRITICAL	SAFE-LIFE	BIAXIAL TENSION (DISCRETE SPECTRA) + BODY BENDING (RANDOM SPECTRA)	143 K (-200F) TO 422 K (300 F)	PARENT METAL - MODERATE WELDS - HIGH	YES (4)	COMPLETELY ACCESSIBLE	INTERIOR SURFACE NOT ACCESSIBLE - EXTERIOR SURFACE ACCESSIBLE BY REMOVAL OF TPS	VISUAL, PENETRANT (BOTH SIDES) ULTRASONIC (RAW MAT'L.)	VISUAL, X-RAY, PENETRANT (WELDS)	VISUAL, X-RAY (WELDS), PENETRANT (WELDS & LOCAL PARENT METAL) ACOUSTIC EMISSION (DURING PROOF)	VISUAL, LEAK DETECTION, PRESSURE DECAY, PENETRANT & X-RAY (LOCAL AREAS)
						RUPTURE	IMMEDIATE CATASTROPHIC											
② LOX TANK CYL. SHELL - FWD. REGION ►	INTEGRAL STIFFENED - WELDED PANELS	2219-T87 ALUMINUM ALLOY PLATE	4100 kg (9100 LB)	3.7	270 MN/m² (39 KSI)	LEAKAGE	TO BE DETERMINED	SAFE-LIFE	BIAXIAL TENSION (DISCRETE SPECTRA) + BODY BENDING (RANDOM SPECTRA)	91 K (-297 F) TO 422 K (300 F)	PARENT METAL - MODERATE WELDS - HIGH	YES (4)	COMPLETELY ACCESSIBLE	INTERIOR SURFACE ACCESSIBLE - (5) EXTERIOR SURFACE ACCESSIBLE BY REMOVAL OF TPS	SAME AS ①	SAME AS ①	SAME AS ①	SAME AS ①
③ LOX TANK CYL. SHELL - AFT REGION ►					345 MN/m² (50 KSI)	RUPTURE	IMMEDIATE CATASTROPHIC											
④ LOX TANK AFT BULKHEAD ►	UNSTIFFENED, WELDED GORE PANELS	2219-T87 ALUMINUM ALLOY SHEET	3700 kg (2) (8200 LB.)	3.3	345 MN/m² 50 KSI	LEAKAGE	TO BE DETERMINED	SAFE-LIFE	BIAXIAL TENSION (DISCRETE SPECTRA)	91 K (-297 F) TO 366 K (200 F)	PARENT METAL - LOW WELDS - HIGH	YES (4)	COMPLETELY ACCESSIBLE	INTERIOR SURFACE ACCESSIBLE - ACCESS TO EXTERIOR SURFACE IS VERY DIFFICULT	SAME AS ①	SAME AS ①	SAME AS ①	SAME AS ①
						RUPTURE	IMMEDIATE CATASTROPHIC											
⑤ CREW COMPARTM'T CYL. SHELL ▷	SKIN, STRINGER, FRAME	2024 ALUMINUM ALLOY SHEET	680 kg (1500 LB.)	0.6		LEAKAGE	MISSION ABORT	SAFE-LIFE & FAIL-SAFE	BIAXIAL TENSION (DISCRETE SPECTRA)	289 K (60 F) TO 311 K (100 F)	LOW	YES	COMPLETELY ACCESSIBLE	LIMITED ACCESS TO INTERIOR & EXTERIOR SURFACES	VISUAL, PENETRANT	VISUAL	VISUAL, PRESSURE DECAY, LEAK CHECK	VISUAL, PRESSURE DECAY, LEAK CHECK
						RUPTURE	IMMEDIATE CATASTROPHIC											
⑥ WING SPARS - LOWER SURFACE ►	MACHINED EXTRUSION	6AL-4V TITANIUM (ANNEALED)	7000 kg (15,400 LB)	6.2	620 MN/m² 90 KSI	TENSILE FRACTURE	DEFERRED CRITICAL	FAIL-SAFE	AXIAL TENSION/COMPRESS. (RANDOM SPECTRA)	273 K (0 F) TO (3) 422 K (300 F)	LOW	NO	LIMITED ACCESS THROUGH INSPECTION PANELS, ABES CAVITIES	LIMITED ACCESS THROUGH INSPECTION PANELS, ABES CAVITIES	VISUAL, PENETRANT, ULTRASONIC (RAW MAT'L.)	VISUAL PENETRANT - (LOCAL WEB/PLATE WELD REGIONS)		VISUAL, AIDED BY FIBER OPTICS
⑦ WING SPARS - UPPER SURFACE					440 MN/m² (64 KSI)	TENSILE FRACTURE, COMPRESSION BUCKLING	DEFERRED CRITICAL											
⑧ ORBITER SUPPORT BULKHEAD (AFT) ▷	MACHINED FORGING	2219-T851 ALUMINUM ALLOY	1200 kg (2700 LB)	1.1	250 MN/m² (36 KSI)	FRACTURE UNDER TENSION & BENDING	IMMEDIATE CATASTROPHIC	SAFE-LIFE	BENDING + AXIAL LOAD (RANDOM SPECTRA)	143 K (-200F) TO (3) 366 K (200 F)	MODERATE	VERY DIFFICULT	COMPLETELY ACCESSIBLE	ACCESSIBLE BY REMOVAL OF TPS	VISUAL, PENETRANT	VISUAL, PENETRANT		VISUAL, PENETRANT
⑨ VERTICAL STABILIZER MAIN BOX ►	3-SPAR BOX, INTEGRAL STIFFENED SKIN PLANKS	6AL-4V TITANIUM (ANNEALED)	2000 kg (4500 LB)	1.8	210 MN/m² (30 KSI)	TENSILE FRACTURE, COMPRESSION BUCKLING	IMMEDIATE CRITICAL (LOSS OF VEHICLE; POSSIBLE CREW SURVIVAL)	FAIL-SAFE	AXIAL TENSION/COMPRESSION (RANDOM SPECTRA)	273 K (0 F) TO 522 K (480 F)	MODERATE	VERY DIFFICULT	EXTERIOR SURFACE ACCESSIBLE - LIMITED ACCESS TO INTERIOR SURFACE	EXTERIOR SURFACE ACCESSIBLE - LIMITED ACCESS TO INTERIOR SURFACE	VISUAL, PENETRANT	VISUAL, AIDED BY FIBER OPTICS		VISUAL, AIDED BY FIBER OPTICS
⑩ INTERTANK ADAPTER - CYL. SHELL ▷	INTEGRAL STIFFENED SKIN, RIVETED TO FRAMES	7075 ALUMINUM ALLOY PLATE	3400 kg (7600 LB.)	3.1	90 MN/m² (13 KSI)	TENSILE FRACTURE, COMPRESSION BUCKLING	IMMEDIATE CATASTROPHIC	SAFE-LIFE	AXIAL TENSION/COMPRESSION (RANDOM SPECTRA)	111 K (-250 F) TO 422 K (300 F)	MODERATE	YES	COMPLETELY ACCESSIBLE	LIMITED ACCESS TO INTERIOR SURFACE - EXTERIOR SURFACE ACCESSIBLE BY REMOVAL OF TPS	VISUAL, PENETRANT, ULTRASONIC (RAW MAT'L)	VISUAL, PENETRANT	VISUAL, PENETRANT	VISUAL, PENETRANT

NOTES:

(1) TOTAL WEIGHT OF STRUCTURAL SYSTEM (EXCLUDING TPS, LANDING, DOCKING) = 112,000 kg (247,000 LB.)
(2) TOTAL WEIGHT OF LOX & LH_2 TANK BULKHEADS
(3) ESTIMATED, BASED ON SKIN TEMPERATURE AND HEAT-SINK CAPACITY OF SUB-STRUCTURE
(4) VALIDITY OF PROOF TEST TO VERIFY NO LEAKAGE DURING SERVICE LIFE IS QUESTIONABLE
(5) INTERIOR SURFACE OF LH_2 TANK BULKHEADS NOT ACCESSIBLE BECAUSE OF FOAM INSULATION

RECOMMENDED SELECTION CODE:

► PRIMARY ELEMENTS FOR STUDY
▷ SECONDARY ELEMENTS FOR STUDY

5.0 FATIGUE AND FRACTURE PROPERTIES

Summarized in this section are fatigue and fracture properties of materials that have been selected or are alternate candidates of interest for the chosen structural elements. Properties have been established from wide-spread literature survey, supplemented by in-house data derived from test programs conducted under other contracts.

5.1 FATIGUE PROPERTIES

5.1.1 2219 Aluminum Alloy

S-N curves for 2210-aluminum alloy are plotted in Fig. 5-1. A family of curves are plotted for various values of stress ratio (maximum stress in cycle divided by minimum stress in cycle). The data are for a theoretical stress concentration factor (K_t) of 4.4, which is considered to be representative or slightly conservative for average design practice as applied to structural assemblies and joints of the propellant tanks. The S-N curves are expressed in terms of percent of material ultimate tensile strength, and are considered to be applicable to both the -T851 and -T878 tempers of the alloy. The curves are based on room temperature data, but may be applied over the temperature range of -300F to +300F with only small error.

The curves are based primarily on the data of Reference 8; however, other sources, such as Reference 9, have been examined to compare and validate the data.

5.1.2 6Al-4V Titanium Alloy

S-N curves for 6Al-4V titanium alloy are plotted in Figure 5-2 (K_t = 3.0) and Figure 5.3 (K_t = 4.5). Again, a family of curves is plotted for various values of stress ratio, and the allowable maximum stress is expressed as a percentage of material ultimate tensile strength. The curves are based on room temperature test data for the annealed material and will be slightly conservative if applied to elevated temperature up to + 650F. Using the allowable stress values determined from these curves with annealed material properties for material in the solution treated and aged (STA) temper should also be conservative.

The S-N curves are based on the data presented in Ref. 8 for titanium which was subjected to a diffusion bond thermal cycle. This is equivalent to a mill anneal temper insofar as strength and fatigue properties are concerned. Data on material in this condition was obtained by extensive testing at the NR Los Angeles Division. Data from other sources, such as References 10 and 11, were also reviewed to verify the validity of the S-N curves.

The S-N curves for K_t = 4.5 are considered to be representative of average design practice applied to joints and attachments; those for

K_t = 3.0 representative of design practice where rather extensive care is taken to minimize stress concentrations and to employ other methods to retard fatigue crack initiation. An interesting comparison is presented in the modified Goodman diagram of Figure 3-4. Superimposed on the constant life curves for K_t = 3.0 and K_t = 4.5 are discrete points representing the results of fatigue tests on structural joints. Spotwelded joint data is taken from Reference 11, riveted joint data from Reference 12. It can be seen that the spotwelded joint and the Hi-Shear rivet joint were approximately comparable to a K_t = 4.5 in the higher cycle range; the riveted joint using Taper-Lok fasteners exhibited better fatigue life than notched specimens with K_t = 3.0. It can also be seen that the allowable stress determined from notched specimens becomes progressively more conservative compared to joint tests as the fatigue life is reduced below 10^5 cycles.

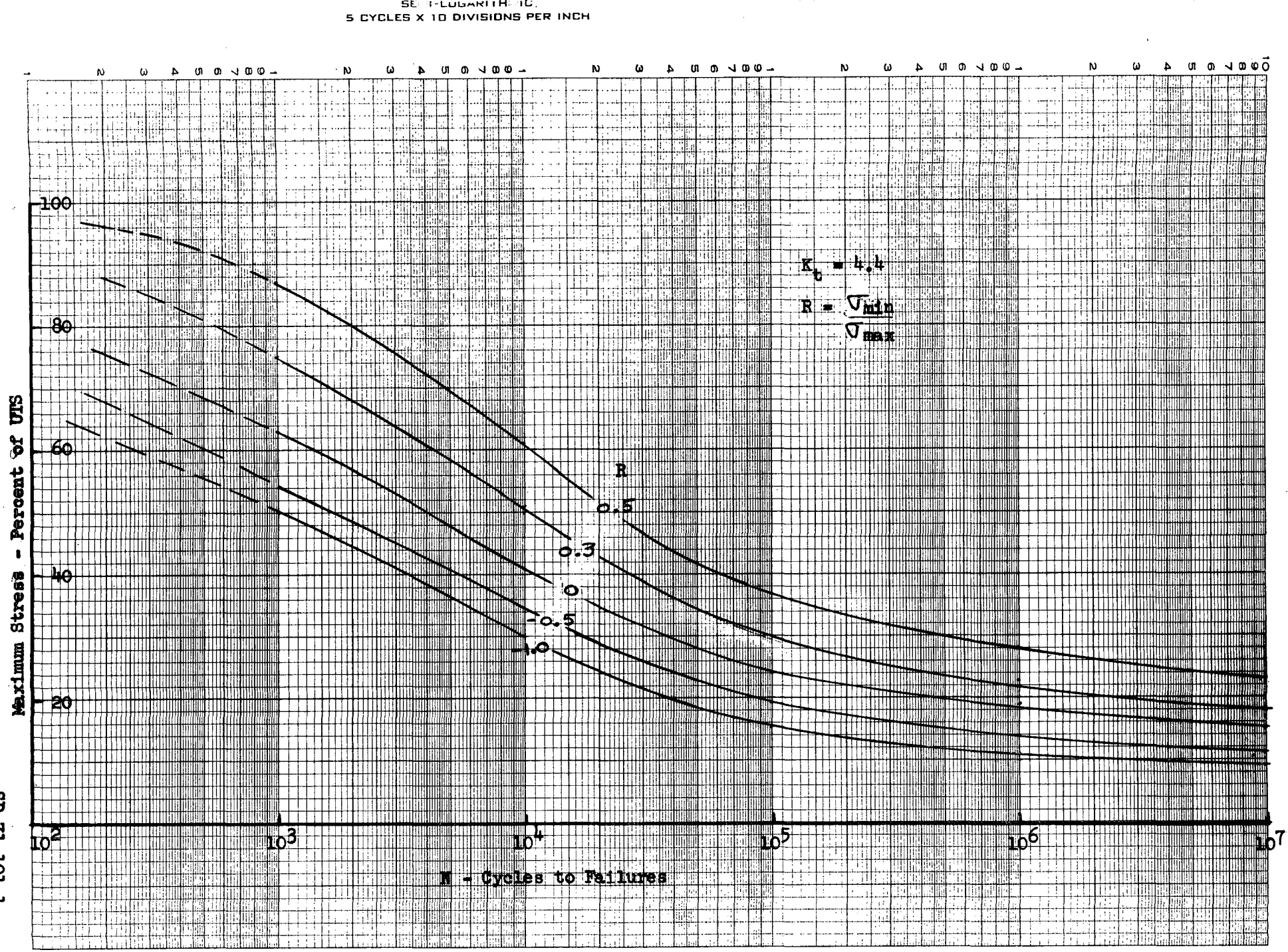

Figure 5-1 S-N Curves for 2219 Aluminum ($K_t = 4.4$)

NO. 340-L510 DIETZGEN GRAPH PAPER
SEMI-LOGARITHMIC
5 CYCLES X 10 DIVISIONS PER INCH
EUGENE DIETZGEN CO.
MADE IN U. S. A.

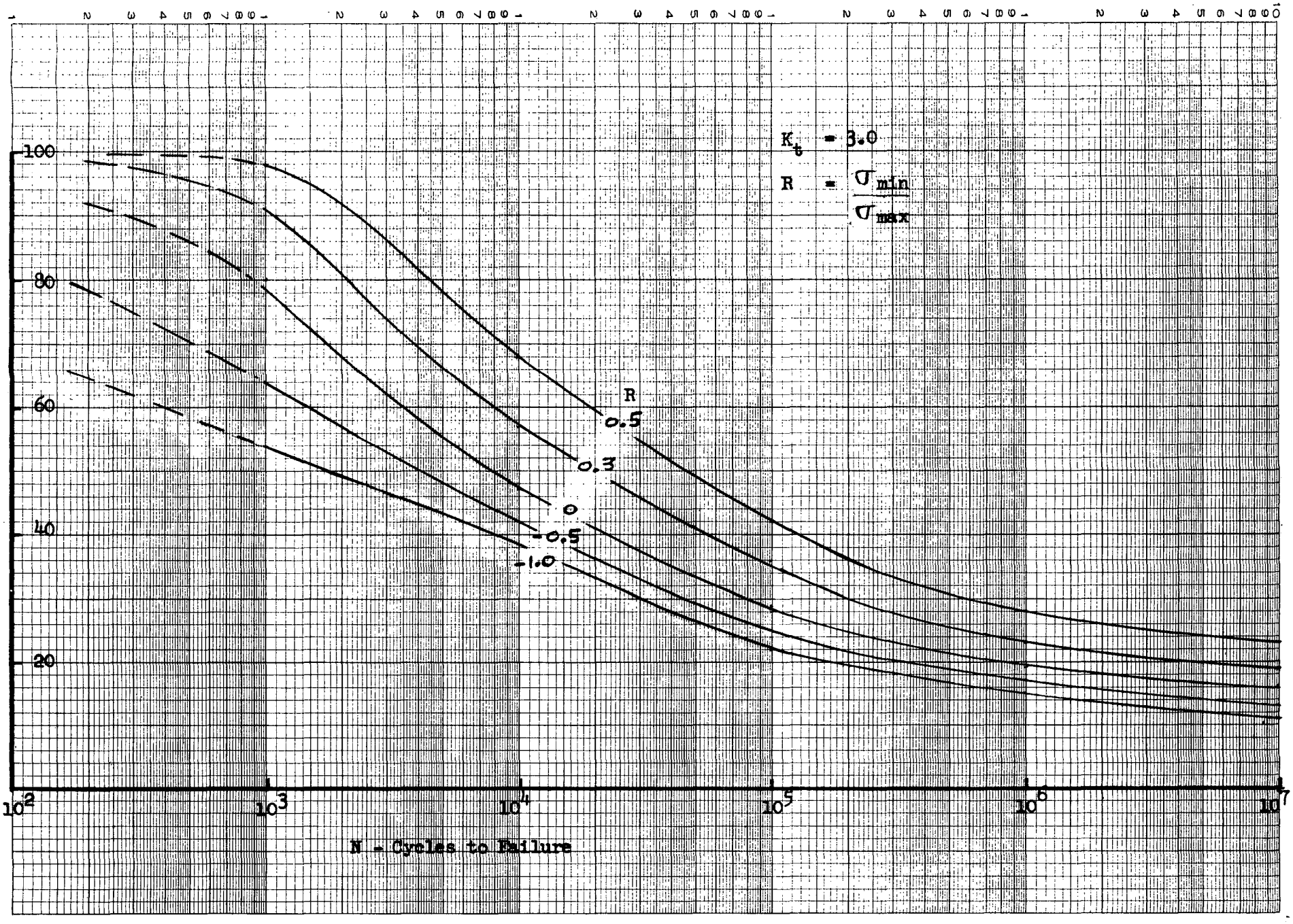

Figure 5-2 S-N Curves for Ti-6Al-4V (K_t = 3.0)

SEMI-LOGARITHMIC
5 CYCLES X 10 DIVISIONS PER INCH
MADE IN U. S. A.

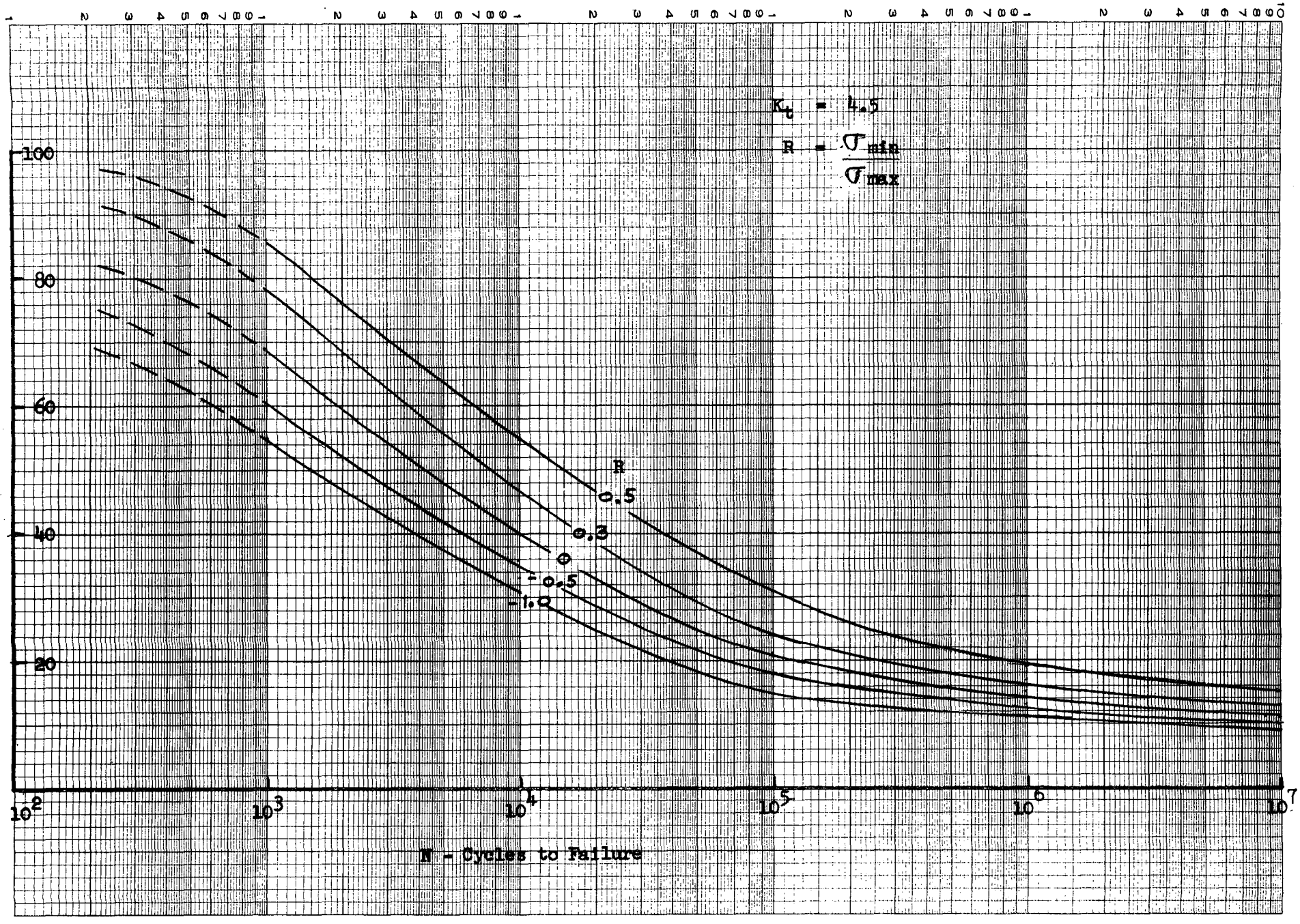

Figure 5-3 S-N Curves for Ti-6Al-4V ($K_t = 4.5$)

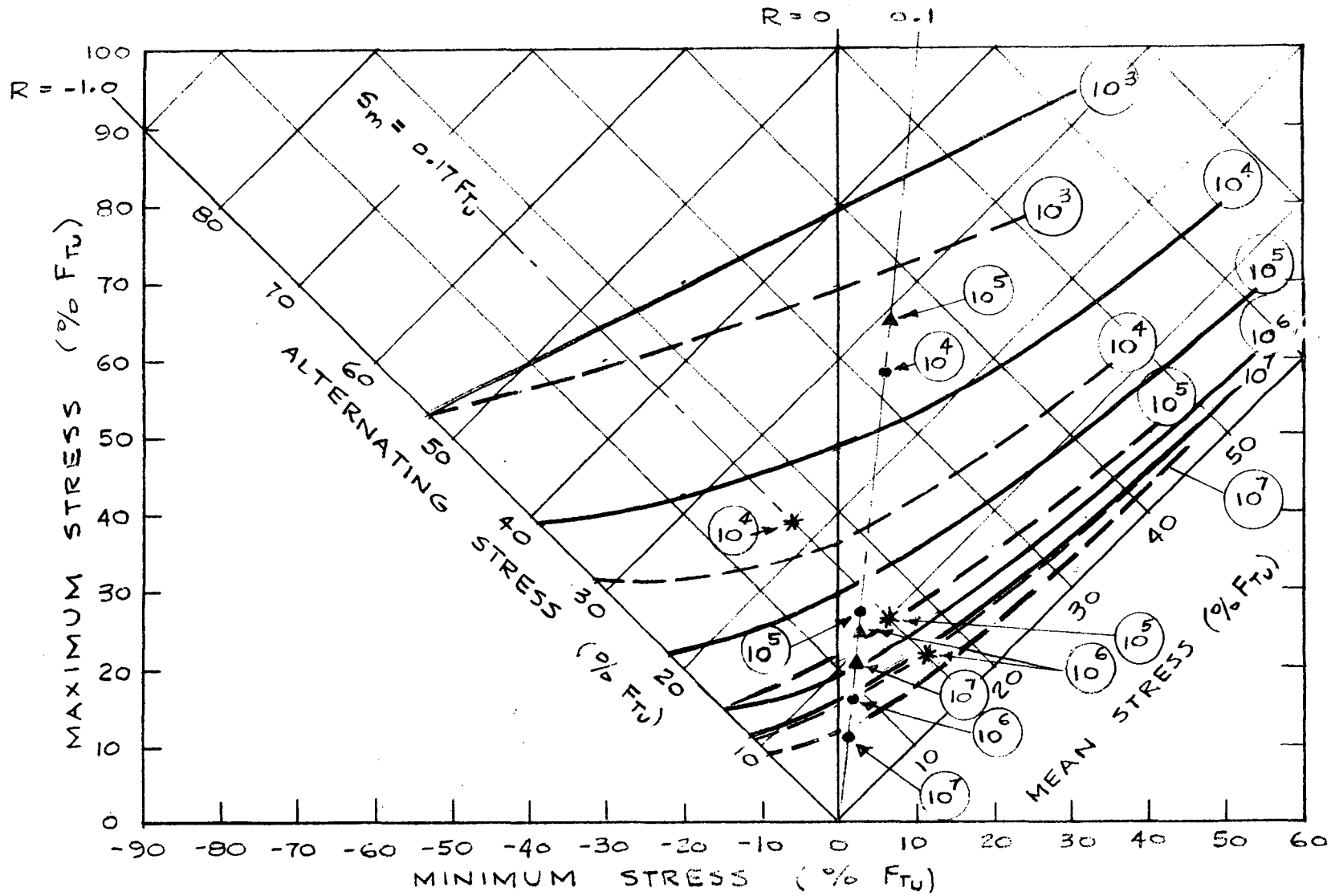

Notched Specimen Tests (Ref. 8) — $K_t = 3.0$; — — — $K_t = 4.5$

Double Lap Joint Tests: ✱ Spotwelds (Ref. 11); ● Hi-Shear Rivets, ▲ Taper-Lok Fasteners (Ref. 12)

Figure 5-4 Modified Goodman Diagram for Ti-6Al-4V (Annealed)

Space Division
North American Rockwell